UNIVERSITY OF CALIFORNIA

SANTA CRUZ

REGULATION OF PP2A^{RTS1} AND ITS ROLE IN CELL SIZE AND ENTRY INTO THE CELL CYCLE

A dissertation submitted in partial satisfaction
of the requirements for the degree of

DOCTOR OF PHILOSOPHY

In

MOLECULAR, CELL AND DEVELOPMENTAL BIOLOGY

by

Jessica Zapata

March 2014

The Dissertation of Jessica Zapata is approved:

_____
Professor Douglas Kellogg, chair

_____
Professor Susan Strome, Ph.D.

_____
Professor Jeremy Sanford, Ph.D

_____
Tyrus Miller
Vice Provost and Dean of Graduate Studies

TABLE OF CONTENTS

Chapter V: Miscellaneous Experiments

LIST OF FIGURES

Chapter I

Chapter II

Chapter III

Chapter IV

Chapter V

LIST OF TABLES

Chapter II

Chapter III

Chapter IV

Chapter V

REGULATION OF CELL SIZE AND ENTRY INTO THE CELL CYCLE BY PP2A^{RTS1}

Jessica Zapata

ABSTRACT

Cell size and shape are essential for the survival and function of all cells. Cell size checkpoints coordinate cell growth and cell division by ensuring passage through G1 and mitosis only occurs when cells reach a critical size; however, the mechanisms that control these checkpoints are largely unknown.

PP2A associated with the Rts1 regulatory subunit (PP2A^{Rts1}) is required for cell size control in budding yeast, but the relevant targets are unknown. Here, we used quantitative proteome-wide mass spectrometry to identify proteins controlled by PP2A^{Rts1}. This revealed that PP2A^{Rts1} controls the two key checkpoint pathways thought to regulate the cell cycle in response to cell growth. To investigate the role of PP2A^{Rts1} in these pathways, we focused on the Ace2 transcription factor, which is thought to delay cell cycle entry by repressing transcription of the G1 cyclin *CLN3*. Diverse experiments suggest that PP2A^{Rts1} promotes cell cycle entry by inhibiting the repressor functions of Ace2.

Furthermore, we found that Rts1 phosphorylation is dependent on the budding yeast homologs of the vertebrate phosphoinositide-dependent kinase 1 (PDK1) and protein kinase C (PKC). We also found that hyperphosphorylation of Rts1 in response to poor nutrients is dependent on PDK1, PKC and casein kinase 1.

Together these results support a model in which Rts1 links nutrient availability and cell size to entry into the cell cycle.

ACKNOWLEDGEMENTS/DEDICATION

I have learned so much through out this time and one of the biggest lessons is that I could not have accomplished all of this without the love and support of many. It is my experience with others and their unfaltering faith that I will cherish forever.

First and foremost I would like to thank my advisor Douglas Kellogg for his continuous guidance and support throughout the years. Thank you for sharing your knowledge, I could not have asked for a better mentor.

I would like to thank my thesis committee members, Susan Strome and Jeremy Sanford. Thank you for your encouragement and for empowering me to follow through with my PhD.

I'd like to extend my gratitude to everyone that has been part of the lab at one time or another. Thank you for making research so much fun. Thank you for the laughs and so many inspiring discussions. Your thoughtful ideas and suggestions helped make this a better project. Thank you for making this and invaluable experience.

Thank you to everyone that contributed to this work, especially Karen Artiles who was fundamental in setting the foundations to this project and Tracy MacDonough who helped me build on those foundations.

Last but not least, I would like to thank my family. My parents and siblings, whose unconditional love and absolute trust in me, gave me the confidence to start this adventure. My husband and daughters who were by my side every step of the way, inspiring and motivating each of the steps that brought me here today.

Finally, I would like to dedicate this work to my family and to my mentor and friend, Doug Kellogg who unknowingly changed my life entirely and in the most difficult time of my life gave me the support and motivation to pursue this dream.

CHAPTER I

INTRODUCTION

THE CELL CYCLE

The events of the eukaryotic cell cycle must be precisely coordinated to ensure that cell division produces two normal daughter cells. These events are driven by highly conserved proteins called cyclins and cyclin-dependent kinases (Cdks). At each stage of the cell cycle, distinct cyclins bind and activate Cdks to initiate specific cell cycle events. Progression through the cell cycle is tightly monitored by cell cycle checkpoints, which ensure that Cdks are only activated when previous cell cycle events have been properly completed. Cell cycle checkpoints act at the three major cell cycle transitions: G1 to S, G2 to M, and Metaphase to Anaphase.

COORDINATION OF CELL GROWTH AND ENTRY INTO THE CELL CYCLE

Cells from the same species or cell type maintain a relatively constant size. In order for cells to maintain a uniform size, cell growth must be coordinated with cell division; otherwise, cells could become smaller or larger with each round of division. Cell size checkpoints coordinate cell growth with cell division by ensuring that key cell cycle transitions occur only when sufficient growth has occurred. Cell size checkpoints have been observed in diverse organisms. In budding yeast, for example, cells divide asymmetrically, yielding a small daughter cell and a large mother cell. The daughter cell will spend a longer time in G1 than the mother cell in order to reach a critical size and enter S phase (Hartwell and Unger, 1977; Johnston

et al., 1977) (Figure 1). Fission yeast cells arrested in S phase continue to grow and become large (Mitchison and Creanor, 1971). Upon release from the arrest, cells return to their normal size by shortening their cell cycle. Once cells readjust their size, the cell cycle length returns to normal (Fantes and Nurse, 1977; Nurse, 1975). Studies in avian erythroblasts and mammalian cell lines have shown that if cell growth is increased by delaying S phase, the subsequent G1 phase will be shorter (Dolznig et al., 2004; Killander and Zetterberg, 1965a; Killander and Zetterberg, 1965b). Furthermore, studies using lymphoblasts showed that they also require a critical size to exit G1, similar to budding yeast (Tzur et al., 2009). All these observations suggest that the mechanisms that coordinate growth and cell division are highly conserved.

In budding yeast, cell size is monitored at the G1 to S transition, which is also called START (Hartwell and Unger, 1977; Johnston et al., 1977). The most upstream event of START is activation of transcription factor SBF, composed of Swi4 and Swi6 (Futcher, 2002). Before cells reach a critical size, SBF is kept inactive by a repressor called Whi5, the functional homolog of protein Rb in mammalian cells (Costanzo et al., 2003; de Bruin et al., 2004) (Figure 2A). When sufficient growth has occurred, Cdk1/Cln3 triggers transcription of late G1 cyclins Cln1 and Cln2 by phosphorylating and inhibiting Whi5 (de Bruin et al., 2004) (Figure 2B). Cln1 and Cln2 are part of a positive feedback loop that further inhibits Whi5, promoting bud emergence and driving entry into the cell cycle (Cross and Tinkelenberg, 1991; Dirick and Nasmyth, 1991). Cell size control also occurs at the G2/M transition. Early evidence for this showed that inhibition of bud growth resulted in a G2/M delay in cells with buds smaller than the critical size (Harvey and Kellogg, 2003).

The G2/M size checkpoint is regulated by the Wee1 kinase and Cdc25 phosphatase (Nurse, 1975; Nurse et al., 1976) (Nurse 1975, 1976). Wee1 phosphorylates and inhibits Cdk1, delaying entry into mitosis, whereas Cdc25 promotes mitotic entry by removing this inhibitory phosphorylation (Dunphy and Kumagai, 1991; Gould and Nurse, 1989; Kumagai and Dunphy, 1991; Russell and Nurse, 1986) (Figure 3A and 3B). Loss of Wee1 causes premature entry into mitosis resulting in small cell size (Nurse, 1975). Conversely, mutations in Cdc25 result in delayed entry into mitosis and a large cell size phenotype (Nurse, 1975; Russell and Nurse, 1986).

Although cell growth and cell division are normally intertwined, there are several examples that show that they can be uncoupled. For instance, the eggs of many vertebrate animals undergo growth without division, and once fertilized, undergo several rounds of division without growth (Newport and Kirschner, 1982). Another example is found in budding yeast, where cells continue to grow during a cell cycle arrest (Johnston et al., 1977).

HOW IS CELL SIZE CONTROLLED?

Cell size checkpoints can measure cell size or growth, yet the nature of the signal that they measure is unknown. They could be measuring cell mass, volume, biosynthetic capacity or growth rate. One approach to discovering how cells measure cell size is to define the pathways that are required for cell size control. In budding yeast, cell size control at START is thought to work through regulation of Cln3 (Tyers et al., 1993). Cell size at entry into the cell cycle is dependent on Cln3 dosage (Cross, 1988; Nash et al., 1988). Thus, cells that overexpress *CLN3* divide at

a smaller size, whereas *cln3*Δ cells spend longer in G1 and are overall larger (Cross, 1988; Nash et al., 1988).

Several models explain how Cln3 might be controlling cell size. The "Cln3 abundance model" suggests that cells monitor abundance of Cln3 (Jorgensen and Tyers, 2004). In this model, Cln3 levels will eventually reach a threshold amount and cells will enter the cell cycle. This observation was puzzling because it was thought that Cln3 levels didn't oscillate significantly throughout the cell cycle (McInery and Breeden, 1997; Tyers et al., 1993). However, recent studies from our lab show that Cln3 levels dramatically change during the cell cycle, peaking at G1 and mitosis (see Chapter II). The "Cln3 abundance model" implies the existence of a fixed parameter against which Cln3 levels are measured. For example, it has been proposed that a fixed amount of Cln3 inhibitor could inhibit Cln3 until levels of Cln3 surpass levels of inhibitor (Alberts et al., 2002). At this point, late G1-cyclin transcription is triggered and cells enter the cell cycle. However, there is no evidence that such an inhibitor exists.

Jorgensen and Tyers proposed a model in which cells measure protein synthesis to assess their size (Jorgensen et al., 2002). This model states that the rate of protein synthesis in response to nutrients or growth factors relays a signal to a "translational sizer". This translational sizer should be constitutively expressed during growth, unstable, and rate-limiting for cell cycle transitions. For instance, in fission yeast, the sizer is proposed to be phosphatase Cdc25 (Rupes, 2002). Cdc25 is a dosage dependent activator of mitotic entry and regulates size control at the G2/M transition (Rupes et al., 2001; Russell and Nurse, 1986). As cells grow during G2, the concentration of Cdc25 also increases (Kovelman and Russell, 1996). In budding

yeast, the sizer is thought to be Cln3 (Turner et al., 2012). The "Cln3 synthesis rate model" suggests that Cln3 is synthesized at a rate proportional to overall protein synthesis (Polymenis and Schmidt, 1997). Evidence supporting this model shows that cells that have reached a critical size cannot pass START until a critical translation rate is met (Unger and Hartwell, 1976). Additionally, treatment with cycloheximide increases the critical cell size threshold and prolongs G1 (Jorgensen et al., 2004; Moore, 1988). As with the "Cln3 abundance model", this model suggests that Cln3 must be normalized to a parameter that remains constant during growth. An interesting hypothesis suggests that Cln3 activity is measured against the fixed number of SBF binding sites (SCBs) (Wang et al., 2009). Evidence supporting this model shows that transformation of yeast with a high-copy plasmid containing several SCBs increases cell size at budding in a Cln3-depedent manner (Wang et al., 2009).

An additional model suggests cell size control is a consequence of differential regulation of Cln3 between mother and daughter cells (Di Talia et al., 2009). Transcription factors Ace2 and Ash1 are daughter-specific and cause a G1-delay by repressing *CLN3* transcription until a critical size is met (Di Talia et al., 2009). Mutations in Ash1 and Ace2 binding sites on the *CLN3* promoter abolish cell size control in daughter cells, causing similar G1 duration in both mother and daughter cells (Di Talia et al., 2009).

An important caveat of all of these models is that cells lacking Cln3 still undergo size-dependent entry into the cell cycle, arguing that Cln3 cannot be solely responsible for cell size control. Furthermore, the models do not explain how a cell size threshold is set. Skotheim and colleagues have proposed a model in which a

Cln1/2-dependent positive feedback loop during G1 converts a gradual size-dependent signal into a switch-like response, triggering entry into the cell cycle (Turner et al., 2012). However, the nature of the size-dependent signal is unknown.

NUTRIENT MODULATION OF CELL SIZE

The cell cycle must adjust to environmental conditions. Budding yeast cells shifted from rich to poor media readjust their size and become overall smaller (Johnston et al., 1979; Tyson et al., 1979) (Figure 4). Conversely, when shifted from poor to rich media, they spend more time in G1 to allow for growth to adjust to a larger critical size. Similarly, fission yeast cells shifted from rich to poor media immediately undergo division, skipping the growth phases to adapt to the lower critical size (Fantes and Nurse, 1977).

Initially, nutrient availability was thought to signal to Cln3 to set a critical size threshold. For instance, low levels of Cln3 in cells shifted to poor nutrients explain the prolonged G1 delay; however, despite having a longer G1, these cells divide at a smaller size and pass START even with very low levels of Cln3 (Polymenis and Schmidt, 1997). Most importantly, *cln3*Δ and *whi5*Δ cells undergo normal nutrient modulation of cell size (Jorgensen et al., 2004; Nash et al., 1988). These observations suggest that size resetting occurs downstream of Cln3 and Whi5.

In an effort to find proteins involved in cell size control in response to nutrients, Tyers and colleagues performed a genome wide analysis of proteins required for nutrient modulation of cell size (Jorgensen et al., 2004). They identified three proteins: protein kinase A (PKA), Sch9 and Sfp1. Loss of function of any of these proteins results in smaller cells incapable of modulating their size in response

to nutrient downshifts (Jorgensen et al., 2004). All three proteins positively regulate ribosomal protein and ribosome biogenesis genes in response to nutrients (Jorgensen et al., 2004). These observations are consistent with the ribosome biogenesis model, which states that nutrients repress G1 cyclin transcription to allow cells to grow and reach a critical size (Jorgensen et al., 2004). A different study from our lab found that the regulatory subunit of protein phosphatase 2A, Rts1, is also required for nutrient-modulation of cell size (Artiles et al., 2009). Loss of Rts1 results in large cells unable to reset their size (Figure 5A).

In multicellular organisms, cells are usually in excess nutrients and need additional mechanisms to regulate their growth and division (Conlon and Raff, 1999). These cells require a signal that instructs them to grow or divide; these signals are known as growth factors and mitogens (Conlon et al., 2001). Nevertheless, nutrient availability is also known to have dramatic effects during development of multicellular organisms. For example, nutrient deprivation during development can decrease a fly's size by 15% (Edgar, 2006).

RTS1 CONTROLS CELL SIZE BY REGULATION OF G1 CYCLINS

PP2A is a highly conserved phosphatase involved in many cellular processes, including cell growth and cell cycle progression (Artiles et al., 2009; Chan and Amon, 2009). It is a trimeric complex composed of a catalytic subunit, a scaffolding subunit and a regulatory subunit. In budding yeast there are two regulatory subunits called Rts1 and Cdc55, which bind PP2A in a mutually exclusive manner to confer specificity to different substrates (Janssens and Goris, 2001; Zhao et al., 1997).

A previous study showed that Rts1 is required for normal accumulation of late G1 cyclins and nutrient modulation of cell size; however, it was unclear where Rts1 was acting upstream of the late G1 cyclins and how it was controlling cell size and cell cycle entry (Artiles et al., 2009) (Figure 5A-B and Figure 6).

Here we investigate the role of $PP2A^{Rts1}$ in cell size control, nutrient sensing and entry into the cell cycle. We find that $PP2A^{Rts1}$ controls cell size by regulating Cln3 levels via Ace2 inhibition, allowing cells to enter the cell cycle once sufficient growth has occurred. We also find that Rts1 is regulated by components of the phosphoinositide-dependent kinase 1 (PDK1) pathway, a very conserved pathway known to regulate growth and cell size in vertebrate cells (Bayascas et al., 2008; Haga et al., 2009; Lawlor et al., 2002). Finally, we find that Rts1 is required for normal accumulation of G1 cyclins in poor nutrients, suggesting a link between nutrient sensing and cell cycle entry.

Defects in the mechanisms that control growth, size and division may lead to uncontrollable cell growth and abnormal cell size and shape. Defects in these mechanisms are a hallmark of diseases like cancer. Therefore, studying how cells coordinate their growth, size and division is critical to understanding and developing cures for diseases like cancer.

REFERENCES

Alberts, B., A. Johnson, J. Lewis, M. Raff, K. Roberts, and W. P. 2002. Molecular Biology of the Cell. Garland Science.

Artiles, K., S. Anastasia, D. McCusker, and D.R. Kellogg. 2009. The Rts1 regulatory subunit of protein phosphatase 2A is required for control of G1 cyclin transcription and nutrient modulation of cell size. *PLoS genetics*. 5:e1000727.

Bayascas, J.R., S. Wullschleger, K. Sakamoto, J.M. Garcia-Martinez, C. Clacher, D. Komander, D.M. van Aalten, K.M. Boini, F. Lang, C. Lipina, L. Logie, C. Sutherland, J.A. Chudek, J.A. van Diepen, P.J. Voshol, J.M. Lucocq, and D.R. Alessi. 2008. Mutation of the PDK1 PH domain inhibits protein kinase B/Akt, leading to small size and insulin resistance. *Mol Cell Biol*. 28:3258-3272.

Chan, L.Y., and A. Amon. 2009. The protein phosphatase 2A functions in the spindle position checkpoint by regulating the checkpoint kinase Kin4. *Genes Dev*. 23:1639-1649.

Conlon, I., and M. Raff. 1999. Size control in animal development. *Cell*. 96:235-244.

Conlon, I.J., G.A. Dunn, A.W. Mudge, and M.C. Raff. 2001. Extracellular control of cell size. *Nat Cell Biol*. 3:918-921.

Costanzo, M., O. Schub, and B. Andrews. 2003. G1 transcription factors are differentially regulated in Saccharomyces cerevisiae by the Swi6-binding protein Stb1. *Mol Cell Biol*. 23:5064-5077.

Cross, F.R. 1988. DAFI, a mutant gene affecting size control, pheromone arrest, and cell cycle kinetics of Saccharomyces cerevisiae. *Mol. Cell. Biol.* 8:4675-4684.

Cross, F.R., and A.H. Tinkelenberg. 1991. A potential positive feedback loop controlling CLN1 and CLN2 gene expression at the start of the yeast cell cycle. *Cell*. 65:875-883.

de Bruin, R.A., W.H. McDonald, T.I. Kalashnikova, J. Yates, 3rd, and C. Wittenberg. 2004. Cln3 activates G1-specific transcription via phosphorylation of the SBF bound repressor Whi5. *Cell*. 117:887-898.

Di Talia, S., H. Wang, J.M. Skotheim, A.P. Rosebrock, B. Futcher, and F.R. Cross. 2009. Daughter-specific transcription factors regulate cell size control in budding yeast. *PLoS biology*. 7:e1000221.

Dirick, L., and K. Nasmyth. 1991. Positive feedback in the activation of G1 cyclins in yeast. *Nature*. 351:754-757.

Dolznig, H., F. Grebien, T. Sauer, H. Beug, and E.W. Mullner. 2004. Evidence for a size-sensing mechanism in animal cells. *Nat Cell Biol*. 6:899-905.

Dunphy, W.G., and A. Kumagai. 1991. The cdc25 protein contains an intrinsic phosphatase activity. *Cell*. 67:189-196.

Edgar, B.A. 2006. How flies get their size: genetics meets physiology. *Nature reviews. Genetics*. 7:907-916.

Fantes, P., and P. Nurse. 1977. Control of cell size in fission yeast by a growth modulated size control over nuclear division. *Exp. Cell Res.* 107:377-386.

Futcher, B. 2002. Transcriptional regulatory networks and the yeast cell cycle. *Curr Opin Cell Biol*. 14:676-683.

Gould, K.L., and P. Nurse. 1989. Tyrosine phosphorylation of the fission yeast $cdc2^{+}$ protein kinase regulates entry into mitosis. *Nature*. 342:39-45.

Haga, S., M. Ozaki, H. Inoue, Y. Okamoto, W. Ogawa, K. Takeda, S. Akira, and S. Todo. 2009. The survival pathways phosphatidylinositol-3 kinase (PI3-K)/phosphoinositide-dependent protein kinase 1 (PDK1)/Akt modulate liver regeneration through hepatocyte size rather than proliferation. *Hepatology*. 49:204-214.

Hartwell, L.H., and M.W. Unger. 1977. Unequal division in *Saccharomyces cerevisiae* and its implications for the control of cell division. *J. Cell. Biol.* 75:422-435.

Harvey, S.L., and D.R. Kellogg. 2003. Conservation of mechanisms controlling entry into mitosis: budding yeast wee1 delays entry into mitosis and is required for cell size control. *Curr. Biol.* 13:264-275.

Janssens, V., and J. Goris. 2001. Protein phosphatase 2A: a highly regulated family of serine/threonine phosphatases implicated in cell growth and signalling. *Biochem J*. 353:417-439.

Johnston, G.C., C.W. Ehrhardt, A. Lorincz, and B.L. Carter. 1979. Regulation of cell size in the yeast Saccharomyces cerevisiae. *Journal of bacteriology*. 137:1-5.

Johnston, G.C., J.R. Pringle, and L.H. Hartwell. 1977. Coordination of growth with cell division in the yeast *Saccharomyces cervisiae*. *Exp. Cell. res.* 105:79-98.

Jorgensen, P., J.L. Nishikawa, B.J. Breitkreutz, and M. Tyers. 2002. Systematic identification of pathways that couple cell growth and division in yeast. *Science*. 297:395-400.

Jorgensen, P., I. Rupes, J.R. Sharom, L. Schneper, J.R. Broach, and M. Tyers. 2004. A dynamic transcriptional network communicates growth potential to ribosome synthesis and critical cell size. *Genes Dev*. 18:2491-2505.

Jorgensen, P., and M. Tyers. 2004. How cells coordinate growth and division. *Curr Biol*. 14:R1014-1027.

Killander, D., and A. Zetterberg. 1965a. A quantitative cytochemical investigation of the relationship between cell mass and initiation of DNA synthesis in mouse fibroblasts in vitro. *Experimental cell research*. 40:12-20.

Killander, D., and A. Zetterberg. 1965b. Quantitative Cytochemical Studies on Interphase Growth. I. Determination of DNA, Rna and Mass Content of Age Determined Mouse Fibroblasts in Vitro and of Intercellular Variation in Generation Time. *Experimental cell research*. 38:272-284.

Kovelman, R., and P. Russell. 1996. Stockpiling of Cdc25 during a DNA replication checkpoint in Schizosaccharomyces pombe. *Molec. Cell. Biol.* 16:86-93.

Kumagai, A., and W.G. Dunphy. 1991. The cdc25 protein controls tyrosine dephosphorylation of the cdc2 protein in a cell-free system. *Cell*. 64:903-914.

Lawlor, M.A., A. Mora, P.R. Ashby, M.R. Williams, V. Murray-Tait, L. Malone, A.R. Prescott, J.M. Lucocq, and D.R. Alessi. 2002. Essential role of PDK1 in regulating cell size and development in mice. *EMBO J*. 21:3728-3738.

McInery, C., and L. Breeden. 1997. A novel Mcm1-dependent element in the SWI4, CLN3, CDC6, and CDC47 promoters activates M/G1-specific transcription. *Genes Dev*. 7:833-843.

Mitchison, J.M., and J. Creanor. 1971. Induction synchrony in the fission yeast. Schizosaccharomyces pombe. *Experimental cell research*. 67:368-374.

Moore, S.A. 1988. Kinetic evidence for a critical rate of protein synthesis in the Saccharomyces cerevisiae yeast cell cycle. *J. Biol. Chem.* 263?:9674-9681.

Nash, R., G. Tokiwa, S. Anand, K. Erickson, and A.B. Futcher. 1988. The WHI1+ gene of Saccharomyces cerevisiae tethers cell division to cell size and is a cyclin homolog. *EMBO J.* 7:4335-4346.

Newport, J., and M. Kirschner. 1982. A major developmental transition in early Xenopus embryos: I. Characterization and timing of cellular changes at the midblastula stage. *Cell*. 30:675-686.

Nurse, P. 1975. Genetic control of cell size at cell division in yeast. *Nature*. 256:547-551.

Nurse, P., P. Thuriaux, and K. Nasmyth. 1976. Genetic control of the cell division cycle in the fission yeast *Schizosaccharomyces pombe*. *Molec. Gen. Genet.* 146:167-178.

Polymenis, M., and E.V. Schmidt. 1997. Coupling of cell division to cell growth by translational control of the G1 cyclin CLN3 in yeast. *Genes Dev*. 11:2522-2531.

Rupes, I. 2002. Checking cell size in yeast. *Trends Genet.* 18:479-485.

Rupes, I., B.A. Webb, A. Mak, and P.G. Young. 2001. G2/M arrest caused by actin disruption is a manifestation of the cell size checkpoint in fission yeast. *Mol. Biol. Cell*. 12:3892-3903.

Russell, P., and P. Nurse. 1986. cdc25+ functions as an inducer in the mitotic control of fission yeast. *Cell*. 45:145-153.

Turner, J.J., J.C. Ewald, and J.M. Skotheim. 2012. Cell size control in yeast. *Current biology : CB*. 22:R350-359.

Tyers, M., G. Tokiwa, and B. Futcher. 1993. Comparison of the Saccharomyces cerevisiae G1 cyclins: Cln3 may be an upstream activator of Cln1, Cln2 and other cyclins. *EMBO J.* 12:1955-1968.

Tyson, C.B., P.G. Lord, and A.E. Wheals. 1979. Dependency of size of Saccharomyces cerevisiae cells on growth rate. *Journal of bacteriology*. 138:92-98.

Tzur, A., R. Kafri, V.S. LeBleu, G. Lahav, and M.W. Kirschner. 2009. Cell growth and size homeostasis in proliferating animal cells. *Science*. 325:167-171.

Unger, M.W., and L.H. Hartwell. 1976. Control of cell division in Saccharomyces cerevisiae by methionyl-t-RNA. *Proc. Natl. Acad. Sci. U.S.A.* 73:1664-1668.

Wang, H., L.B. Carey, Y. Cai, H. Wijnen, and B. Futcher. 2009. Recruitment of Cln3 cyclin to promoters controls cell cycle entry via histone deacetylase and other targets. *PLoS biology*. 7:e1000189.

Zhao, Y., G. Boguslawski, R.S. Zitomer, and A.A. DePaoli-Roach. 1997. Saccharomyces cerevisiae homologs of mammalian B and B' subunits of protein phosphatase 2A direct the enzyme to distinct cellular functions. *The Journal of biological chemistry*. 272:8256-8262.

Figure 1: Entry into the cell cycle occurs when cells reach a critical cell size. Budding yeast cells divide asymmetrically, yielding a large mother cell and a small daughter cell. The large mother cell is already at the critical size and speed through G1, whereas the small daughter cell will spend a longer time growing in G1 in order to reach the critical cell size.

Figure 1

Figure 2: Entry into the cell cycle in budding yeast.

A) Before cells reach a critical size, transcription of late G1 cyclins, Cln1 and Cln2, is kept inactive by transcriptional repressor Whi5. Whi5 binds to transcription factor SBF (composed of Swi4 and Swi6) and inhibits its function. B) Once cells reach a critical cell size, the Cdk1/Cln3 complex phosphorylates Whi5 causing it to dissociate from SBF. Activation of SBF leads to transcription of late G1 cyclins Cln1 and Cln2 and therefore, entry into S phase.

Figure 2

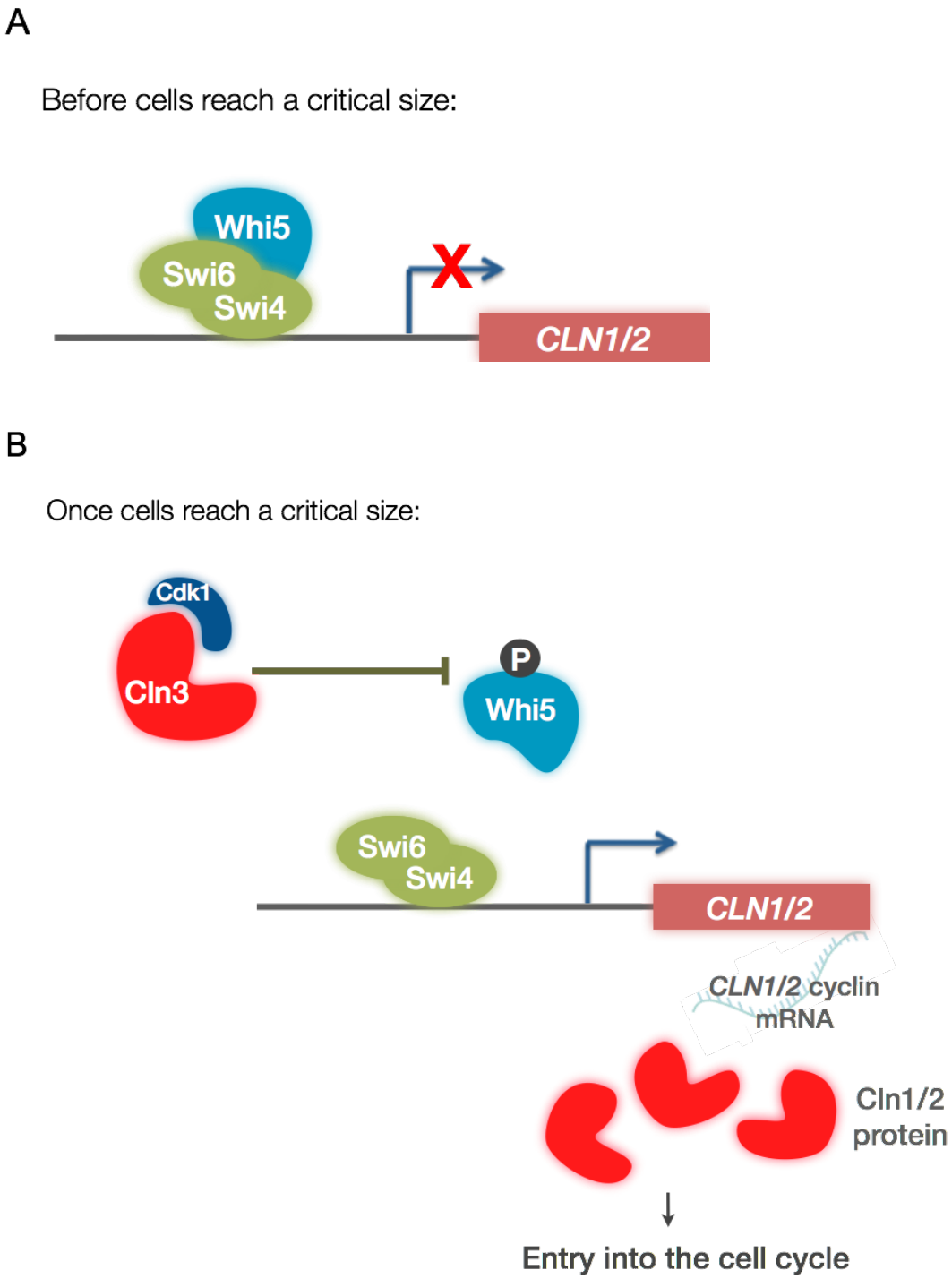
A
Before cells reach a critical size:
Whi5
Swi6
Swi4
X
CLN1/2
B
Once cells reach a critical size:
Cdk1
Cln3
P
Whi5
Swi6
Swi4
CLN1/2
CLN1/2 cyclin mRNA
Cln1/2 protein
Entry into the cell cycle

Figure 3: Entry into mitosis in budding yeast.

A) Inhibitory phosphorylation of mitotic Cdk1 by Wee1 keeps cells from entering mitosis prematurely. B) Once cells are ready to enter mitosis, phosphatase Cdc25 dephosphorylates mitotic Cdk1,. Activation of mitotic Cdk1 drives entry into mitosis.

Figure 3

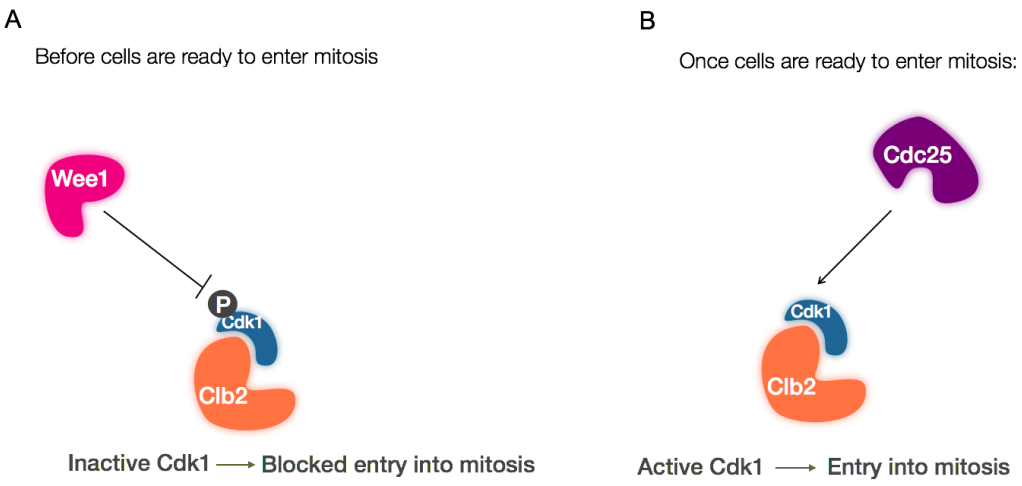
A
Before cells are ready to enter mitosis
Wee1
P
Cdk1
Clb2
Inactive Cdk1 → Blocked entry into mitosis
B
Once cells are ready to enter mitosis:
Cdc25
Cdk1
Clb2
Active Cdk1 → Entry into mitosis

Figure 4: Nutrient modulation of cell size.

Cell size distribution graph of cells grown to log phase in either rich media (Dextrose) or poor media (Glycerol/Ethanol). In rich media the average cell size is 30 fL, whereas in poor media, size is reduced by approximately 50%. This result clearly shows a link between cell size control and nutrient availability.

Figure 4

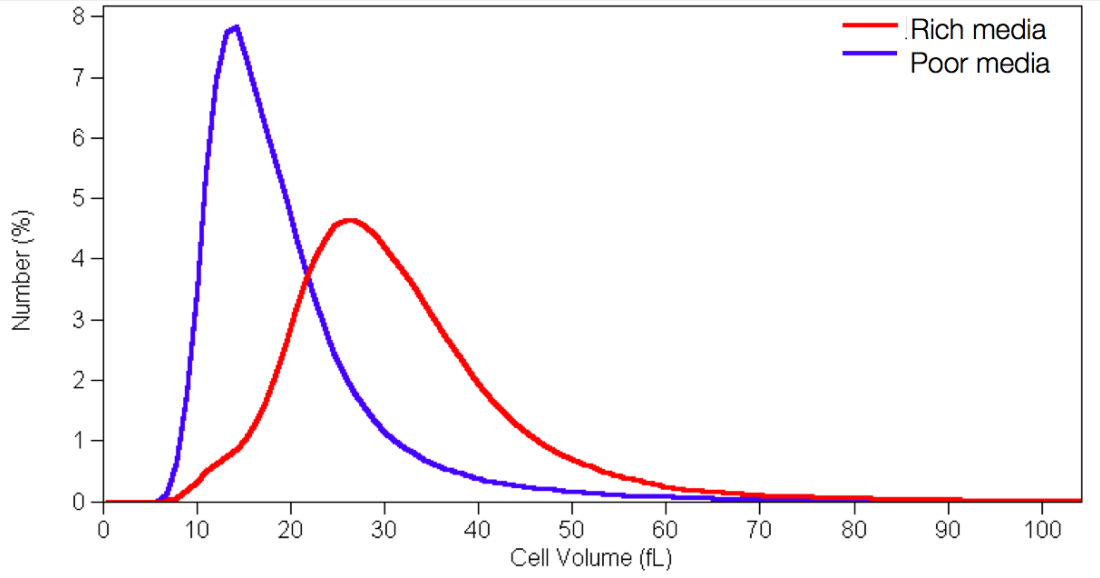
Rich media
Poor media
Number (%)
Cell Volume (fL)
0
1
2
3
4
5
6
7
8
0
10
20
30
40
50
60
70
80
90
100

Figure 5: Loss of Rts1 abolishes nutrient modulation of cell size and causes a delay in G1.

A) Cell size distribution graph of wild type and *rts1*Δ cells grown to log phase in either rich media (Dextrose) or poor media (Glycerol/Ethanol). In rich media, wild type cell undergo normal nutrient modulation of cell size. *rts1*Δ cells are unable to regulate their cell size in response to nutrient availability and remain large. B) Western blots showing G1 cyclin, Cln2, accumulation in wild type and *rts1*Δ cells coming out of a G1 or metaphase arrest. Loss of Rts1 causes a delay in Cln2 accumulation in comparison to wild type.

Figure 5

A

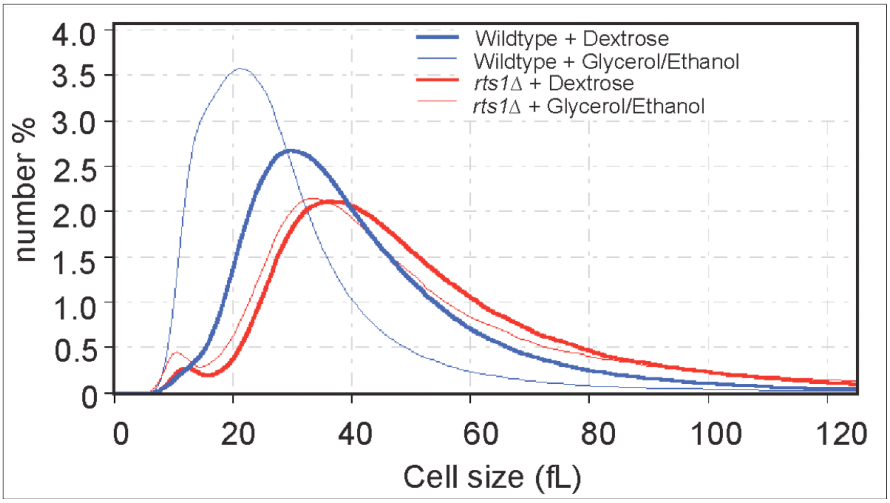
Wildtype + Dextrose
Wildtype + Glycerol/Ethanol
rts1Δ + Dextrose
rts1Δ + Glycerol/Ethanol
number %
4.0
3.5
3.0
2.5
2.0
1.5
1.0
0.5
0
0
20
40
60
80
100
120
Cell size (fL)

B

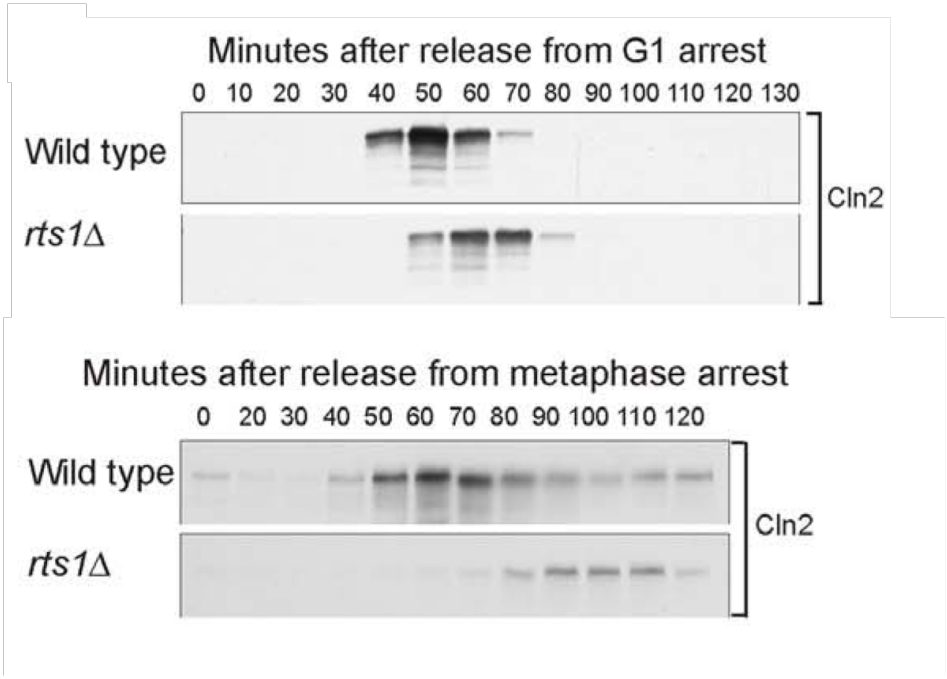
Minutes after release from G1 arrest
0 10 20 30 40 50 60 70 80 90 100 110 120 130
Wild type
rts1Δ
Cln2
Minutes after release from metaphase arrest
0 20 30 40 50 60 70 80 90 100 110 120
Wild type
rts1Δ
Cln2

Figure 6: Where does $PP2A^{Rts1}$ act upstream of the G1 cyclins and how does it control cell size and entry into the cell cycle?

A schematic representation of the major question we aim to answer in this dissertation.

Figure 6

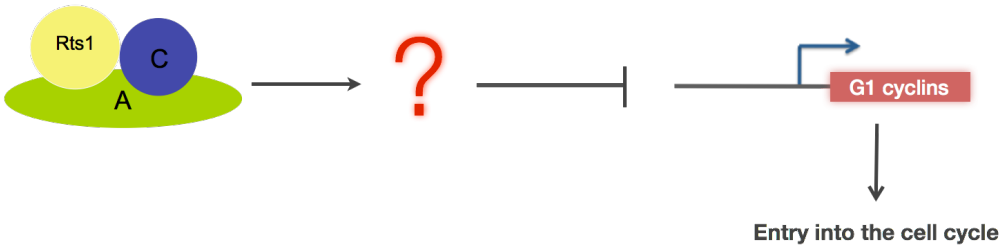

CHAPTER II

PP2A^{RTS1} IS A MASTER REGULATOR OF PATHWAYS THAT CONTROL CELL SIZE

ABSTRACT

Cell size checkpoints ensure that passage through G1 and mitosis occurs only when sufficient growth has occurred. The mechanisms by which these checkpoints work are largely unknown. PP2A associated with the Rts1 regulatory subunit (PP2A^{Rts1}) is required for cell size control in budding yeast, but the relevant targets are unknown. Here, we used quantitative proteome-wide mass spectrometry to identify proteins controlled by PP2A^{Rts1}. This revealed that PP2A^{Rts1} controls the two key checkpoint pathways thought to regulate the cell cycle in response to cell growth. To investigate the role of PP2A^{Rts1} in these pathways, we focused on the Ace2 transcription factor, which is thought to delay cell cycle entry by repressing transcription of the G1 cyclin *CLN3*. Diverse experiments suggest that PP2A^{Rts1} promotes cell cycle entry by inhibiting the repressor functions of Ace2. We hypothesize that control of Ace2 by PP2A^{Rts1} plays a role in mechanisms that link G1 cyclin accumulation to cell growth.

INTRODUCTION

Cell size must be tightly controlled to ensure function and survival (Jorgensen and Tyers, 2004; Turner et al., 2012). Control of cell size in dividing cells is achieved via cell size checkpoints, which delay key cell cycle transitions until sufficient growth has occurred. Despite their name, it is uncertain whether cell size checkpoints monitor a parameter linked to cell size, such as volume or surface area, or whether they monitor parameters linked to growth or biosynthetic capacity. Discovery of checkpoint signals that link the cell cycle to cell growth is thus an essential step towards understanding how cell size is controlled.

Cell size checkpoints operate at entry into the cell cycle in G1 and again at mitosis. The mitotic checkpoint works through the Wee1 kinase, which delays mitosis via inhibitory phosphorylation of Cdk1 (Gould and Nurse, 1989; Nurse, 1975). Wee1 is a dose-dependent regulator of cell size. Thus, loss of Wee1 in fission yeast causes premature entry into mitosis at a reduced cell size, while increased activity of Wee1 causes delayed entry into mitosis and increased cell size (Nurse, 1975; Russell and Nurse, 1987). The signals that connect Cdk1 inhibitory phosphorylation to cell growth are poorly understood.

The G1 cell size checkpoint is best understood in budding yeast. Cell division in budding yeast is asymmetric, yielding a large mother cell and a small daughter cell. The observation that the small daughter cell spends more time undergoing growth in G1 provided early evidence for the existence of cell size checkpoints (Hartwell and Unger, 1977; Johnston et al., 1977). It also focused attention on the mechanisms that control cell cycle entry, and how they might be linked to cell size. The key molecular event that drives cell cycle entry is activation of

Cdk1 by G1 cyclins (Cross, 1990; Richardson et al., 1989). There are three G1 cyclins that bind and activate Cdk1 in budding yeast, called Cln1, Cln2 and Cln3 (Hadwiger et al., 1989; Richardson et al., 1989). Transcription of *CLN3* is initiated in early G1, and the Cln3/Cdk1 complex helps trigger transcription of the late G1 cyclins *CLN1* and *CLN2* (Dirick and Nasmyth, 1991). Cln1/2 drive growth of a new daughter cell, which marks commitment to a new round of cell division (Cross, 1990; McCusker et al., 2007; Richardson et al., 1989).

Early evidence pointed to Cln3 as playing a critical role in cell size control. Loss of *CLN3* causes a prolonged delay in entry into the cell cycle. Cell growth continues during the delay, leading to increased cell size (Cross, 1988). Conversely, overexpression of *CLN3* causes premature entry into the cell cycle at a reduced cell size (Cross, 1988; Nash et al., 1988). Together, these observations suggested that Cln3, like Wee1, is a critical dose-dependent regulator of cell size (Cross, 1988; Nash et al., 1988). In this view, cell size in G1 phase could be controlled by mechanisms that link production of active Cln3/Cdk1 to attainment of a critical cell size. A number of observations, however, indicate this kind of model is too simplistic. First, *cln3*Δ cells still show size-dependent entry into the cell cycle (Di Talia et al., 2009; Ferrezuelo et al., 2012). Thus, although *cln3*Δ cells are significantly larger than wild type cells, small unbudded *cln3*Δ cells spend more time undergoing growth in G1 than larger unbudded cells. In addition, *cln3*Δ cells undergo normal nutrient modulation of cell size, in which cells reduce their size in response to poor nutrients (Jorgensen et al., 2004). Together, these observations indicate that modulation of Cln3 alone is insufficient to explain cell size control in G1.

Although Wee1 and G1 cyclins clearly play roles in cell size control, it is unlikely that they are involved in the mechanisms that determine size. Both are capable of accelerating or delaying the cell cycle in a dose-dependent manner, which suggests that they respond to checkpoint signals that determine the duration of growth at specific phases of the cell cycle. Thus, they appear to be downstream effectors of a global mechanism of cell size control. The nature of this global mechanism has remained deeply mysterious.

We recently discovered that a specific form of protein phosphatase 2A (PP2A) is required for cell size control (Artiles et al., 2009). Canonical PP2A is a trimeric complex composed of a catalytic subunit, a scaffolding subunit, and a regulatory subunit (Janssens and Goris, 2001; Zhao et al., 1997). In budding yeast, there are two regulatory subunits, referred to as Rts1 and Cdc55, that form two distinct complexes: $PP2A^{Rts1}$ and $PP2A^{Cdc55}$ (Zhao et al., 1997). We previously discovered that *rts1*Δ causes increased cell size and a failure to undergo nutrient modulation of cell size (Artiles et al., 2009). In addition, *rts1*Δ causes a prolonged delay in transcription of the G1 cyclin Cln2, a prolonged delay in mitosis, and defects in regulatory phosphorylation of Wee1 (Artiles et al., 2009; Harvey et al., 2011). Together, these observations suggest that $PP2A^{Rts1}$ functions in both G1 and mitotic cell size checkpoints. However, the targets of $PP2A^{Rts1}$ that mediate these functions were unknown. Here, we used proteome-wide mass spectrometry to identify targets of $PP2A^{Rts1}$. This revealed that $PP2A^{Rts1}$ controls key elements of both cell size checkpoints, which suggests that it functions in the mysterious cell size control mechanisms that send signals to G1 cyclins and Wee1. We further discovered that

$PP2A^{Rts1}$ controls the transcription factor Ace2, which likely contributes to mechanisms that link *CLN3* transcription to cell growth.

RESULTS

A proteomic screen for targets of PP2A^{Rts1}

To identify targets of PP2A^{Rts1}, we used quantitative phosphoproteomics to search for proteins that become hyperphosphorylated in *rts1*Δ cells. Since we previously found that PP2A^{Rts1} is required for control of G1 cyclin transcription, we were particularly interested in G1 targets of PP2A^{Rts1} (Artiles et al., 2009). We therefore synchronized wild type and *rts1*Δ cells and collected samples for mass spectrometry 10 minutes before the G1 cyclin Cln2 appeared, which is when the decision to initiate G1 cyclin transcription is made. Proteolytic peptides from each strain were covalently modified by reductive dimethylation to generate light (wild type) and heavy (*rts1*Δ) stable isotope labeled pools. After combining, phosphopeptides were enriched by strong cation exchange followed by TiO2 affinity chromatography and identified via LC-MS/MS (Figure 1A) (Kettenbach and Gerber, 2011; Villen and Gygi, 2008).

The heavy to light ratios of phosphorylated peptides in *rts1*Δ cells versus wild type cells were $\log_2$ transformed. Thus, positive values indicate increased phosphorylation in *rts1*Δ, while negative values indicate decreased phosphorylation. A parallel analysis of sample matched unphosphorylated peptides was used to generate protein abundance ratios that were used to correct for differences in protein abundance between the two samples (Table S1). Three biological replicates of the experiment were carried out, which allowed calculation of average $\log_2$ ratios and standard deviations for most peptides. The complete data set appears in Tables S1, S2 and S3. Table S1 lists all protein quantification data, Table S2 lists all identified

phosphorylation sites along with quantitative data, and Table S3 provides detailed information for each of the 78,204 phosphopeptides that were detected.

A total of 10807 sites were identified on 2066 proteins. Of these, 9255 sites on 1937 proteins could be quantified. We focused on sites that were quantified in at least two of three biological replicates. This high-quality set includes 5159 sites on 1544 proteins (Figure 1B). Note that the analysis is not comprehensive; many peptides are not detected due to poor ionization, loss during chromatography, or low abundance.

Relative peptide abundances were calculated as the ratio of corresponding heavy and light peptide pairs as determined from their extracted ion chromatograms. A visual representation of this is shown for a single phosphopeptide in Figure S1. For each phosphorylation site, we calculated an average ratio from all quantified peptides harboring each site. We used a two-fold standard deviation from the mean, representing a ~2.5-fold change in either direction, to define significant changes in phosphorylation (Figure 1C). At this threshold, we identified 241 sites on 156 proteins that were hyperphosphorylated in *rts1*Δ cells (Table S4). We observed fewer sites whose phosphorylation decreased: 59 sites on 45 proteins (Table S5).

PP2A^{Rts1} is required for normal regulation of key effectors of cell size control

Table S4 lists proteins that underwent significant hyperphosphorylation in *rts1*Δ cells. It is likely that additional regulated sites whose ratios fell below our cutoff exist in the data. Several of the regulated proteins are linked to known roles of PP2A^{Rts1}. For example, PP2A^{Rts1} controls Kin4 in the spindle orientation checkpoint (Chan and Amon, 2009). A site in Kin4, serine 351, was upregulated nearly 3-fold in

*rts1*Δ cells. $PP2A^{Rts1}$ also controls chromosome cohesion (Yu and Koshland, 2007). Here, we identified two proteins involved in chromosome cohesion as new targets of $PP2A^{Rts1}$-dependent regulation: Pds1 and Ulp2.

We focused on targets of $PP2A^{Rts1}$ that could provide clues to its role in cell size control. The analysis identified multiple proteins involved in cell size control in G1, including three factors that control G1 cyclin transcription: Swi4, Swi5, and Ace2. Swi4 is a transcriptional activator of the late G1 cyclins *CLN1* and *CLN2* (Nasmyth and Dirick, 1991; Ogas et al., 1991). Swi5 and Ace2 are related factors that control transcription of genes expressed in late mitosis/early G1 (Dohrmann et al., 1992; Doolin et al., 2001). Ace2 is a repressor of *CLN3* transcription, while Swi5 controls transcription of the G1 cyclin Pcl2, which activates Pho85 and acts redundantly with Cln1/2 to promote bud emergence (Aerne et al., 1998; Di Talia et al., 2009; Laabs et al., 2003; Moffat and Andrews, 2004). Bck2, an upstream regulator of *CLN1/2* transcription, was hyperphosphorylated in one of the biological replicates (Table S2)(Bastajian et al., 2013; Di Como et al., 1995). Thus, $PP2A^{Rts1}$ appears to control transcription of all of the key G1 cyclins. The analysis also identified Ydj1, which is thought to control Cln3 localization and stability (Verges et al., 2007; Yaglom et al., 1996). Loss of Ace2, Swi4, or Ydj1 causes defects in cell size control (Breeden and Mikesell, 1991; Caplan and Douglas, 1991; Di Talia et al., 2009; Dohrmann et al., 1992; Ferrezuelo et al., 2012).

The analysis also identified proteins involved in cell size control during mitosis. For example, the inhibitory site on Cdk1 that is phosphorylated by Wee1 showed one of the most dramatic increases, being upregulated >25-fold in *rts1*Δ cells. Moreover, Swe1, the budding yeast homolog of Wee1, was

hyperphosphorylated on multiple sites that were previously found to be required for its activation (Harvey et al., 2005; Harvey et al., 2011). This is consistent with our previous finding that *rts1*Δ causes Swe1 to accumulate in a hyperphosphorylated active form, which is the likely cause of a prolonged mitotic delay (Harvey et al., 2011). We also identified three related kinases that are required for Swe1 inactivation: Hsl1, Gin4 and Kcc4 (Barral et al., 1999; Longtine et al., 2000; Ma et al., 1996; McMillan et al., 1999). Loss of these kinases can cause delayed entry into mitosis and severe cell size defects (Altman and Kellogg, 1997; Barral et al., 1999). Loss of these kinases also causes Swe1 to accumulate in a hyperphosphorylated active form, similar to *rts1*Δ (Okuzaki et al., 2003; Shulewitz et al., 1999). Together, these observations suggest that $PP2A^{Rts1}$ controls Swe1 via Hsl1, Gin4 and Kcc4. The fission yeast homologs of Hsl1, Gin4 and Kcc4 are required for nutrient modulation of cell size (Belenguer et al., 1997; Young and Fantes, 1987).

The mass spectrometry data show that $PP2A^{Rts1}$ controls both of the known targets of cell size control: G1 cyclin expression and inhibitory phosphorylation of Cdk1. Thus, $PP2A^{Rts1}$ may be a component of global cell size control mechanisms. Here, we focused on the Ace2 transcription factor. Table I shows data for all identified Ace2 phosphorylation sites, which includes four significantly regulated sites: S122, S253, S709, and T713. Ace2 is asymmetrically segregated into the nuclei of small daughter cells, where it is thought to delay cell cycle entry via inhibition of *CLN3* transcription (Di Talia et al., 2009; Laabs et al., 2003). (Di Talia et al., 2009). However, regulation of Ace2 has not been linked to signals that relay information about cell growth or size. Ace2 also functions as a transcriptional activator for genes involved in septation (Dohrmann et al., 1992).

Loss of PP2A^{Rts1} causes defects in phosphorylation of the Ace2 transcription factor

To extend the mass spectrometry data, we assayed Ace2 phosphorylation in synchronized wild type and *rts1*Δ cells. Phosphorylation of Ace2 causes an electrophoretic mobility shift that can be assayed by western blotting (Mazanka and Weiss, 2010; Sbia et al., 2008). We first assayed Ace2 after release from a G1 arrest imposed by mating pheromone. The mitotic cyclin Clb2 was assayed in the same samples as a marker for cell cycle progression. In wild type cells, Ace2 was present at low levels early in the cell cycle and began to accumulate and undergo extensive hyperphosphorylation as cells entered mitosis, consistent with previous reports that Ace2 is phosphorylated by mitotic Cdk1 (Figure 2A) (Mazanka and Weiss, 2010; O'Conallain et al., 1999; Sbia et al., 2008). In *rts1*Δ cells, the mitotic hyperphosphorylation of Ace2 was delayed by approximately 20 minutes, consistent with a previously reported G1 delay in *rts1*Δ cells (Artiles et al., 2009). To compare differences in Ace2 phosphorylation during G1, we loaded the initial time points from Figure 2A in an intercalated manner (Figure 2B). This revealed that a fraction of Ace2 was hyperphosphorylated in *rts1*Δ cells during G1.

We also assayed Ace2 phosphorylation and Clb2 levels after release from a metaphase arrest. Ace2 was phosphorylated in metaphase-arrested wild type cells and was dephosphorylated as cells exited mitosis (Figure 2C). Ace2 underwent a transient phosphorylation at 30 minutes and became phosphorylated again at 50 minutes as cells entered the next mitosis. Ace2 was dramatically hyperphosphorylated in *rts1*Δ cells relative to wild type cells (Figure 2C). In addition,

Ace2 dephosphorylation and destruction of Clb2 were delayed by approximately 20 minutes in *rts1*Δ cells, which indicated that $PP2A^{Rts1}$ is required for normal mitotic exit.

Since we did not observe a drop in Ace2 levels as cells traversed G1 after release from a metaphase arrest (Figure 2C), it is likely that low levels of Ace2 after release from a G1 arrest (Figure 2A) is caused by the prolonged arrest, rather than by a mechanism that degrades Ace2 during G1 in every cell cycle.

Cbk1 contributes to hyperphosphorylation of Ace2 in *rts1*Δ cells

We next searched for the kinase that hyperphosphorylates Ace2 in *rts1*Δ cells. Cdk1 is thought to phosphorylate Ace2 during mitosis to block its nuclear import (Mazanka and Weiss, 2010; O'Conallain et al., 1999; Sbia et al., 2008). If Cdk1 and $PP2A^{Rts1}$ acted on the same sites, one would predict that dephosphorylation of Ace2 would fail to occur or would occur more slowly when Cdk1 was inactivated in *rts1*Δ cells. To test this, we utilized an analog-sensitive allele of *CDK1* (*cdk1-as1*) that can be rapidly and specifically inhibited by addition of 1NM-PP1 (Bishop et al., 2000). Ace2 phosphorylation was assayed after addition of 1NM-PP1 to rapidly growing wild type, *cdk1-as1*, *rts1*Δ, and *cdk1-as1 rts1*Δ cells. Inhibition of Cdk1 caused rapid dephosphorylation of Ace2 in both *cdk1-as1* and *cdk1-as1 rts1*Δ cells (Figure 3A). This suggests that Cdk1 and $PP2A^{Rts1}$ do not act on the same sites, but does not rule out a more complex model in which $PP2A^{Rts1}$ acts redundantly with another phosphatase on Cdk1 target sites. None of the 4 high confidence hyperphosphorylated sites on Ace2 correspond to the optimal mitotic Cdk1 consensus site (S/TPXXR/K), although 3 of the 4 correspond to the minimal Cdk1 consensus site (S/TP).

Ace2 is also phosphorylated by Cbk1, a member of the nuclear Dbf2 related (NDR)/Lats kinase family that plays roles in bud growth and mitotic exit (Mazanka et al., 2008). During late mitosis, Cbk1 is asymmetrically localized to the daughter nucleus, where it phosphorylates Ace2 on several sites that inhibit nuclear export (Colman-Lerner et al., 2001; Mazanka et al., 2008; Weiss et al., 2002). Cbk1 could therefore inhibit nuclear export of Ace2 to delay *CLN3* transcription in newborn daughter cells. One of the high confidence Ace2 sites corresponds to a Cbk1 consensus site (S122) that is phosphorylated in vitro and in vivo in a Cbk1-dependent manner (Mazanka et al., 2008). Western blotting with a phospho-specific antibody (Mazanka and Weiss, 2010) demonstrated that this site is hyperphosphorylated in *rts1*Δ cells (Figure 3B). Thus, Cbk1 is likely responsible for hyperphosphorylating at least one site on Ace2 in *rts1*Δ cells. However, most of the sites that were hyperphosphorylated in *rts1*Δ cells do not correspond to Cbk1 consensus sites, which suggests that multiple kinases may be involved.

To further test the roles of Cdk1 and Cbk1, we reconstituted phosphorylation of Ace2 in vitro. Cdk1 caused a shift in the electrophoretic mobility of Ace2 that was similar to the Cdk1-dependent shift observed in vivo (Figures 3A and 3C). Cbk1 also shifted the electrophoretic mobility of Ace2, but the extent of the shift appeared to be less than the shift caused by *rts1*Δ in vivo (Figure 3C). We considered the possibility that efficient phosphorylation of Ace2 by Cbk1 requires priming by Cdk1; however, Cdk1 did not appear to enhance Cbk1 phosphorylation of Ace2 in vitro (Figure 3C).

Since there was the possibility that the reconstituted reactions lacked key factors necessary for efficient phosphorylation of Ace2 by Cbk1, we also tested the role of Cbk1 in vivo. We attempted to use an analog-sensitive allele of Cbk1 to test

whether hyperphosphorylation of Ace2 after release from a mitotic arrest depended on Cbk1 activity. However, for unknown reasons *rts1*Δ *cbk1-as* cells expressed very low levels of Ace2 when arrested in mitosis, so we were unable to obtain a clear result. Instead, we assayed hyperphosphorylation of Ace2 in log phase wild type, *rts1*Δ, *cbk1*Δ and *rts1*Δ *cbk1*Δ cells. The majority of Ace2 phosphorylation that can be detected in log phase cells is due to mitotic Cdk1; however, a hyperphosphorylated form of Ace2 could be faintly detected in both *rts1*Δ and *rts1*Δ *cbk1*Δ cells (arrow, Figure 3D). This observation provides further evidence that Cbk1 is not solely responsible for hyperphosphorylation of Ace2 in *rts1*Δ cells.

PP2A^{Rts1} is likely a negative regulator of Ace2

Since *rts1*Δ causes a prolonged G1 delay, we hypothesized that PP2A^{Rts1} inhibits repressor functions of Ace2. In this model, inactivation of PP2A^{Rts1} causes Ace2 to become hyperphosphorylated, which makes it hyperactive as a repressor of *CLN3* transcription. We first used genetics to test this model. If PP2A^{Rts1} is an inhibitor of Ace2, then *ace2*Δ could rescue temperature-dependent growth defects caused by *rts1*Δ. To test this, we assayed rate of colony formation in wild type, *rts1*Δ, *ace2*Δ and *rts1*Δ *ace2*Δ cells at 30°C and 37°C. We found that *ace2*Δ partially rescued the temperature-dependent growth defect caused by *rts1*Δ (Figure 4A). Because *ace2*Δ causes a cell separation defect, colonies could appear larger because they start from a clump of cells rather than a single cell. We therefore used a Bioscreen apparatus to measure rates of growth of each strain. This confirmed that *ace2*Δ partially rescued the slow growth phenotype of *rts1*Δ cells at both 30°C and 34°C (Figure 4B)

We also discovered that overexpression of Ace2 from the *GAL1* promoter was lethal in *rts1*Δ cells, consistent with the idea that $PP2A^{Rts1}$ inhibits transcriptional repressor functions of Ace2 (Figure 4C). The lethality of *ACE2* overexpression in *rts1*Δ suggests that hyperactive Ace2 must have targets in addition to *CLN3* because deletion of *CLN3* alone is not lethal.

Overexpression of *CLN3* partially rescues cell size defects caused by *rts1*Δ

Loss of *RTS1* or *CLN3* causes cells to become abnormally large (Artiles et al., 2009; Cross, 1988). We hypothesized that hyperactive Ace2 in *rts1*Δ cells causes failure to produce normal levels of Cln3, leading to increased cell size. To test this, we overexpressed *CLN3* from the *GAL1* promoter in *rts1*Δ cells. This reduced the size of *rts1*Δ cells to nearly the same size as wild type cells, consistent with the hypothesis (Figure 5). Previous studies found that *CLN3* overexpression causes cells to become significantly smaller than wild type cells (Tyers et al., 1992) (Figure 5). Thus, *GAL1-CLN3* does not cause the same size reduction in wild type and *rts1*Δ cells, which indicates that cell size defects caused by *rts1*Δ are not due solely to a failure to produce normal levels of Cln3. This is consistent with the discovery that $PP2A^{Rts1}$ controls diverse pathways required for cell size control.

$PP2A^{Rts1}$ is required for normal control of Cln3 protein and mRNA levels

To further test the hypothesis that $PP2A^{Rts1}$ controls production of Cln3 via Ace2, we assayed *CLN3* mRNA accumulation in wild type, *rts1*Δ, *ace2*Δ, and *rts1*Δ *ace2*Δ cells after release from a G1 arrest. *CLN3* mRNA levels were assayed both by qRT-PCR and by northern blotting, which gave similar results. Accumulation of

Cln3-6XHA protein was assayed in identical time courses, and the mitotic cyclin Clb2 was assayed in the same samples to provide a marker for cell cycle progression.

In wild type cells, *CLN3* mRNA and protein peaked in G1 at 20-30 minutes (Figures 6A-C and S2). There was a second peak of *CLN3* mRNA and protein later in the cell cycle that appeared at the same time as peak levels of the mitotic cyclin Clb2, indicating that Cln3 is produced in mitosis (Figures 6A-D). In *rts1*Δ cells, accumulation of *CLN3* mRNA and protein was reduced and delayed (Figures 6A-C and S2). The defect in *CLN3* mRNA accumulation caused by *rts1*Δ early in the cell cycle (time points 10-20 minutes) appeared to be rescued by *ace2*Δ *(*see Figure 6B legend*)*. In addition, *ace2*Δ advanced the peak of Cln3 protein early in the cell cycle in *rts1*Δ cells, consistent with a rescue of *CLN3* mRNA levels. However, defects in *CLN3* mRNA accumulation that occurred later in the cell cycle (time points 50-100 minutes) were not rescued by *ace2*Δ (Figures 6A-6C).

We carried out similar experiments in cells released from a metaphase arrest. In wild type cells, *CLN3* mRNA and protein were present at the metaphase arrest and then increased as Clb2 levels declined, reaching a peak 20 minutes after release from the arrest (Figures 7A-7C). Cln3 protein was present throughout most of G1, decreased before mitosis, and then accumulated again during the second mitosis. The decline in *CLN3* mRNA and protein at 30 minutes was correlated with hyperphosphorylation of Ace2, consistent with a role for Ace2 hyperphosphorylation in repression of *CLN3* transcription (compare wild type samples in Figures 2C, 7A and 7B). In *rts1*Δ cells, destruction of Clb2 was delayed, indicating a delay in exit from mitosis, and *CLN3* mRNA and protein failed to accumulate to normal levels as

cells exited mitosis (Figures 7A-C). Defects in *CLN3* mRNA accumulation in *rts1*Δ cells were not rescued by *ace2*Δ (Figures 7A-B).

Together, these observations show that *ace2*Δ may rescue some, but not all, defects in *CLN3* mRNA accumulation caused by *rts1*Δ. A possible explanation is that $PP2A^{Rts1}$ controls an additional repressor of *CLN3* transcription. The only other known repressor of *CLN3* transcription is Yox1 (Bastajian et al., 2013; Pramila et al., 2002). The mass spectrometry analysis identified a hyperphosphorylated Yox1 peptide in *rts1*Δ cells with high confidence in one of the biological replicates (Table S3). In addition, *yox1*Δ improved the growth rate of *rts1*Δ *ace2*Δ cells at 34°C (Figure 7D). Finally, *rts1*Δ increased the toxicity caused by expression of *YOX1* from the *GAL1* promoter (Figure 7E). $PP2A^{Rts1}$ may therefore control multiple repressors of *CLN3* transcription.

$PP2A^{Rts1}$ is required for normal control of transcriptional activator functions of Ace2

In addition to its repressor functions, Ace2 is a transcriptional activator for genes involved in cell separation, including *CTS1* (Dohrmann et al., 1992). To test whether $PP2A^{Rts1}$ controls transcriptional activator functions of Ace2, we assayed *CTS1* mRNA levels in wild type, *rts1*Δ, *ace2*Δ and *rts1*Δ *ace2*Δ cells after release from a G1 arrest (Figure 8). Levels of *CTS1* mRNA showed a significant increase in *rts1*Δ cells that was dependent upon *ACE2*. Thus, Ace2 is hyperactive as a transcriptional activator in *rts1*Δ cells.

PP2A^{Rts1} is required for normal binding of Ash1 to the *CLN3* promoter

Ace2 is thought to collaborate with Ash1 to repress *CLN3* transcription (Di Talia et al., 2009). Like Ace2, Ash1 is asymmetrically segregated into the daughter cell at the end of cell division (Bobola et al., 1996). Chromatin immunoprecipitation (ChIP) experiments have shown that Ace2 and Ash1 bind to the *CLN3* promoter (Di Talia et al., 2009). To further investigate regulation of *CLN3* transcription by PP2A^{Rts1}, we assayed binding of Ace2 and Ash1 to the *CLN3* promoter. Loss of Rts1 did not cause significant effects on binding of Ace2 to the *CLN3* promoter; however, binding of Ash1 was significantly increased (Figures 9A and 9B). In addition, binding of Ace2 was dependent upon Ash1, and binding of Ash1 was strongly dependent upon Ace2 (Figures 9C and 9D). These findings suggest that hyperphosphorylation of Ace2 causes increased recruitment of Ash1, leading to transcriptional repression.

Ace2 is hyperphosphorylated in small-unbudded daughter cells

The preceding experiments show that Ace2 is hyperphosphorylated in *rts1*Δ cells, which likely activates it to repress transcription of *CLN3*. We next investigated regulation of Ace2 in wild type cells. It is thought that Ace2 causes a G1 delay in small daughter cells by repressing *CLN3* transcription (Di Talia et al., 2009; Laabs et al., 2003). However, the signals that control the duration of the delay are unknown. The discovery that PP2A^{Rts1} controls Ace2 suggested that it could play a role in determining the duration of the G1 delay. We reasoned that one way to test this would be to monitor Ace2 hyperphosphorylation, as well as levels of *CLN3* mRNA and protein, during G1 in newborn daughter cells. If PP2A^{Rts1} plays a role in

enforcing a G1 delay, then Ace2 should be hyperphosphorylated in newborn daughter cells and dephosphorylation of Ace2 should be correlated with accumulation of Cln3.

Cells synchronized via a cell cycle arrest cannot be used to study events that occur in small newborn daughter cells because cells grow during the arrest. To circumvent this problem, we used centrifugal elutriation to isolate small daughter cells. To enrich for very small daughter cells, the cells were grown in media containing a poor carbon source prior to elutriation. After isolation, the cells were released into rich media and samples were taken to assay Ace2 phosphorylation and levels of *CLN3* mRNA and protein as the cells underwent growth and entry into the cell cycle. We also measured cell size as a function of time to monitor cell growth, and the fraction of cells undergoing bud emergence to determine when cells enter the cell division cycle. We used northern blotting to assay *CLN3* mRNA levels because qRT-PCR requires normalization to an internal standard RNA, which could undergo significant changes as cells grow. By using northern blotting to probe the same fraction of total RNA at each time point we could assay levels of *CLN3* mRNA per cell.

The small newborn daughter cells underwent continuous growth and initiated bud emergence at 130 minutes (Figures 10A and 10B). Ace2 was hyperphosphorylated in the small unbudded cells and underwent gradual dephosphorylation (Figure 10C). Maximal dephosphorylation of Ace2 occurred at 70-80 minutes. Cln3 was first detectable at 10 minutes and then accumulated gradually, reaching peak levels around the time of maximal Ace2 dephosphorylation (Figure 10C). Thus, Ace2 dephosphorylation and Cln3 protein accumulation

occurred gradually during growth and were correlated. *CLN3* mRNA accumulated gradually during growth, similar to Cln3 protein (Figure 10D). We consistently observed a transient increase in *CLN3* mRNA at 5 minutes, and Cln3 protein began to accumulate shortly thereafter. This burst of *CLN3* mRNA was not correlated with Ace2 phosphorylation.

As expected, the mitotic cyclin Clb2 was not detectable, which indicates that phosphorylation of Ace2 in this context was not due to mitotic Cdk1 activity. It was not possible to isolate unbudded *rts1*Δ cells due to their severe cell size defects: centrifugal elutriation yielded a mixture of budded and unbudded cells that were of similar size.

DISCUSSION

Identification of PP2A^{Rts1} targets by proteome-wide mass spectrometry

To identify targets of PP2A^{Rts1}-dependent regulation, we used quantitative proteome-wide mass spectrometry to search for proteins that undergo changes in phosphorylation in *rts1*Δ cells. Proteome-wide mass spectrometry should prove to be a powerful tool for identifying phosphatase targets, since one searches for proteins that undergo hyperphosphorylation, which is unlikely to be due to indirect or toxic effects caused by inactivation of the phosphatase.

The analysis identified 156 proteins that undergo significant hyperphosphorylation when PP2A^{Rts1} is inactivated. These likely include direct targets of PP2A^{Rts1}, but also appear to delineate entire pathways regulated by PP2A^{Rts1}. For example, several components of a pathway that regulates mitosis via Cdk1 inhibitory phosphorylation were identified. In this pathway, three related kinases called Gin4, Hsl1 and Kcc4 promote entry into mitosis by inactivating Swe1. Gin4 and Hsl1 are controlled by the septins, which were also identified as potential targets of PP2A^{Rts1}-dependent regulation (Table S2). Previous work found that *rts1*Δ causes a mitotic delay and defects in Swe1 phosphorylation; however, the underlying mechanisms were unknown. The mass spectrometry data suggest that PP2A^{Rts1} regulates mitosis via a pathway that includes the septins, Gin4/Hsl1/Kcc4 and Swe1.

In addition to identifying targets of PP2A^{Rts1}-dependent regulation, the mass spectrometry identified 10,807 phosphorylation sites on 2066 proteins. These sites significantly expand phosphorylation site data in budding yeast. Nevertheless, it must be kept in mind that proteome-wide mass spectrometry is not comprehensive.

Thus, little can be inferred from the absence of proteins or sites in the data. In addition, the analysis generally does not provide sufficient sequence coverage to warrant mutagenesis of identified sites to test their functions. Rather, further site mapping must be carried out using purified proteins to yield more comprehensive identification of sites.

PP2A^{Rts1} as a master regulator of cell size control pathways

Swe1 and the G1 cyclins play important roles in mechanisms that control cell size. Both serve as downstream effectors of cell size control mechanisms that accelerate or delay the cell cycle to allow more or less time for cell growth. The cell size control mechanisms that signal to Swe1 and the G1 cyclins have proven remarkably difficult to discover.

In previous work we found that PP2A^{Rts1} is required for normal control of cell size, as well as nutrient modulation of cell size. Here, we discovered that PP2A^{Rts1} regulates pathways that control both Swe1 and G1 cyclins. Together, these observations suggest the possibility that PP2A^{Rts1} is a component of the enigmatic cell size control mechanisms that signal to Swe1 and G1 cyclins.

In G1 phase, PP2A^{Rts1} controls phosphorylation of two key transcription factors for G1 cyclins: Ace2 and Swi4. Ace2 is a repressor of *CLN3* transcription (Di Talia et al., 2009; Laabs et al., 2003), while Swi4 is a transcriptional activator for late G1 cyclins *CLN1* and *CLN2* (Nasmyth and Dirick, 1991; Ogas et al., 1991). Since Cln3 appears first and helps promote transcription of *CLN1* and *CLN2*, it was initially thought that size control in G1 works through *CLN3*. However, although *cln3*Δ are abnormally large, they still show size-dependent entry into the cell cycle and nutrient

modulation of cell size, which shows that cell size control in G1 can not work solely through *CLN3* (Di Talia et al., 2009; Ferrezuelo et al., 2012; Jorgensen et al., 2004; Nasmyth and Dirick, 1991). The discovery that $PP2A^{Rts1}$ controls both Ace2 and Swi4 suggests that a common mechanism could link transcription of both early and late G1 cyclins to cell size or growth. Thus, size dependent entry into the cell cycle in *cln3*Δ cells could work through $PP2A^{Rts1}$ and Swi4-dependent control of *CLN1* and *CLN2* transcription.

In mitosis, $PP2A^{Rts1}$ regulates a pathway that controls inhibitory phosphorylation of Cdk1. Although much emphasis has been placed on control of cell size at G1 in budding yeast, it is likely that size is also controlled in mitosis. Loss of Swe1, or regulators of Swe1, cause defects in cell size (Harvey et al., 2005; Harvey and Kellogg, 2003; Jorgensen et al., 2002; Kellogg, 2003; Longtine et al., 2000; Ma et al., 1996; Shulewitz et al., 1999; Sreenivasan and Kellogg, 1999). Moreover, nutrients almost certainly modulate cell size at both G1 and mitosis. Classic experiments carried out over 30 years ago discovered that daughter cells exit mitosis at a smaller size in poor nutrients (Johnston et al., 1977). More recent work has confirmed that the smallest cells in a population of cells growing in poor nutrients are smaller than the smallest cells in rich nutrients, which can only occur if daughter cells exit mitosis at a smaller size [see, for example, Figure 3A in (Jorgensen et al., 2004) or Figure 11A in (Artiles et al., 2009)]. This suggests the existence of a mechanism that drives progression through mitosis at a smaller bud size when cells are growing in poor nutrients. Since $PP2A^{Rts1}$ is required for nutrient modulation of cell size and regulates mitosis, it may be an essential component of this mechanism. $PP2A^{Rts1}$ appears to control mitosis via the related kinases Gin4, Hsl1 and Kcc4.

Fission yeast homologs of these kinases (Cdr1 and Cdr2) are required for nutrient modulation of cell size at entry into mitosis, which suggests a conserved mechanism (Young and Fantes, 1987).

PP2A^{Rts1} controls G1 cyclin transcription via the Ace2 transcription factor

We focused on Ace2 as a starting point for characterizing proteins controlled by PP2A^{Rts1}. Ace2 is thought to delay cell cycle entry in small daughter cells via repression of *CLN3* transcription (Colman-Lerner et al., 2001; Laabs et al., 2003). The signals that control the length of the Ace2-dependent delay could control cell size, but have been largely unknown. Our analysis suggests that PP2A^{Rts1} controls Ace2, which likely influences the duration of G1 and cell size.

Diverse experiments support a model in which hyperphosphorylated Ace2 is active as a repressor of *CLN3* transcription, and that PP2A^{Rts1} dephosphorylates Ace2 to promote *CLN3* transcription (Figure 10E). In *rts1*Δ cells, Ace2 was hyperphosphorylated, which correlated with decreased *CLN3* mRNA and protein. In wild type cells, there was a decrease in *CLN3* mRNA and protein 30 minutes after release from metaphase arrest that correlated with Ace2 hyperphosphorylation. Finally, in small unbudded cells undergoing growth, dephosphorylation of Ace2 occurred gradually and was correlated with gradually increasing Cln3 protein levels.

Genetic analysis provided additional support for the model: overexpression of *ACE2* was lethal in *rts1*Δ cells, and *ace2*Δ partially rescued the reduced growth rate of *rts1*Δ cells at elevated temperatures. In addition, *ace2*Δ rescued defects in *CLN3* mRNA levels in *rts1*Δ cells early in the cell cycle. However, *ace2*Δ did not cause increased *CLN3* mRNA levels in wild type cells, and it did not rescue reduced levels

of *CLN3* mRNA in *rts1*Δ cells exiting mitosis. There are several potential explanations for these observations. First, previous work suggests that Ace2 represses *CLN3* transcription only in small unbudded daughter cells; however, we were not able to test effects of *rts1*Δ and *ace2*Δ upon *CLN3* transcription in small daughter cells for two reasons. First, small daughter cells grow during cell cycle arrests and are therefore lost in synchronized cells. Second, *ace2*Δ and *rts1*Δ cause cell clumping or size defects that preclude isolation of small daughter cells by centrifugal elutriation. Thus, we could not analyze the effects of *rts1*Δ and *ace2*Δ in the context most likely to show strong effects. Another consideration is that $PP2A^{Rts1}$ could also activate factors that promote *CLN3* transcription, in which case inactivation of the repressor would not be sufficient to rescue *CLN3* mRNA levels in *rts1*Δ cells. Finally, $PP2A^{Rts1}$ could regulate multiple repressors of *CLN3* transcription. Consistent with this, we found evidence that $PP2A^{Rts1}$ controls Yox1, another repressor of *CLN3* transcription (Bastajian et al., 2013; Pramila et al., 2002). The *CLN3* gene has an unusually large 5' untranslated region and is subject to complex regulation (Polymenis and Schmidt, 1997).

What is the kinase that hyperphosphorylates Ace2 in *rts1*Δ cells? Previous work found that Ace2 is phosphorylated by Cbk1, which drives asymmetric localization of Ace2 into daughter cell nuclei (Mazanka et al., 2008). There is also evidence that Cbk1 controls additional Ace2 functions (Mazanka et al., 2008). The mass spectrometry identified a Cbk1 target site (S122), and western blotting with a phospho-specific antibody confirmed that the site is hyperphosphorylated in *rts1*Δ cells. However, purified Cbk1 did not appear to be capable of phosphorylating Ace2 in vitro to the same extent observed in vivo in *rts1*Δ cells. In addition, the mass

spectrometry identified numerous sites that have not been attributed to Cbk1. Thus, it is likely that at least one additional kinase regulates Ace2. We found no clear evidence that hyperphosphorylation of Ace2 in *rts1*Δ cells is due to Cdk1. Moreover, the *rts1*Δ phenotype is not consistent with hyperphosphorylation of Ace2 on mitotic Cdk1 sites, since previous work suggests that this should lead to constitutive cytoplasmic localization of Ace2, where it could not repress *CLN3* transcription (O'Conallain et al., 1999; Sbia et al., 2008).

$PP2A^{Rts1}$ could act directly on Ace2, or it could act further upstream to inhibit a kinase or activate a phosphatase that acts on Ace2. We found that purified $PP2A^{Rts1}$ was not able to dephosphorylate Ace2; however, we could not demonstrate that the $PP2A^{Rts1}$ was active so the experiment was inconclusive.

$PP2A^{Rts1}$ may contribute to gradual Cln3 accumulation during growth of small cells

Cln3 has been difficult to detect by western blotting, so its behavior during the cell cycle has been little characterized. We used highly sensitive western blotting techniques to gain an unprecedented view of Cln3 protein during the cell cycle. This revealed that Cln3 shows significant periodic oscillations. One peak of Cln3 occurs in G1, as expected for a G1 cyclin, and a second peak occurs as the mitotic cyclin Clb2 reaches peak levels. The functions of Cln3 during mitosis are unknown.

We also assayed Cln3 and Ace2 during growth of newborn daughter cells. An important hypothesis for cell size control suggests that Cln3 levels are proportional to cell growth or size, and that cell cycle entry is triggered when Cln3 levels reach a threshold (Jorgensen and Tyers, 2004; Turner et al., 2012). However,

Cln3 has never been assayed in growing newborn daughter cells to test this model. We found that Cln3 was initially absent in newborn daughter cells and then accumulated gradually during growth. Cln3 reached peak levels at approximately 90 minutes and bud emergence began 40 minutes later. The striking correlation between Cln3 protein levels and cell growth is consistent with the Cln3 threshold model. The delay between peak Cln3 levels and bud emergence may correspond to a previously described size-independent delay in G1 that occurs prior to bud emergence (Di Talia et al., 2007; Di Talia et al., 2009). Alternatively, the delay may reflect additional size-dependent mechanisms that regulate the activity or localization of Cln3 (Verges et al., 2007). Mechanisms that restrain the ability of *CLN3* to trigger cell cycle entry during early daughter cell growth may play a role in setting a size threshold.

Ace2 was hyperphosphorylated in newborn daughter cells and underwent gradual dephosphorylation during cell growth, reaching maximal dephosphorylation at approximately the same time that Cln3 protein reached peak levels. This observation suggests the possibility that the extent of Ace2 dephosphorylation could help set the level of *CLN3* transcription.

Cell size checkpoints must translate a parameter related to growth into a proportional checkpoint signal that can be read by downstream components to determine when sufficient growth has occurred. The nature of the proportional checkpoint signal is one of the central enigmas of cell size control. The discovery that Ace2 phosphorylation is proportional to growth suggests that it may respond to a proportional checkpoint signal. Moreover, the central role of $PP2A^{Rts1}$ in control of both Ace2 phosphorylation and cell size suggests that it could be responsible for

generating or relaying a proportional checkpoint signal to Ace2, thereby ensuring that Cln3 levels are proportional to growth. $PP2A^{Rts1}$ could also play a role in setting the threshold. In this case, poor nutrients could regulate $PP2A^{Rts1}$ to lower the threshold, thereby allowing cells to go through the cell cycle at a reduced cell size. This kind of model could explain the puzzling observation that cells growing in poor nutrients enter the cell cycle at a reduced size, despite having reduced levels of Cln3 (Hall et al., 1998; Newcomb et al., 2003). If poor nutrients reduce the threshold, lower levels of Cln3 would be required for cell cycle entry. Further analysis of the targets of $PP2A^{Rts1}$, as well as the signals that control $PP2A^{Rts1}$, will likely provide important new clues to how cell division is linked to cell growth.

MATERIALS AND METHODS

Yeast strains, culture conditions and plasmids

All strains are in the W303 background (*leu2-3,112 ura3-1 can1-100 ade2-1 his3-11,15 trp1-1 GAL+ ssd1-d2*). The genotypes of the strains used for this study are listed in **Table II**. Full length *CLN3* was expressed from the GAL1 promoter using the integrating plasmid pDK93A [*GAL1-CLN3 URA3*]. One-step PCR-based gene replacement was used for construction of deletions and epitope tags at the endogenous locus. Strains that contain *GAL1-CDC20* strains were made by genetic crosses (Bhoite et al., 2001) or by using a PCR-based approach to integrate the *GAL1* promoter in front of the endogenous *CDC20* gene in the appropriate background.

Cells were grown in YEPD media (1% yeast extract, 2% peptone, 2% dextrose) supplemented with 40mg/L adenine or in YEP media (1% yeast extract, 2% peptone) supplemented with an added carbon source, as noted.

Preparation of samples for mass spectrometry

To prepare samples for mass spectrometry, wild type and *rts1*Δ cells containing *CLN2-3XHA* were grown in YEPD medium overnight at room temperature. Cells were arrested in G1 with mating pheromone and released from the arrest at 30ºC at an OD_{600} of 0.7. Samples were taken for Cln2-3XHA western blots every 10 minutes following the arrest, which were used to confirm that samples for mass spectrometry were taken just before Cln2 could be detected by western blotting. At 20 min post-release, 25 ml of the culture were harvested by centrifuging 95s at 3800

rpm and 1 ml of ice cold lysis buffer (8 M urea, 75 mM NaCl, 50 mM Tris-HCl pH 8.0, 50 mM NaF, 50 mM β-glycerophosphate, 1 mM sodium orthovanadate, 10 mM sodium pyrophosphate, 1 mM PMSF) was added to the cells and used to transfer them to a wide-bottom 1.6 ml screw-top tube. The cells were pelleted again and the supernatant was removed. Approximately 0.5 ml of glass beads were added and the cells were frozen in liquid nitrogen. The cells were lysed by addition of 750 ul of lysis buffer, followed by bead-beating using a Biospec Multibeater-8 at top speed for three cycles of 1 min, each followed by a 1 min incubation on ice to avoid over-heating of the lysates. Samples were centrifuged at 13000 rpm for 15 s and the supernatants were transferred to fresh 1.6 ml tubes, which were centrifuged at 13000 rpm for 10 min at 4ºC. The supernatants from this spin were transferred to fresh 1.6 ml tubes and frozen in liquid nitrogen. This procedure yielded 0.7 ml of extract at 2-5 mg/ml.

Disulfide bonds were reduced by adding dithiothreitol to a final concentration of 2.5 mM and incubating at 56°C for 40 min. The extract was allowed to cool to room temperature and the reduced cysteines were alkylated by adding iodoacetamide to 7.5 mM and incubating for 40 min in the dark at room temperature. Alkylation was quenched with an additional 5 mM dithiothreitol.

Peptide digestion and labeling by reductive dimethylation

Proteins were diluted 2.5-fold into 25 mM (final concentration) Tris-HCl, pH 8.8 and digested by the addition of lysyl endopeptidase (lysC) (Wako USA, #12-02541) to a final concentration of 10 ng/µl with gentle agitation overnight at room temperature. Digested peptides were acidified by the addition of neat formic acid (FA) to 1% final concentration and the resultant precipitate was pelleted by

centrifuging for 2 min at 21k x g. The supernatants were loaded onto pre-wet 200 mg tC18, reverse-phase solid phase extraction cartridges (Waters, Milford, MA, #WAT054925). The columns were washed with 6 ml of 1% FA followed by 3 ml of phosphate/citrate buffer (227 mM Na_2HPO_4, 86 mM $NaH_2C_6H_5O_7$, pH 5.5). Peptides were labeled by reductive dimethylation (Boersema et al., 2009) with 6 ml of "light" reductive dimethylation reaction mix [0.8% formaldehyde (Sigma, #F1635), 120 mM $NaCNBH_3$ (Sigma, #296945), in phosphate/citrate buffer] or with 6 ml of "heavy" reductive dimethylation reaction mix [0.8% D2-formaldehyde (Isotec, #492620), 120 mM $NaCNBD_3$ (CDN, #D-1797), in phosphate/citrate buffer]. The columns were washed with 6ml of 1% FA and the peptides were eluted with 1 ml of 70% acetonitrile (ACN), 1% FA. Equal amounts of wild type ("light") and *rts1*Δ ("heavy") peptides were combined and dried in a speed-vac.

Phosphopeptide enrichment by SCX/TiO2

Phosphopeptides were enriched using a modified version of the two-step, SCX-IMAC/TiO_2 protocol employing step elution from self-packed solid-phase extraction strong cation exchange (SCX) chromatography cartridges as previously described with some changes (Dephoure and Gygi, 2011; Villen and Gygi, 2008). Peptides were resuspended in 1 ml SCX buffer A (7 mM KH_2PO_4, pH 2.65, 30% ACN) and loaded onto pre-equilibrated syringe-barrel columns packed with 500 mg of 20 µm, 300 Å, polysulfoethylA resin (poly LC). Peptides were eluted by the sequential addition of 3 ml of SCX buffer A containing increasing concentrations of KCl. Twelve fractions were collected after elution with 0 (flow-through), 10, 20, 30, 40, 50, 60, 70, 80, 90, 100, and 200 mM KCl. All fractions were frozen in liquid nitrogen,

lyophilized, resuspended in 1 ml of 1% FA, and desalted on 50 mg Sep-paks. Peptides were eluted with 500 µl of 70% ACN, 1% FA. Five percent of each fraction was taken off for protein abundance analysis. The remaining peptides were dried in a speed vac. TiO_2 enrichment was performed by either of two protocols. For replicate one, peptides from fractions 8-11 were pooled after desalting (fraction 12 was not used for phosphopeptide analysis). Dried peptides were resuspended in 50 µl wash/binding buffer (30% ACN, 1% FA, 70 mM glutamic acid) and incubated with 500 µg of Titansphere TiO_2 beads (GL Sciences, #5020-75000) with vigorous shaking for 60 minutes at room temperature. The beads were washed three times with 200 µl of wash/binding buffer and once with 1% FA. Phosphopeptides were eluted in two steps by sequential treatments with 50 µl 0.5 M KH_2PO_4, pH 7.5. The eluates were acidified by the addition of FA to 1% final concentration, desalted on STAGE tips (Rappsilber et al., 2003), and dried in a speed vac. Eight fractions corresponding to 0, 10, 20, 30, 40, 50, 60, and the pooled 70-100 mM KCl steps were analyzed by LC-MS/MS.

SCX for peptides from replicates two and three was performed as for set one, but 11 fractions were taken with steps of 0, 10, 20, 30, 40, 50, 60, 70, 80, 90, and 200 mM KCl. Fractions 9-11 were pooled prior to TiO_2 enrichment. TiO_2 phosphopeptide enrichment was performed using a modified protocol (Kettenbach and Gerber, 2011) using 2 mg of TiO_2 resin for each fraction and a wash/binding buffer composed of 50% ACN, 2M lactic acid.

Mass spectrometry

SCX fractions for protein abundance level analysis were analyzed on a LTQ Orbitrap Velos mass spectrometer using a data-dependent Top20-MS2 method. For each cycle, one full MS scan of m/z = 300-1500 was acquired in the Orbitrap. Each full scan was followed by the selection of the most intense ions, up to 20, for CID and MS2 analysis in the LTQ. Ions selected for MS2 analysis were excluded from re-analysis for 90 seconds.

Phosphopeptide samples were analyzed on a LTQ Orbitrap Velos mass spectrometer (Thermo Fisher Scientific) equipped with an Accela 600 quaternary pump (Thermo Fisher Scientific) and a Famos microautosampler (LC Packings, Sunnyvale, CA). Nanospray tips were hand-pulled using 100 µm I.D. fused-silica tubing and packed with 0.5 cm of Magic C4 resin (5µm, 100 Å, Michrom Bioresources, Auburn, CA) followed by 20 cm of Maccel C18AQ resin (3µm, 200 Å, Nest Group, Southborough, MA). Peptides were separated using a gradient of 3% to 28% ACN in 0.125% FA over 70 min with an in column flow rate of ~300-500 nl/min. Peptides were detected using a data-dependent Top20-MS2 method. For each cycle, one full MS scan of m/z = 300-1500 was acquired in the Orbitrap at a resolution of 60,000 at m/z = 400 with AGC target = $1x10^6$ and maximum ion accumulation time of 500 mS. Each full scan was followed by the selection of the most intense ions, up to 20, for collision induced dissociation (CID) and MS2 analysis in the LTQ. An AGC target of $2x10^3$ and maximum ion accumulation time of 150 mS was used for MS2 scans. Ions selected for MS2 analysis were excluded from re-analysis for 60 sec. Precursor ions with charge = 1+ or unassigned were excluded from selection for MS2 analysis. Lockmass, employing atmospheric polydimethylsiloxane (m/z =

445.120025) as an internal standard was used in all runs to calibrate orbitrap MS precursor masses. For replicate one, eight fractions were analyzed once each. For replicates two and three, sufficient material was recovered to shoot samples in duplicate for most fractions. For replicate two, all nine fractions were analyzed in duplicate. For replicate three, fractions 1-6 were analyzed in duplicate while fractions 7-9 were analyzed once.

For protein abundance analysis, 5% of each SCX fraction was removed before phosphopeptide enrichment, desalted on a STAGE tip, resuspended in 5% FA and analyzed in a single run for each fraction as described in the previous paragraphs for phosophopeptides, but using a 90 min gradient of 3-25% buffer B and 75 sec dynamic exclusion.

Peptide identification and filtering

MS2 spectra were searched using SEQUEST v.28 (rev. 13) (Eng et al., 1994) against a composite database containing the translated sequences of all predicted open reading frames of *Saccharomyces cerevisiae* (http://downloads.yeastgenome.org, downloaded 10/30/2009) and its reversed complement, using the following parameters: a precursor mass tolerance of ±20 ppm; 1.0 Da product ion mass tolerance; lysC digestion; up to two missed cleavages; static modifications of carbamidomethylation on cysteine (+57.0214), dimethyl adducts (+28.0313) on lysine and peptide amino termini; and dynamic modifications for methionine oxidation (+15.9949), heavy dimethylation (+6.0377) on lysine and peptide amino termini, and phosphate (+79.9663) on serine, threonine, and tyrosine for phosphopeptide enriched samples.

Peptide spectral matches were filtered to 1% FDR using the target-decoy strategy (Elias and Gygi, 2007) combined with linear discriminant analysis (LDA) (Huttlin et al., 2010) using several different parameters including Xcorr, ΔCn', precursor mass error, observed ion charge state, and predicted solution charge state. Linear discriminant models were calculated for each LC-MS/MS run using peptide matches to forward and reversed protein sequences as positive and negative training data. Peptide spectral matches within each run were sorted in descending order by discriminant score and filtered to a 1% FDR as revealed by the number of decoy sequences remaining in the data set. The data were further filtered to control protein level FDRs. Peptides from all fractions in each experiment were combined and assembled into proteins. Protein scores were derived from the product of all LDA peptide probabilities, sorted by rank, and filtered to 1% FDR as described for peptides. The FDR of the remaining peptides fell dramatically after protein filtering. Remaining peptide matches to the decoy database were removed from the final dataset.

For inclusion in quantitative calculations, peptides were required to have a minimum signal-to-noise ratio of ≥ 5 or a maximum value ≥ 10 for heavy and light species. Protein abundance ratios were calculated using the median $\log_2$ ratio of all peptides for each protein. This was done independently for each of the three biological replicate experiments and only those proteins for which we quantified ≥ 2 unique peptides were retained in the dataset (Table S1). Ratios were normalized to recenter the distribution at 1:1 ($\log_2 = 0$). Phosphopeptide ratios were adjusted for changes in protein abundance where possible using the corresponding protein ratio from the matched experiment. However, corrections were only applied if protein

levels were available for all experiments in which the phosphosite was quantified (7230 of 9255 quantified sites were corrected for protein level abundance and 3983 of 5159 high quality sites quantified in two or more replicates). We note that although we were unable to normalize all phosphorylation site quantifications to protein level changes, the vast majority of proteins undergo almost no change in abundance between the two samples (log2Ratio StDev = 0.32), thus most uncorrected are unlikely to be significantly skewed. Phosphorylation site ratios were calculated from the median of all quantified phosphopeptides harboring each site in each replicate.

Phosphorylation site localization analysis was done using the Ascore algorithm (Beausoleil et al., 2006). These values appear in Table S2.

Cell cycle time courses and log phase cells

To ensure that protein loading was normalized in time course experiments, we determined optical densities of cultures from each strain that yield equal amounts of extracted protein. This was necessary because large cells (i.e. *rts1*Δ cells) or clumpy cells (i.e. *ace2*Δ cells) scatter light differently. Samples of cultures from each strain at varying optical densities were harvested and the cells were lysed by bead beating. The protein concentration in extracts from each strain was then measured to determine which optical densities yield comparable amounts of extracted protein. We found that optical densities of 0.6 (wild type), 0.8 (*rts1*Δ), 0.5 (*ace2*Δ) and 0.5 (*rts1*Δ *ace2*Δ) yielded protein concentrations with differences of less than two fold. We also used multiple background bands in western blots to ensure that protein loading between strains and individual samples was normalized.

To synchronize cells in G1 with mating pheromone, cells were grown to log phase in YEPD overnight at room temperature prior to synchronization. Cells at an OD_{600} of 0.6 were arrested in G1 by addition of 0.5 μg/ml of α factor for 3.5 hours. Cells were released into a synchronous cell cycle by washing 3X with fresh YEPD pre-warmed to 30ºC. Time courses were carried out at 30ºC unless otherwise noted. To prevent cells from re-entering the cell cycle, α factor was added back at 65 minutes post-release.

To synchronize cells at metaphase, cells containing *GAL1-CDC20* were grown overnight in YEP media containing 2% raffinose and 2% galactose. Cells were arrested by washing into media containing 2% raffinose and incubated at room temperature for 4 hours. Cells were released from the metaphase arrest by adding 2% galactose and were then shifted to 30ºC for western blotting experiments or 25ºC for *CLN3* mRNA analysis.

For induced expression experiments, cells were grown overnight in YEP medium containing 2% glycerol and 2% ethanol. Expression of genes from the *GAL1* promoter was induced by addition of 2% galactose and the cells were shifted to 30ºC.

For time courses using analog-sensitive alleles, cells were grown overnight in YEPD without adenine. The adenine-analog inhibitor 1NMPP1 was added to log phase cells at a final concentration of 25μM, the cells were then shifted to 30ºC.

To analyze log phase cells, cultures were grown in YEPD, YEPD+2% galactose or YEPD+2% glycerol/ethanol overnight at room temperature. 1.6ml of cells at an OD_{600} of 0.6 were collected and centrifuged at 13000rpm for 30s, the

supernatant was removed and 250ul of glass beads were added before freezing in liquid nitrogen.

Western blotting

To collect samples for western blotting, 1.6 ml samples were collected at each time point and centrifuged at 13000 rpm for 30s. The supernatant was removed and 250μl of glass beads were added before freezing in liquid nitrogen. Cells were lysed using 140μl of 1X sample buffer (65mM Tris-HCl pH 6.8, 3% SDS, 10% glycerol, 50mM NaF, 100mM β-glycerophosphate, 5% 2-mercaptoethanol, bromophenol blue). Phenyl methyl sulfonyl fluoride (PMSF) was added to the sample buffer to 2mM immediately before use. Cells were lysed in a Biospec Multibeater-8 at top speed for 2 minutes. The samples were removed and centrifuged for 15s at 13000 rpm in a microfuge and placed in boiling water for 5 min. After boiling, the samples were centrifuged for 5min at 13000 rpm and loaded on a SDS polyacrylamide gel.

To assay phosphorylation of Ace2 serine 122, cells were grown overnight in YEPD media at room temperature to OD_{600}=0.6. Cells from 50 ml of culture were pelleted, resuspended 1 ml of ice cold 50 mM Hepes, pH 7.6, and pelleted in a wide-bottomed 1.6 ml screw top tube. Cells were lysed by bead-beating in 600 ul lysis buffer (50 mM Tris-HCl, pH7.5,150 mM NaCl,1% Triton-X 100, 10% glycerol, 120 mM beta-glycerophosphate, 2 mM sodium orthovanadate) containing 2 mM PMSF. Ace2-3XHA was immunoprecipitated with mouse monoclonal 12CA5 antibody western blots were probed with rabbit anti-phospho-S122 antibody as previously described, except that the antibody was used at a dilution of 1:30,000 in TBST (10

mM Tris-Cl, pH 7.5, 100 mM NaCl, 0.1% Tween 20) containing 4% BSA (Mazanka and Weiss, 2010).

SDS-PAGE was carried out as previously described (Harvey et al., 2005). Gels were run at a constant current of 20 mA. For Ace2, Clb2 and Cln3, electrophoresis was carried out on 10% polyacrylamide gels until a 29kD prestained marker ran to the bottom of the gel. Protein was transferred to nitrocellulose membranes for 1h 30min at 800 mA at 4ºC in a Hoeffer transfer tank in buffer containing 20 mM Tris base, 150 mM glycine, and 20% methanol. Blots were probed overnight at 4ºC with affinity-purified rabbit polyclonal antibodies raised against, Ace2, Clb2 or HA peptide; or mouse monoclonal antibody against HA peptide. Cln3-6XHA blots were probed with the 12CA5 anti-HA monoclonal antibody. All blots were probed with an HRP-conjugated donkey anti-rabbit secondary antibody (GE Healthcare) or HRP-conjugated donkey anti-mouse antibody for 45-90 minutes at room temperature. Secondary antibodies were detected via chemiluminescence with Advansta ECL or Quantum reagents (Menlo Park, CA).

RNA analysis

qRT-PCR was used to measure *CLN3* mRNA levels as described using RPR1 RNA as the internal control (Voth et al., 2007)(*CLN3* primers: *5'-CAGCGATCAGCGAATACAATAA-3'* and *5'-TGATAATGAACCGCGAGGAA-3'*; *RPR1* control primers: *5'-CACCTATGGGCGGGTTATCAG-3'* and *5'CCTAGGCCGAACTCCGTGA-3'*).

Northern blotting probes for *CLN3* and *ACT1* RNA were made using gel-purified PCR products (*CLN3* oligos: *5'-*

GCGGGATCCATGGCCATATTGAAGGATAC-3', 5'-GCGGAGCTCTCAGCGAGTTTTCTTGAGGT-3'; *ACT1* oligos *5'-TCATACCTTCTACAACGAATTGAGA-3'*, 5'-*ACACTTCATGATGGAGTTGTAAGT-3'*). Probes were labeled using the Megaprime DNA labeling kit (GE Healthcare Amersham). RNA for northern blotting was isolated as previously described (Cross and Tinkelenberg, 1991; Kellogg and Murray, 1995). Briefly, 1.6 ml samples were collected at each time point and centrifuged for 30s at 13,000rpm. The supernatant was removed and 200μl of acid-washed beads were added before freezing on liquid nitrogen. 350μl of NETS buffer (0.3M NaCl, 1mM EDTA, 10mM Tris-HCl pH 7.5, 0.2% SDS) and 350μl of phenol/chloroform were added to each cell pellet and cells were lysed by shaking in a Biospec Multibeater-8 at full speed for 2 minutes. Samples were then centrifuged at 15,000xg for 5 minutes and 300μl of the aqueous phase was transferred to a new tube. RNA was ethanol-precipitated and resuspended in TE buffer (10 mM Tris-HCl pH 7.5, 1mM EDTA) containing 0.2% SDS followed by incubation at 65˚C for 10 minutes. The samples were run in a 1% formaldehyde-agarose gel at 5V/cm2. The same fraction of total extracted RNA was loaded at each time point. This typically corresponded to 8 ug RNA at the zero time point. *CLN3* blots were stripped and re-probed for *ACT1* to control for loading.

Chromatin immunoprecipitation

Chromatin immunoprecipitations (ChIPs) were performed as described (Voth et al., 2007). Yeast cells were collected at optical density 0.6 - 0.8 and crosslinked in 1% formaldehyde for 20 minutes at room temperature. Crosslinking was quenched with 0.125M glycine for 5 minutes, and cells were washed twice with 1x TBS. Cell

pellets were resuspended in lysis buffer (0.1% deoxycholic acid, 1mM EDTA, 50mM HEPES pH 7.5, 140mM NaCl, 1% Triton X-100 supplemented with 0.8mM DTT and protease inhibitors) and were lysed with 0.5mm zirconia beads (BioSpec) in a Mini-Beadbeater (BioSpec). Following centrifugation, the pellet was washed with lysis buffer and sonicated to a shearing size of <500 nucleotides using a Biorupter XL bath sonicator (Diagenode). The sonicated material was centrifuged, and the supernatant containing the chromatin was quantitated by Bradford assay.

Immunoprecipitations were performed overnight at 4°C using 500 to 700 ug of chromatin, 4A6 monoclonal antibody to the Myc epitope (Millipore), and Pan-Mouse Dyna Beads IgG (Invitrogen). The beads were washed twice with lysis buffer, twice with high salt buffer (lysis buffer with 500mM NaCl), twice with LiCl buffer (0.5% deoxycholic acid, 1mM EDTA, 250mM LiCl, 0.5% NP-40, 10mM Tris-HCl pH 8.0) and once with TE. Cross-links were reversed overnight in elution buffer (10mM EDTA, 1% SDS, 50mM Tris-HCl pH 8.0) at 65°C. DNA was purified using the QIAGEN QIAquick PCR purification kit. qPCR reactions were performed using a Roche LightCycler480 II. A standard curve representing a range of concentrations of input samples was used for quantitating the amount of product for each sample with each primer set. All ChIP samples were normalized to corresponding input control samples, to a genomic reference region on chromosome I, and to genetically identical untagged strain as a control. (ChIP primers for the *CLN3* promoter region: *5'-TACATTCTGTGCTGGCGACC-3'; 5'-TTTGAGCACAGCGTTTGGTTG-3'; 5'-ATTCGTCTCGTTTGAAC-GCTTG-3'; 5'-GCCAAGCGTTCAAACGAGAC-3';* ChIP primers for the chromosome I control region 5'-

GTTTATAGCGGGCATTATGCGTAGATCAG-3'; 5'-

GTTCCTCTAGAATTTTTCCACTCGCACATTC-3')

Analysis of cell size, bud emergence and cell proliferation

Triplicate cell cultures were grown overnight to log phase at room temperature in YEPD or YEP containing 2% galactose. A 0.9 ml sample of each culture was fixed with 100 μl of 37% formaldehyde for 1 hour, and then washed twice with 1X PBS+0.04% sodium azide +0.02% Tween-20. Cell size was measured using a Channelizer Z2 Coulter counter as previously described (Jorgensen et al., 2002). Briefly, 150μl of fixed culture was diluted in 20ml of Isoton II® diluent (Beckman Coulter) and sonicated for 20 seconds prior to cell sizing. Each plot is the average of three independent experiments in which three independent samples were analyzed per strain. The size of elutriated cells was measured in the same manner except that the cells were not sonicated. The percentage of budded cells was measured by counting the number of small-unbudded cells over a total of at least 200 cells using a Zeiss phase contrast microscope with a 40X/0.65 Zeiss objective.

To assay the rate of cell proliferation on plates, cells were grown O/N in YEPD at room temperature and adjusted to an OD_{600} of 1.0. 5-fold serial dilutions were spotted onto YEPD or YEP containing 2% galactose media and incubated for at 30°C or 37°C. To assay the growth rate in liquid cultures, eight independent cultures of each strain were grown overnight, and each was diluted 100 fold in inoculating 0.2 ml cultures in a 100 well plate where growth was monitored in a Bioscreen C Apparatus (Growth Curves USA).

Immunoaffinity Purifications and in vitro Assays

Immunoaffinity purification of Ace2-3XHA, Cbk1-3XHA was carried out in the presence of 1M KCl as previously described with the following changes (Mortensen et al., 2002). Affinity beads were prepared by binding 0.6mg of anti-HA antibody to 0.5 ml of protein A beads overnight at 4˚C. 14 grams of frozen cell powder was resuspended in 30 ml of lysis buffer (50 mM HEPES-KOH pH7.6, 1 M KCL, 1 mM EGTA, 1 mM $MgCl_2$, 0.25% Tween-20, 5% glycerol) containing 1mM PMSF by stirring at 4˚C for 15 min. The cell extract was centrifuged at 40,000 rpm for 1 h. The elution buffer contained 50 mM HEPES-KOH pH 7.6, 250 mM KCl, 1 mM EGTA, 1 mM $MgCl_2$, 5% glycerol, 0.5mg/ml HA dipeptide. The Ace2-3XHA was treated with λ phosphatase before elution.

To test if Cbk1 directly phosphorylates Ace2, purified Ace2 and Cbk1 were mixed in the presence of 1 mM ATP and kinase assay buffer (50mM HEPES-KOH pH 7.6, 1 mM $MgCl_2$, 1 mM DTT, 5% glycerol, 0.05% Tween-20, 10 ng/μl BSA). The reactions were incubated for 30 min at 30°C and then quenched with 4X SDS-PAGE sample buffer (260mM Tris-HCl pH 6.8, 12% SDS, 40% Glycerol, 0.04% bromophenol blue). The samples were loaded onto a 10% SDS-PAGE gel, which was transferred to nitrocellulose and probed with anti-Ace2. Similar approaches were used to test the effects of purified Cdk1/Clb2 (Harvey et al., 2011).

Centrifugal Elutriation

Cells for elutriation were grown overnight at room temperature in YEP medium containing 2% glycerol and 2% ethanol to increase the fraction of very small unbudded cells. Centrifugal elutriation was carried out as previously described

(Futcher, 1999; McCusker et al., 2012). Briefly, cells were elutriated at 4°C in a Beckman J6-MI centrifuge with a JE-5.0 rotor at 2700 rpm. Small-unbudded cells were released into fresh YEPD media at 25°C and samples were taken at 10 minute intervals.

ACKNOWLEDGEMENTS

I would like to thank my advisor Doug Kellogg who guided this project and our collaborators for letting me use their data in this dissertation. Tracy MacDonough provided figures 2B, 3C, 4A, 7B, 7C and 10C. Noah Dephoure and Steven Gygi provided figure 1, S1 and tables I, S1, S2, S3, S4, and S5. Yaxin Yu, Emily Partnell, and David Stillman provided figures figure 4B, 6B, 7A, 7D and 8. All supplementary material can be obtained online.

I thank members of the laboratory for advice and support, and Vu Thai for help with protein purification and in vitro assays. I also thank Eric Weiss for the Ace2 phosphospecific antibody. This work was supported by NIH grant GM053959 (D. Kellogg) and NIH grant GM39067 (D. Stillman).

REFERENCES

Aerne, B.L., A.L. Johnson, J.H. Toyn, and L.H. Johnston. 1998. Swi5 controls a novel wave of cyclin synthesis in late mitosis. *Mol Biol Cell*. 9:945-956.

Altman, R., and D.R. Kellogg. 1997. Control of mitotic events by Nap1 and the Gin4 kinase. *J. Cell Biol.* 138:119-130.

Artiles, K., S. Anastasia, D. McCusker, and D.R. Kellogg. 2009. The Rts1 regulatory subunit of protein phosphatase 2A is required for control of G1 cyclin transcription and nutrient modulation of cell size. *PLoS genetics*. 5:e1000727.

Barral, Y., M. Parra, S. Bidlingmaier, and M. Snyder. 1999. Nim1-related kinases coordinate cell cycle progression with the organization of the peripheral cytoskeleton in yeast. *Genes Dev.* 13:176-187.

Bastajian, N., H. Friesen, and B.J. Andrews. 2013. Bck2 acts through the MADS box protein Mcm1 to activate cell-cycle-regulated genes in budding yeast. *PLoS genetics*. 9:e1003507.

Beausoleil, S.A., J. Villen, S.A. Gerber, J. Rush, and S.P. Gygi. 2006. A probability-based approach for high-throughput protein phosphorylation analysis and site localization. *Nature biotechnology*. 24:1285-1292.

Belenguer, P., L. Pelloquin, M.L. Oustrin, and B. Ducommun. 1997. Role of the fission yeast nim 1 protein kinase in the cell cycle response to nutritional signals. *Biochemical and biophysical research communications*. 232:204-208.

Bhoite, L.T., Y. Yu, and D.J. Stillman. 2001. The Swi5 activator recruits the Mediator complex to the HO promoter without RNA polymerase II. *Genes Dev*. 15:2457-2469.

Bishop, A.C., J.A. Ubersax, D.T. Petsch, D.P. Matheos, N.S. Gray, J. Blethrow, E. Shimizu, J.Z. Tsien, P.G. Schultz, M.D. Rose, J.L. Wood, D.O. Morgan, and K.M. Shokat. 2000. A chemical switch for inhibitor-sensitive alleles of any protein kinase. *Nature*. 407:395-401.

Bobola, N., R.P. Jansen, T.H. Shin, and K. Nasmyth. 1996. Asymmetric accumulation of Ash1p in postanaphase nuclei depends on a myosin and restricts yeast mating-type switching to mother cells. *Cell*. 84:699-709.

Boersema, P.J., R. Raijmakers, S. Lemeer, S. Mohammed, and A.J. Heck. 2009. Multiplex peptide stable isotope dimethyl labeling for quantitative proteomics. *Nature protocols*. 4:484-494.

Breeden, L., and G.E. Mikesell. 1991. Cell cycle-specific expression of the SWI4 transcription factor is required for the cell cycle regulation of HO transcription. *Genes Dev*. 5:1183-1190.

Caplan, A.J., and M.G. Douglas. 1991. Characterization of YDJ1: a yeast homologue of the bacterial dnaJ protein. *J Cell Biol*. 114:609-621.

Chan, L.Y., and A. Amon. 2009. The protein phosphatase 2A functions in the spindle position checkpoint by regulating the checkpoint kinase Kin4. *Genes Dev*. 23:1639-1649.

Colman-Lerner, A., T.E. Chin, and R. Brent. 2001. Yeast Cbk1 and Mob2 activate daughter-specific genetic programs to induce asymmetric cell fates. *Cell*. 107:739-750.

Cross, F. 1990. Cell cycle arrest caused by CLN gene deficiency in Saccharomyces cerevisiae resembles START-I arrest and is independent of the mating-pheromone signalling pathway. *Mol. Cell. Biol.* 10:6482-6490.

Cross, F.R. 1988. DAFI, a mutant gene affecting size control, pheromone arrest, and cell cycle kinetics of Saccharomyces cerevisiae. *Mol. Cell. Biol.* 8:4675-4684.

Cross, F.R., and A.H. Tinkelenberg. 1991. A potential positive feedback loop controlling CLN1 and CLN2 gene expression at the start of the yeast cell cycle. *Cell*. 65:875-883.

Dephoure, N., and S.P. Gygi. 2011. A solid phase extraction-based platform for rapid phosphoproteomic analysis. *Methods*. 54:379-386.

Di Como, C.J., H. Chang, and K.T. Arndt. 1995. Activation of CLN1 and CLN2 G1 cyclin gene expression by BCK2. *Molec. Cell. Biol.* 15:1835-1846.

Di Talia, S., J.M. Skotheim, J.M. Bean, E.D. Siggia, and F.R. Cross. 2007. The effects of molecular noise and size control on variability in the budding yeast cell cycle. *Nature*. 448:947-951.

Di Talia, S., H. Wang, J.M. Skotheim, A.P. Rosebrock, B. Futcher, and F.R. Cross. 2009. Daughter-specific transcription factors regulate cell size control in budding yeast. *PLoS biology*. 7:e1000221.

Dirick, L., and K. Nasmyth. 1991. Positive feedback in the activation of G1 cyclins in yeast. *Nature*. 351:754-757.

Dohrmann, P.R., G. Butler, K. Tamai, S. Dorland, J.R. Greene, D.J. Thiele, and D.J. Stillman. 1992. Parallel pathways of gene regulation: homologous regulators SWI5 and ACE2 differentially control transcription of HO and chitinase. *Genes Dev*. 6:93-104.

Doolin, M.T., A.L. Johnson, L.H. Johnston, and G. Butler. 2001. Overlapping and distinct roles of the duplicated yeast transcription factors Ace2p and Swi5p. *Mol Microbiol*. 40:422-432.

Elias, J.E., and S.P. Gygi. 2007. Target-decoy search strategy for increased confidence in large-scale protein identifications by mass spectrometry. *Nat Methods*. 4:207-214.

Eng, J.K., A.L. McCormack, and J. Yates, 3rd. 1994. An approach to correlate tandem mass spectral data of peptides with amino acid sequences in a protein database. *J. Am. Soc. Spectrom.* 5:976-989.

Ferrezuelo, F., N. Colomina, A. Palmisano, E. Gari, C. Gallego, A. Csikasz-Nagy, and M. Aldea. 2012. The critical size is set at a single-cell level by growth rate to attain homeostasis and adaptation. *Nature communications*. 3:1012.

Futcher, B. 1999. Cell cycle synchronization. *Methods in cell science*. 21:79-86.

Gould, K.L., and P. Nurse. 1989. Tyrosine phosphorylation of the fission yeast cdc2^{+} protein kinase regulates entry into mitosis. *Nature*. 342:39-45.

Hadwiger, J.A., C. Wittenberg, H.E. Richardson, M. de Barros Lopes, and S.I. Reed. 1989. A family of cyclin homologs that control the G1 phase in yeast. *Proc Natl Acad Sci U S A*. 86:6255-6259.

Hall, D.D., D.D. Markwardt, F. Parviz, and W. Heideman. 1998. Regulation of the Cln3-Cdc28 kinase by cAMP in Saccharomyces cerevisiae. *EMBO J*. 17:4370-4378.

Hartwell, L.H., and M.W. Unger. 1977. Unequal division in *Saccharomyces cerevisiae* and its implications for the control of cell division. *J. Cell. Biol.* 75:422-435.

Harvey, S.L., A. Charlet, W. Haas, S.P. Gygi, and D.R. Kellogg. 2005. Cdk1-dependent regulation of the mitotic inhibitor Wee1. *Cell*. 122:407-420.

Harvey, S.L., G. Enciso, N.E. Dephoure, S.P. Gygi, J. Gunawardena, and D.R. Kellogg. 2011. A phosphatase threshold sets the level of Cdk1 activity in early mitosis. *Mol Biol. Cell*. 22:3595-3608.

Harvey, S.L., and D.R. Kellogg. 2003. Conservation of mechanisms controlling entry into mitosis: budding yeast wee1 delays entry into mitosis and is required for cell size control. *Curr. Biol.* 13:264-275.

Huttlin, E.L., M.P. Jedrychowski, J.E. Elias, T. Goswami, R. Rad, S.A. Beausoleil, J. Villen, W. Haas, M.E. Sowa, and S.P. Gygi. 2010. A tissue-specific atlas of mouse protein phosphorylation and expression. *Cell*. 143:1174-1189.

Janssens, V., and J. Goris. 2001. Protein phosphatase 2A: a highly regulated family of serine/threonine phosphatases implicated in cell growth and signalling. *Biochem J*. 353:417-439.

Johnston, G.C., J.R. Pringle, and L.H. Hartwell. 1977. Coordination of growth with cell division in the yeast *Saccharomyces cervisiae*. *Exp. Cell. res.* 105:79-98.

Jorgensen, P., J.L. Nishikawa, B.J. Breitkreutz, and M. Tyers. 2002. Systematic identification of pathways that couple cell growth and division in yeast. *Science*. 297:395-400.

Jorgensen, P., I. Rupes, J.R. Sharom, L. Schneper, J.R. Broach, and M. Tyers. 2004. A dynamic transcriptional network communicates growth potential to ribosome synthesis and critical cell size. *Genes Dev*. 18:2491-2505.

Jorgensen, P., and M. Tyers. 2004. How cells coordinate growth and division. *Curr Biol*. 14:R1014-1027.

Kellogg, D.R. 2003. Wee1-dependent mechanisms required for coordination of cell growth and cell division. *J Cell Sci*. 116:4883-4890.

Kellogg, D.R., and A.W. Murray. 1995. NAP1 acts with Clb2 to perform mitotic functions and suppress polar bud growth in budding yeast. *J. Cell Biol.* 130:675-685.

Kettenbach, A.N., and S.A. Gerber. 2011. Rapid and reproducible single-stage phosphopeptide enrichment of complex peptide mixtures: application to general and phosphotyrosine-specific phosphoproteomics experiments. *Analytical chemistry*. 83:7635-7644.

Laabs, T.L., D.D. Markwardt, M.G. Slattery, L.L. Newcomb, D.J. Stillman, and W. Heideman. 2003. ACE2 is required for daughter cell-specific G1 delay in Saccharomyces cerevisiae. *Proc Natl Acad Sci U S A*. 100:10275-10280.

Longtine, M.S., C.L. Theesfeld, J.N. McMillan, E. Weaver, J.R. Pringle, and D.J. Lew. 2000. Septin-dependent assembly of a cell cycle-regulatory module in Saccharomyces cerevisiae. *Mol. Cell. Biol.* 20:4049-4061.

Ma, X.J., Q. Lu, and M. Grunstein. 1996. A search for proteins that interact genetically with histone H3 and H4 amino termini uncovers novel regulators of the Swe1 kinase in Saccharomyces cerevisiae. *Genes Dev*. 10:1327-1340.

Mazanka, E., J. Alexander, B.J. Yeh, P. Charoenpong, D.M. Lowery, M. Yaffe, and E.L. Weiss. 2008. The NDR/LATS family kinase Cbk1 directly controls transcriptional asymmetry. *PLoS biology*. 6:e203.

Mazanka, E., and E.L. Weiss. 2010. Sequential counteracting kinases restrict an asymmetric gene expression program to early G1. *Mol Biol Cell*. 21:2809-2820.

McCusker, D., C. Denison, S. Anderson, T.A. Egelhofer, J.R. Yates, 3rd, S.P. Gygi, and D.R. Kellogg. 2007. Cdk1 coordinates cell-surface growth with the cell cycle. *Nat Cell Biol*. 9:506-515.

McCusker, D., A. Royou, C. Velours, and D. Kellogg. 2012. Cdk1-dependent control of membrane-trafficking dynamics. *Mol Biol Cell*. 23:3336-3347.

McMillan, J.N., M.S. Longtine, R.A.L. Sia, C.L. Theesfeld, E.S.G. Bardes, J.R. Pringle, and D.J. Lew. 1999. The morphogenesis checkpoint in Saccharomyces cerevisiae: cell cycle control of Swe1p degradation by Hsl1p and Hsl7p. *Molec. Cell Biol.* 19:6929-6939.

Moffat, J., and B. Andrews. 2004. Late-G1 cyclin-CDK activity is essential for control of cell morphogenesis in budding yeast. *Nat Cell Biol*. 6:59-66.

Mortensen, E., H. McDonald, J. Yates, and D.R. Kellogg. 2002. Cell cycle-dependent assembly of a Gin4-septin complex. *Molec. Biol. Cell*. 13:2091-2105.

Nash, R., G. Tokiwa, S. Anand, K. Erickson, and A.B. Futcher. 1988. The WHI1+ gene of Saccharomyces cerevisiae tethers cell division to cell size and is a cyclin homolog. *EMBO J.* 7:4335-4346.

Nasmyth, K., and L. Dirick. 1991. The role of SWI4 and SWI6 in the activity of G1 cyclins in yeast. *Cell*. 66:995-1013.

Newcomb, L.L., J.A. Diderich, M.G. Slattery, and W. Heideman. 2003. Glucose regulation of Saccharomyces cerevisiae cell cycle genes. *Eukaryotic cell*. 2:143-149.

Nurse, P. 1975. Genetic control of cell size at cell division in yeast. *Nature*. 256:547-551.

O'Conallain, C., M.T. Doolin, C. Taggart, F. Thornton, and G. Butler. 1999. Regulated nuclear localisation of the yeast transcription factor Ace2p controls

expression of chitinase (CTS1) in Saccharomyces cerevisiae. *Molecular & general genetics : MGG*. 262:275-282.

Ogas, J., B.J. Andrews, and I. Herskowitz. 1991. Transcriptional regulation of CLN1 and CLN2 and a putative new G1 cyclin (HCS26) by SWI4, a positive regulator of G1-specific transcription. *Cell*. 66:1015-1026.

Okuzaki, D., T. Watanabe, S. Tanaka, and H. Nojima. 2003. The Saccharomyces cerevisiae bud-neck proteins Kcc4 and Gin4 have distinct but partially-overlapping cellular functions. *Genes & genetic systems*. 78:113-126.

Polymenis, M., and E.V. Schmidt. 1997. Coupling of cell division to cell growth by translational control of the G1 cyclin CLN3 in yeast. *Genes Dev*. 11:2522-2531.

Pramila, T., S. Miles, D. GuhaThakurta, D. Jemiolo, and L.L. Breeden. 2002. Conserved homeodomain proteins interact with MADS box protein Mcm1 to restrict ECB-dependent transcription to the M/G1 phase of the cell cycle. *Genes Dev*. 16:3034-3045.

Rappsilber, J., Y. Ishihama, and M. Mann. 2003. Stop and go extraction tips for matrix-assisted laser desorption/ionization, nanoelectrospray, and LC/MS sample pretreatment in proteomics. *Analytical chemistry*. 75:663-670.

Richardson, H.E., C.W. Wittenberg, F. Cross, and S.I. Reed. 1989. An essential G1 function for cyclin-like proteins in yeast. *Cell*. 59:1127-1133.

Russell, P., and P. Nurse. 1987. Negative regulation of mitosis by wee1+, a gene encoding a protein kinase homolog. *Cell*. 49:559-567.

Sbia, M., E.J. Parnell, Y. Yu, A.E. Olsen, K.L. Kretschmann, W.P. Voth, and D.J. Stillman. 2008. Regulation of the yeast Ace2 transcription factor during the cell cycle. *The Journal of biological chemistry*. 283:11135-11145.

Shulewitz, M.J., C.J. Inouye, and J. Thorner. 1999. Hsl7 localizes to a septin ring and serves as an adapter in regulatory pathway that relieves tyrosine phosphorylation of Cdc28 protein kinase in Saccharomyces cerevisiae. *Mol. Cell. Biol.* 19:7123-7137.

Sreenivasan, A., and D. Kellogg. 1999. The Elm1 kinase functions in a mitotic signaling network in budding yeast. *Mol. Cell. Biol.* 19:7983-7994.

Turner, J.J., J.C. Ewald, and J.M. Skotheim. 2012. Cell size control in yeast. *Current biology : CB*. 22:R350-359.

Tyers, M., G. Tokiwa, R. Nash, and B. Futcher. 1992. The Cln3-Cdc28 kinase complex of S. cerevisiae is regulated by proteolysis and phosphorylation. *EMBO J.* 11:1773-1784.

Verges, E., N. Colomina, E. Gari, C. Gallego, and M. Aldea. 2007. Cyclin Cln3 is retained at the ER and released by the J chaperone Ydj1 in late G1 to trigger cell cycle entry. *Mol Cell*. 26:649-662.

Villen, J., and S.P. Gygi. 2008. The SCX/IMAC enrichment approach for global phosphorylation analysis by mass spectrometry. *Nature protocols*. 3:1630-1638.

Voth, W.P., Y. Yu, S. Takahata, K.L. Kretschmann, J.D. Lieb, R.L. Parker, B. Milash, and D.J. Stillman. 2007. Forkhead proteins control the outcome of transcription factor binding by antiactivation. *EMBO J*. 26:4324-4334.

Weiss, E.L., C. Kurischko, C. Zhang, K. Shokat, D.G. Drubin, and F.C. Luca. 2002. The Saccharomyces cerevisiae Mob2p-Cbk1p kinase complex promotes polarized growth and acts with the mitotic exit network to facilitate daughter cell-specific localization of Ace2p transcription factor. *J Cell Biol*. 158:885-900.

Yaglom, J.A., A.L. Goldberg, D. Finley, and M.Y. Sherman. 1996. The molecular chaperone Ydj1 is required for the p34CDC28-dependent phosphorylation of the cyclin Cln3 that signals its degradation. *Mol Cell Biol*. 16:3679-3684.

Young, P.G., and P.A. Fantes. 1987. Schizosaccharomyces pombe mutants affected in their division response to starvation. *J. Cell Sci.* 88:295-304.

Yu, H.G., and D. Koshland. 2007. The Aurora kinase Ipl1 maintains the centromeric localization of PP2A to protect cohesin during meiosis. *J Cell Biol*. 176:911-918.

Zhao, Y., G. Boguslawski, R.S. Zitomer, and A.A. DePaoli-Roach. 1997. Saccharomyces cerevisiae homologs of mammalian B and B' subunits of protein phosphatase 2A direct the enzyme to distinct cellular functions. *The Journal of biological chemistry*. 272:8256-8262.

Table I: Ace2 Phosphorylation Sites

Site	local sequence	#Identified Peptides	#Quantified Peptides	#Replicates Quantified	Avg Ratio	Std Dev
S122	SHKRGL**S**GTAIFG	2	2	2	2.51	0.72
T135	FLGHNK**T**LSISSL	1	1	1	2.41	
S137	GHNKTL**S**ISSLQQ	2	0	0		
S140	KTLSIS**S**LQQSIL	3	0	0		
T245	KLVSGA**T**NSNSKP	6	2	1	2.44	
S249	GATNSN**S**KPGSPV	6	5	2	0.93	0.02
S253	SNSKPG**S**PVILKT	8	7	2	1.43	0.73
S709	KKSLLD**S**PHDTSP	9	9	3	1.54	0.29
T713	LDSPHD**T**SPVKET	9	7	2	1.62	0.24
S714	DSPHDT**S**PVKETI	4	4	2	1.27	0.05

The table shows all identified and quantified phosphosites in Ace2. Six sites were identified in two out of three biological replicates and out of those six, four showed increased phosphorylation above the log2 threshold: S122, S253, S709 and T713. Bold letters represent the identified phosphosite and its surrounding amino acids.

Table II: Strains used in this study

Strain	*MAT*	Genotype	Reference or Source
DK186	a	*bar1*	Altman *et al*., 1997
DK351	a	*bar1 cdk1::cdk1-as1*	Bishop *et al*., 2000
DK647	a	*bar1 rts1Δ::kanMX6*	Artiles *et al*., 2009
DK751	a	*bar1 CLN2-3XHA::LEU2 rts1Δ::kanMX6*	Artiles *et al*., 2009
DK968	a	*bar1 cdk1::cdk1-as1 rts1Δ::HIS*	Bishop *et al*., 2000
DK1307	a	*bar1 CLN2-3XHA::LEU2 rts1Δ::HIS*	Artiles *et al*., 2009
DK1907	a	*bar1 CLN2-3XHA::LEU2 rts1Δ::HIS ace2Δ::kanMX4*	This study
DK1908	a	*bar1 CLN2-3XHA::LEU2 ace2Δ::kanMX4*	This study
DK1929	a	*bar1 CLN2-3XHA::LEU2 GAL1-ACE2::HIS5*	This study
DK1930	a	*bar1 CLN2-3XHA::LEU2 GAL1-ACE2::HIS5 rts1Δ::kanMX6*	This study
DK2010	a	*bar1* pDK93A [*GAL1-CLN3::URA*]	This study
DK2011	a	*bar1* pDK93A [*GAL1-CLN3::URA*] *rts1Δ::kanMX4*	This study
DK2017	a	*bar1 CLN3-6XHA::HIS*	This study
DK2019	a	*bar1 CLN3-6XHA::HIS rts1Δ::kanMX4*	This study
DK2049	a	*bar1 CLN3-6XHA::HIS rts1Δ::kanMX4 ace2Δ::hphNT1*	This study
DK2053	a	*bar1 CLN2-3XHA::LEU GAL1-YOX1::HIS*	This study
DK2054	a	*bar1 CLN2-3XHA::LEU GAL1-YOX1::HIS rts1Δ::kanMX4*	This study
DK2055	a	*bar1 CLN3-6XHA::HIS ace2Δ::natMX4*	This study
DK2056	a	*bar1 GAL1-CDC20::NatNT2 CLN3-6XHA::HIS*	This study
DK2057	a	*bar1 GAL1-CDC20::NatNT2 CLN3-6XHA::HIS rts1Δ::kanMX4*	This study
DK2058	a	*bar1 GAL1-CDC20::NatNT2 CLN3-6XHA::HIS rts1Δ::kanMX4 ace2Δ::hphNT1*	This study
DK2093	a	*bar1 cbk1Δ::HIS*	This study
DK2136	a	*bar1 GAL1-CDC20::NatNT2 CLN3-6XHA::HIS ace2Δ::kanMX4*	This study
DK2149	a	*bar1 ACE2-GFP::klTRP rts1Δ::kanMX4*	This study
DK2171	a	*bar1 cbk1Δ::HIS rts1Δ::kanMX4*	This study
DK2490	a	*bar1 ACE2-3XHA::kanMX6 cbk1Δ::HIS*	This study
DY150	a		Thomas *et al*., 1989
DY151	α		Thomas *et al*., 1989
DY3924	α	*ace2Δ::HIS3 lys2*	This study
DY5923	a	*ACE2-MYC(13)::kanMX*	This study
DY8309	a	*ASH1-MYC(13)::kanMX*	Takahata *et al*., 2011
DY9719	a	*ash1Δ::TRP1 lys2 met15*	This study
DY10788	a	*GAL1-CDC20::ADE2 lys2*	Sbia *et al*., 2008
DY15549	a	*GAL1-CDC20::ADE2 lys2 ace2::HIS3*	This study
DY15723	α	*rts1Δ::kanMX lys2*	This study
DY15729	α	*ace2Δ::HIS rts1Δ::kanMX6 lys2 met15*	This study
DY15995	a	*GAL1-CDC20::ADE2 lys2 rts1::kanMX lys2*	This study
DY15996	a	*GAL1-CDC20::ADE2 lys2 rts1::kanMX ace2::HIS3 lys2*	This study
DY16269	a	*ACE2-MYC(13)::kanMX rts1Δ::hphMX4*	This study
DY16273	a	*ASH1-MYC(13)::kanMX rts1Δ::hphMX4 lys2*	This study
DY17134	a	*GAL1-CDC20::ADE2 yox1::natMX*	This study
DY17236	a	*GAL1-CDC20::ADE2 yox1::natMX ace2Δ::HIS3*	This study
DY17240	a	*GAL1-CDC20::ADE2 yox1::natMX rts1Δ::kanMX*	This study
DY17242	a	*GAL1-CDC20::ADE2 yox1::natMX rts1Δ::kanMX ace2Δ::HIS*	This study
ZZ41	a	*bar1 CLN2-3XHA::LEU2*	Artiles *et al*., 2009

Figure 1: A phosphoproteomic screen for proteins regulated by $PP2A^{Rts1}$.

(A) A schematic summary of the approach used to search for targets of $PP2A^{Rts1}$. (B) A total of 9,255 sites were quantified in three biological replicates. The overlap of sites quantified from each replicate is shown. (C) The log2 distribution of 5159 sites quantified in at least two replicates. The areas outside the dotted lines indicate sites that change by two standard deviations or greater. The log2 distribution of the 2702 quantified proteins is shown in the inset.

Figure 1

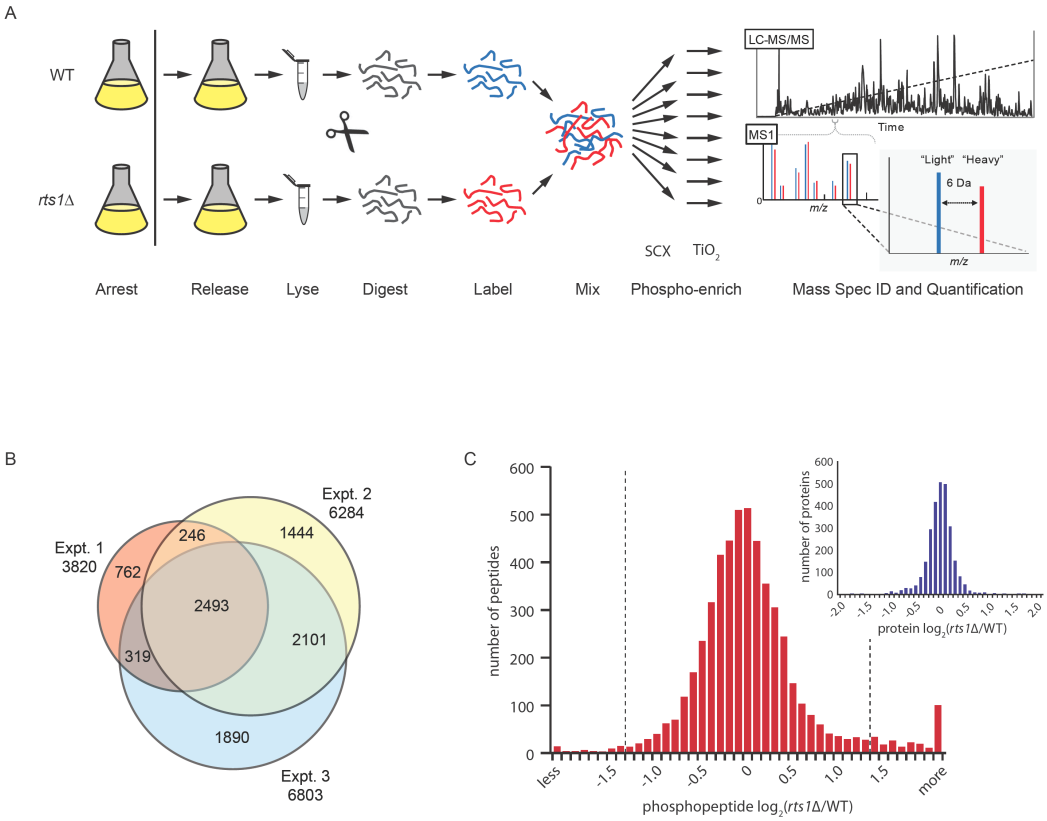
A
WT
rts1Δ
LC-MS/MS
Time
MS1
m/z
"Light" "Heavy"
6 Da
m/z
SCX
TiO2
Arrest
Release
Lyse
Digest
Label
Mix
Phospho-enrich
Mass Spec ID and Quantification
B
Expt. 1
3820
Expt. 2
6284
Expt. 3
6803
246
1444
762
2493
2101
319
1890
C
number of peptides
600
500
400
300
200
100
0
less
-1.5
-1.0
-0.5
0
0.5
1.0
1.5
more
phosphopeptide log2(rts1Δ/WT)
number of proteins
protein log2(rts1Δ/WT)
-2.0

Figure 2: The Ace2 transcription factor is hyperphosphorylated in *rts1*Δ cells. (A) Cells were released from a G1 arrest and the behavior of Ace2 and Clb2 was assayed by western blot. (B) The same samples shown in Figure 2B were loaded in an intercalated manner to visualize differences in Ace2 between wild type and *rts1*Δ cells. (C) Cells were released from a metaphase arrest and the behavior of Ace2 and Clb2 was assayed by western blot.

Figure 2

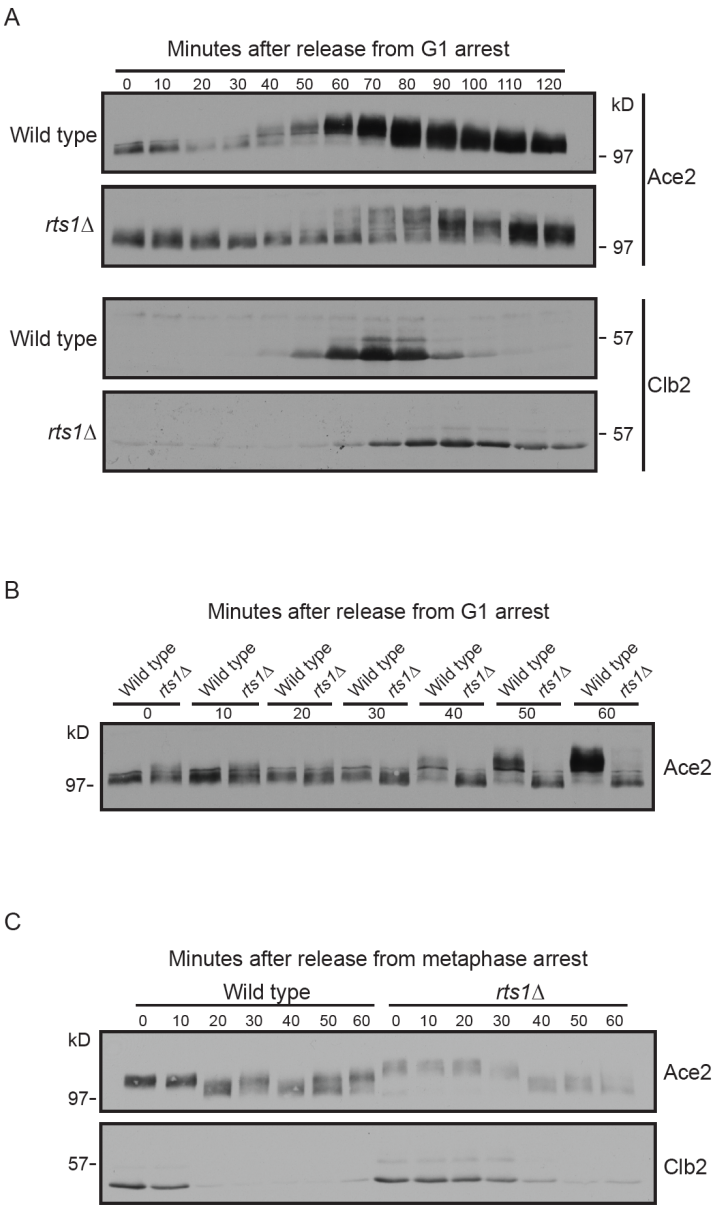
A
Minutes after release from G1 arrest
0 10 20 30 40 50 60 70 80 90 100 110 120
kD
Wild type
97
Ace2
rts1Δ
97
Wild type
57
Clb2
rts1Δ
57
B
Minutes after release from G1 arrest
Wild type
rts1Δ
0 10 20 30 40 50 60
kD
97-
Ace2
C
Minutes after release from metaphase arrest
Wild type
rts1Δ
0 10 20 30 40 50 60 0 10 20 30 40 50 60
kD
97-
Ace2
57-
Clb2

Figure 3: Multiple kinases contribute to hyperphosphorylation of Ace2 in *rts1*Δ cells.

(A) Samples were taken at the indicated times after addition of 1NM-PP1 to log phase cells and phosphorylation of Ace2 was assayed by western blot. (B) Ace2-3XHA was immunoprecipitated from wild type, *rts1*Δ or *cbk1*Δ cells and probed with anti-Ace2 antibody or with an antibody that recognizes phosphorylated S122. Ace2-3XHA was immunoprecipitated from the *cbk1*Δ cells as a control to demonstrate that the phospho-specific antibody recognizes a site phosphorylated by Cbk1. (C) Kinase reactions containing affinity purified Ace2-3XHA, Cbk1-3XHA and Cdk1/Clb2-3XHA in the indicated combinations were initiated by addition of ATP. Ace2-3XHA phosphorylation was assayed by western blotting with anti-HA mouse monoclonal antibody. (D) Cells were grown to log phase at room temperature and Ace2 phosphorylation was assayed by western blot. The arrow indicates a hyperphosphorylated form of Ace2.

Figure 3

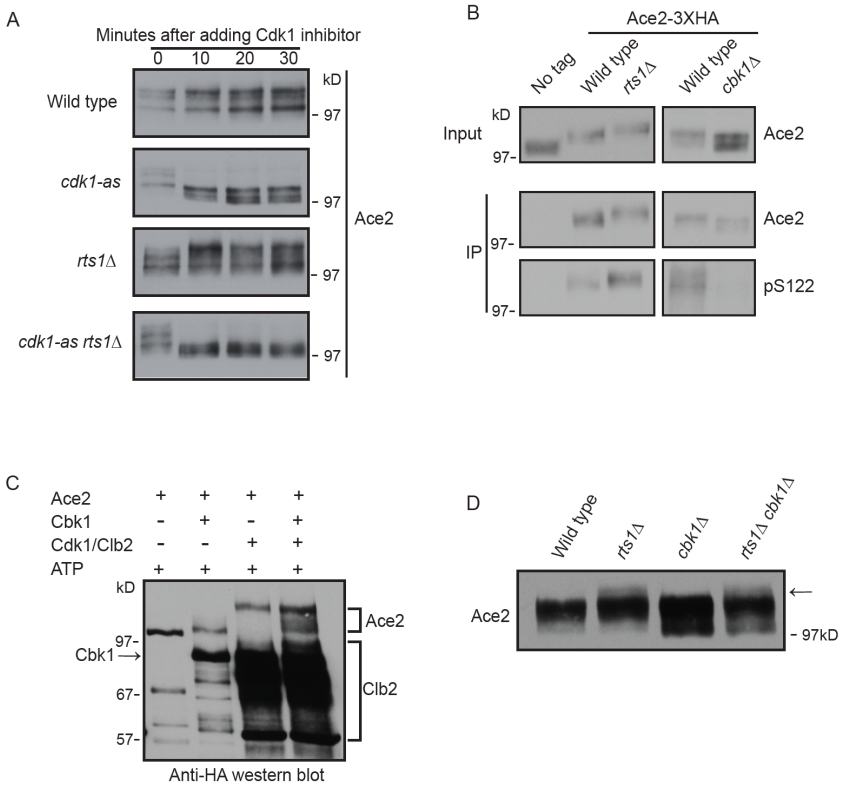
A
Minutes after adding Cdk1 inhibitor
0 10 20 30
kD
Wild type
cdk1-as
rts1Δ
cdk1-as rts1Δ
97
Ace2
B
Ace2-3XHA
No tag
Wild type
rts1Δ
Wild type
cbk1Δ
Input
kD
97-
Ace2
IP
97-
Ace2
pS122
C
Ace2 + + + +
Cbk1 - + - +
Cdk1/Clb2 - - + +
ATP + + + +
kD
97-
Cbk1
67-
57-
Ace2
Clb2
Anti-HA western blot
D
Wild type
rts1Δ
cbk1Δ
rts1Δ cbk1Δ
Ace2
97kD

Figure 4: Genetic analysis suggests that PP2A^{Rts1} is a negative regulator of Ace2.

(A) A series of 5-fold dilutions of cells were grown on YPD media at 30˚C or 37˚C. (B) Eight independent colonies grown overnight at 23°C were diluted into fresh medium and grown in a Bioscreen C apparatus. The average growth of the eight cultures was plotted, with standard deviations shown**.** (C) A series of 5-fold dilutions of cells were grown at 30˚C on YEP media containing either dextrose or galactose.

Figure 4

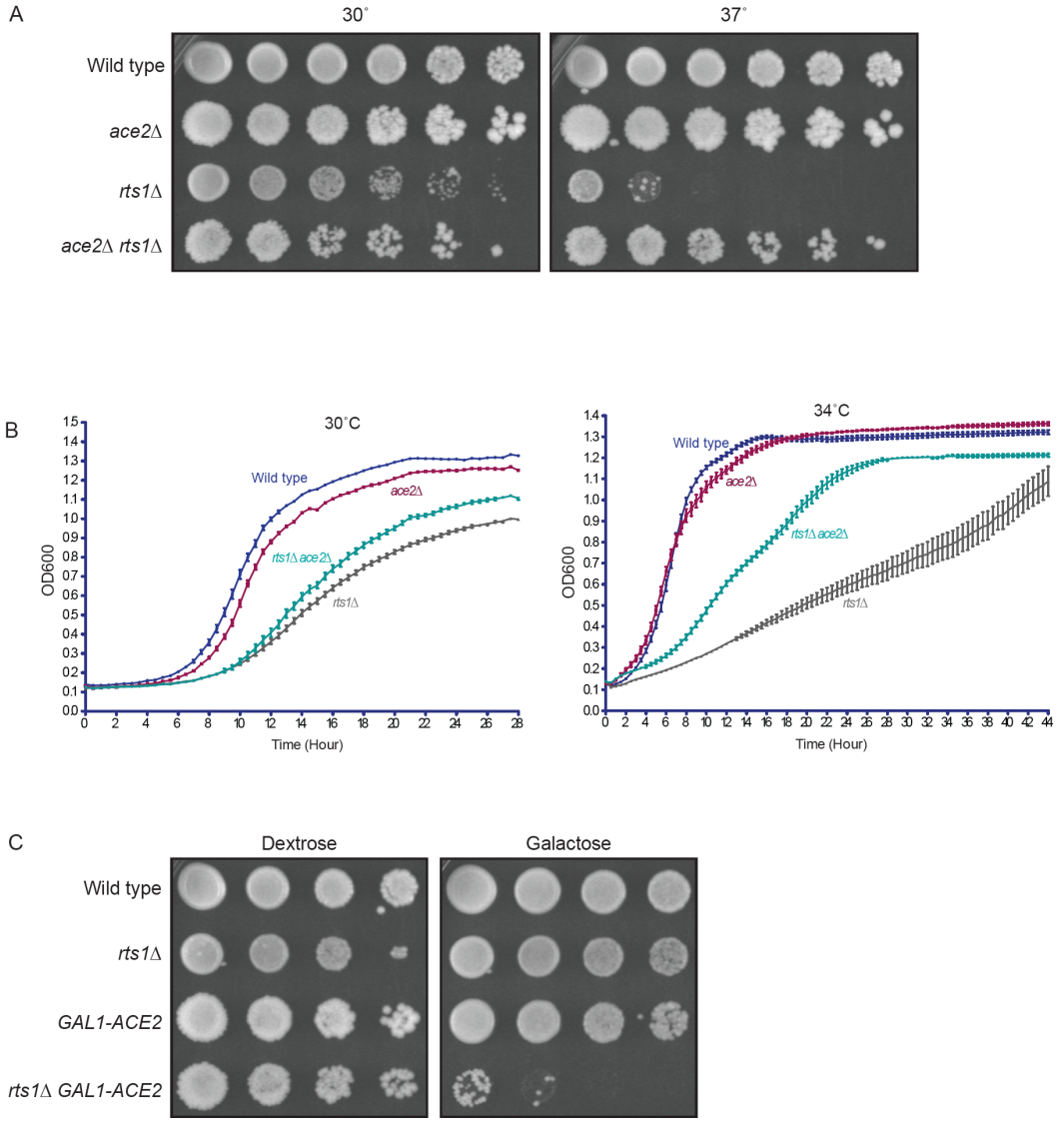
A
30˚
37˚
Wild type
ace2Δ
rts1Δ
ace2Δ rts1Δ
B
30˚C
34˚C
Wild type
ace2Δ
rts1Δ ace2Δ
rts1Δ
OD600
Time (Hour)
C
Dextrose
Galactose
Wild type
rts1Δ
GAL1-ACE2
rts1Δ GAL1-ACE2

Figure 5: Overexpression of *CLN3* partially rescues the cell size defects caused by *rts1*Δ.

Cells were grown to log phase in media containing 2% galactose and cell size distributions were determined using a Coulter counter. Each plot represents the average of three independent biological replicates in which three independent samples were analyzed for each strain.

Figure 5

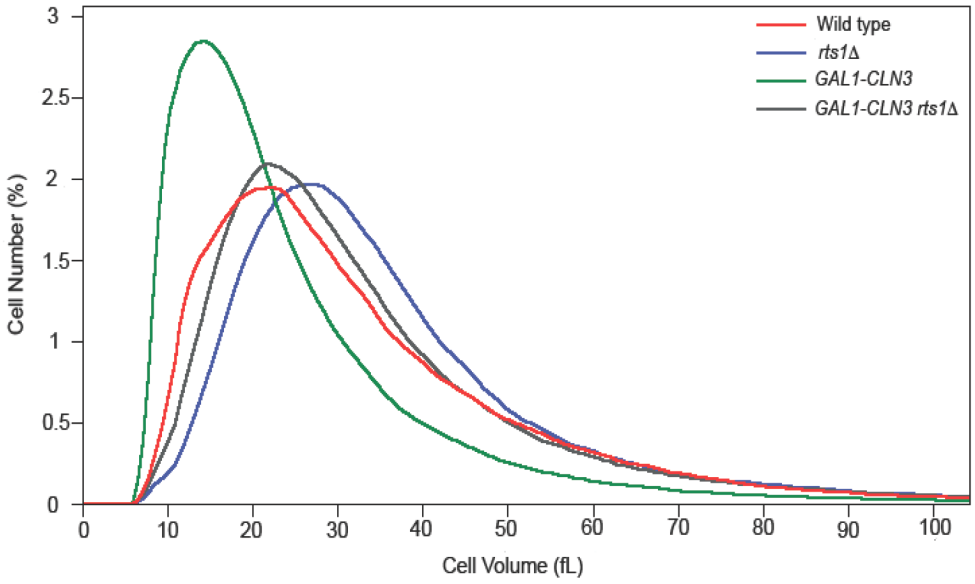
Wild type
rts1Δ
GAL1-CLN3
GAL1-CLN3 rts1Δ
Cell Number (%)
Cell Volume (fL)
0
0.5
1
1.5
2
2.5
3
0
10
20
30
40
50
60
70
80
90
100

Figure 6: $PP2A^{Rts1}$ is required for normal control of *CLN3* mRNA and protein levels in cells released from a G1 arrest.

(A-D) Wild type, *rts1*Δ, *ace2*Δ, and *rts1*Δ *ace2*Δ cells were released from G1 arrest at 30˚C and the level of *CLN3* mRNA was assayed by northern blotting (A) or qRT-PCR (B). Independent samples were probed for Cln3-6XHA (C) and Clb2 (D) by western blot. The Cln3-6XHA and Clb2 western blots were from the same samples to allow direct comparison of the timing of cell cycle events. Loading controls for the northern blot and the western blots are shown Figure S2.

Figure 6

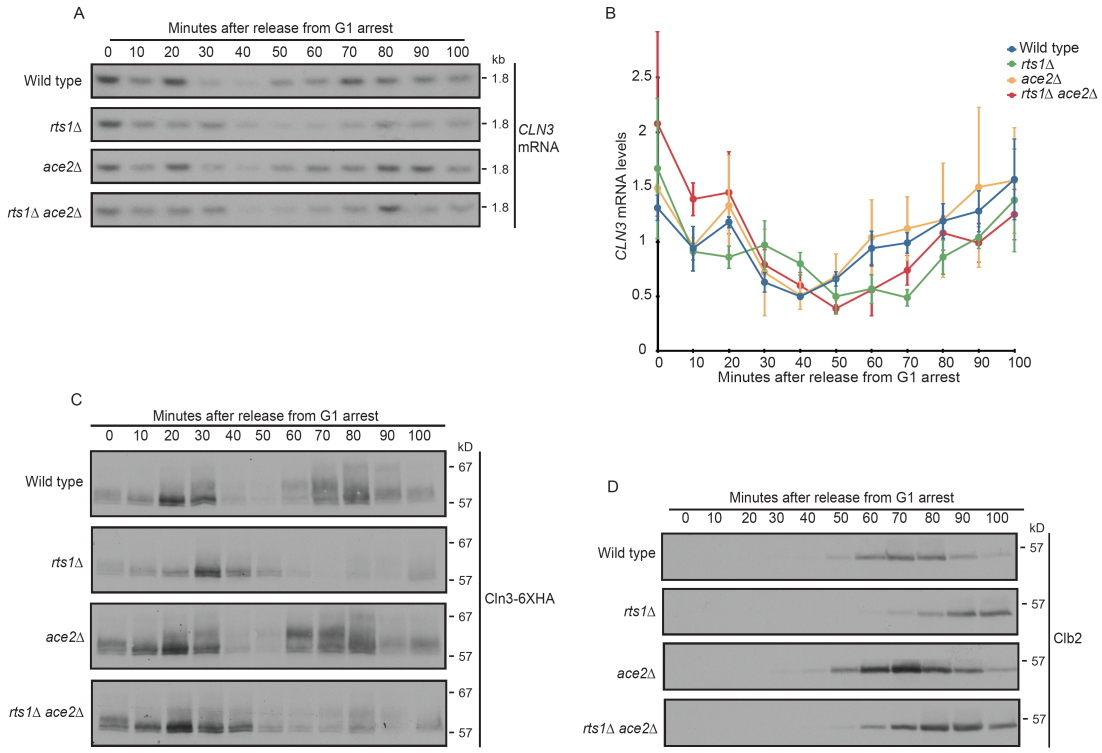
A
Minutes after release from G1 arrest
0 10 20 30 40 50 60 70 80 90 100
kb
Wild type
rts1Δ
ace2Δ
rts1Δ ace2Δ
1.8
CLN3 mRNA
B
Wild type
rts1Δ
ace2Δ
rts1Δ ace2Δ
CLN3 mRNA levels
0 0.5 1 1.5 2 2.5
0 10 20 30 40 50 60 70 80 90 100
Minutes after release from G1 arrest
C
Minutes after release from G1 arrest
0 10 20 30 40 50 60 70 80 90 100
kD
Wild type
rts1Δ
ace2Δ
rts1Δ ace2Δ
67
57
Cln3-6XHA
D
Minutes after release from G1 arrest
0 10 20 30 40 50 60 70 80 90 100
kD
Wild type
rts1Δ
ace2Δ
rts1Δ ace2Δ
57
Clb2

Figure 7: $PP2A^{Rts1}$ is required for normal control of *CLN3* mRNA and protein levels in cells released from a metaphase arrest.

(A-C) *GAL-CDC20*, *GAL-CDC20 rts1*Δ, *GAL-CDC20 ace2*Δ and *GAL-CDC20 ace2*Δ *rts1*Δ cells were released from a metaphase arrest at 30˚C and samples were analyzed by qRT-PCR (A). Independent samples were probed for Cln3-6XHA (B) and Clb2 (C) by western blot. The Cln3-6XHA and Clb2 western blots were from the same samples to allow direct comparison of the timing of cell cycle events. (D) Cell growth rate was analyzed using a Bioscreen C apparatus. (E) A series of 10-fold dilutions of cells were grown at 25˚C on YEP media containing either dextrose or galactose.

Figure 7

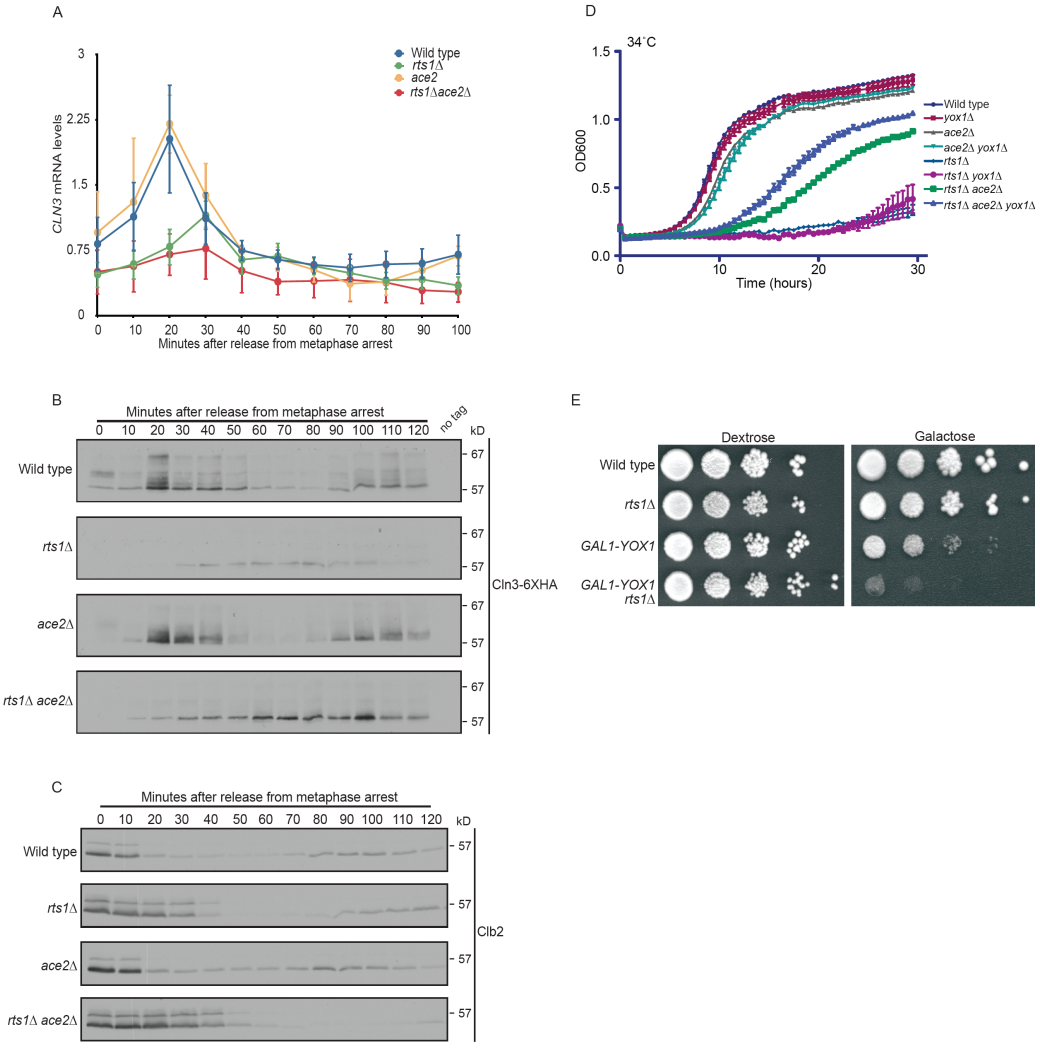
A
Wild type
rts1Δ
ace2
rts1Δace2Δ
CLN3 mRNA levels
Minutes after release from metaphase arrest
B
Minutes after release from metaphase arrest
no tag
kD
Wild type
rts1Δ
ace2Δ
rts1Δ ace2Δ
Cln3-6XHA
C
Minutes after release from metaphase arrest
kD
Wild type
rts1Δ
ace2Δ
rts1Δ ace2Δ
Clb2
D
34˚C
OD600
Time (hours)
Wild type
yox1Δ
ace2Δ
ace2Δ yox1Δ
rts1Δ
rts1Δ yox1Δ
rts1Δ ace2Δ
rts1Δ ace2Δ yox1Δ
E
Dextrose
Galactose
Wild type
rts1Δ
GAL1-YOX1
GAL1-YOX1 rts1Δ

Figure 8: $PP2A^{Rts1}$ is required for normal control of *CTS1* mRNA levels

Wild type, *rts1*Δ, *ace2*Δ, and *rts1*Δ *ace2*Δ cells were released from a G1 arrest at 30˚C and the behavior of *CTS1* mRNA was assayed by qRT-PCR.

Figure 8

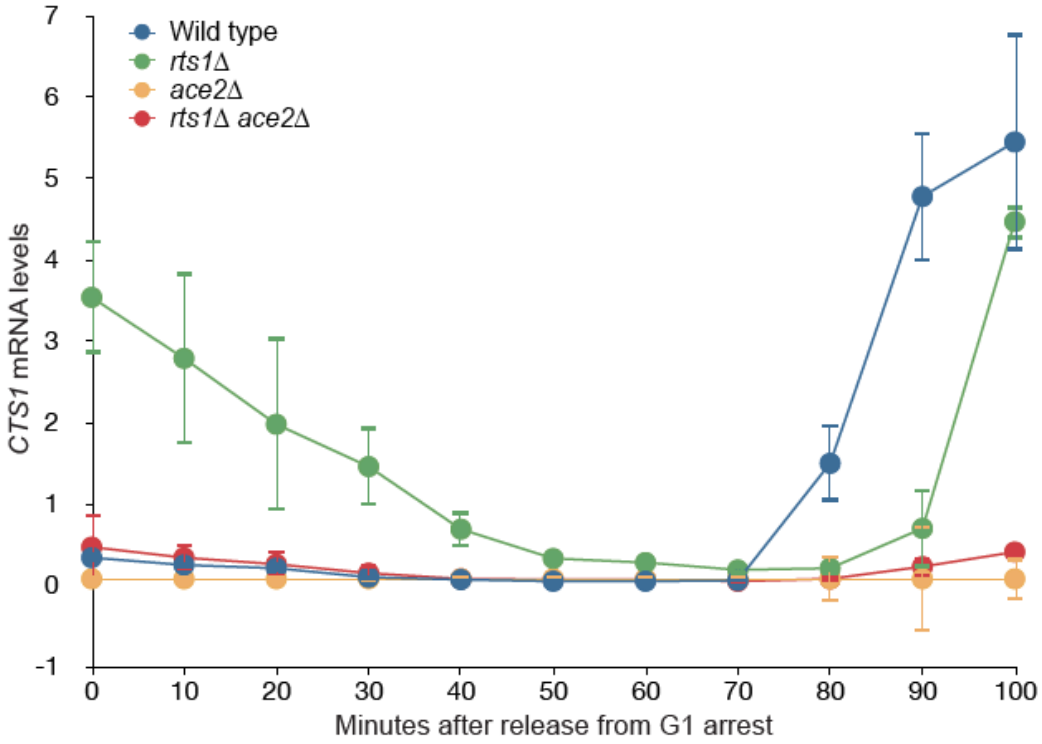
Wild type
rts1Δ
ace2Δ
rts1Δ ace2Δ
CTS1 mRNA levels
7
6
5
4
3
2
1
0
-1
0
10
20
30
40
50
60
70
80
90
100
Minutes after release from G1 arrest

Figure 9: Loss of PP2A^{Rts1} causes increased binding of Ash1 to the *CLN3* promoter.

ChIP experiments were performed using Ace2-Myc, Ash1-Myc, or untagged control strains. Transcription factor binding was measured for two regions of the *CLN3* promoter, *CLN3*-A (-1026 to -830) and *CLN3*-B (-853 to -642), in distance from the ATG. Data from at least three replicates were analyzed by an unpaired two-tailed t test to test for statistically significant differences.

Figure 9

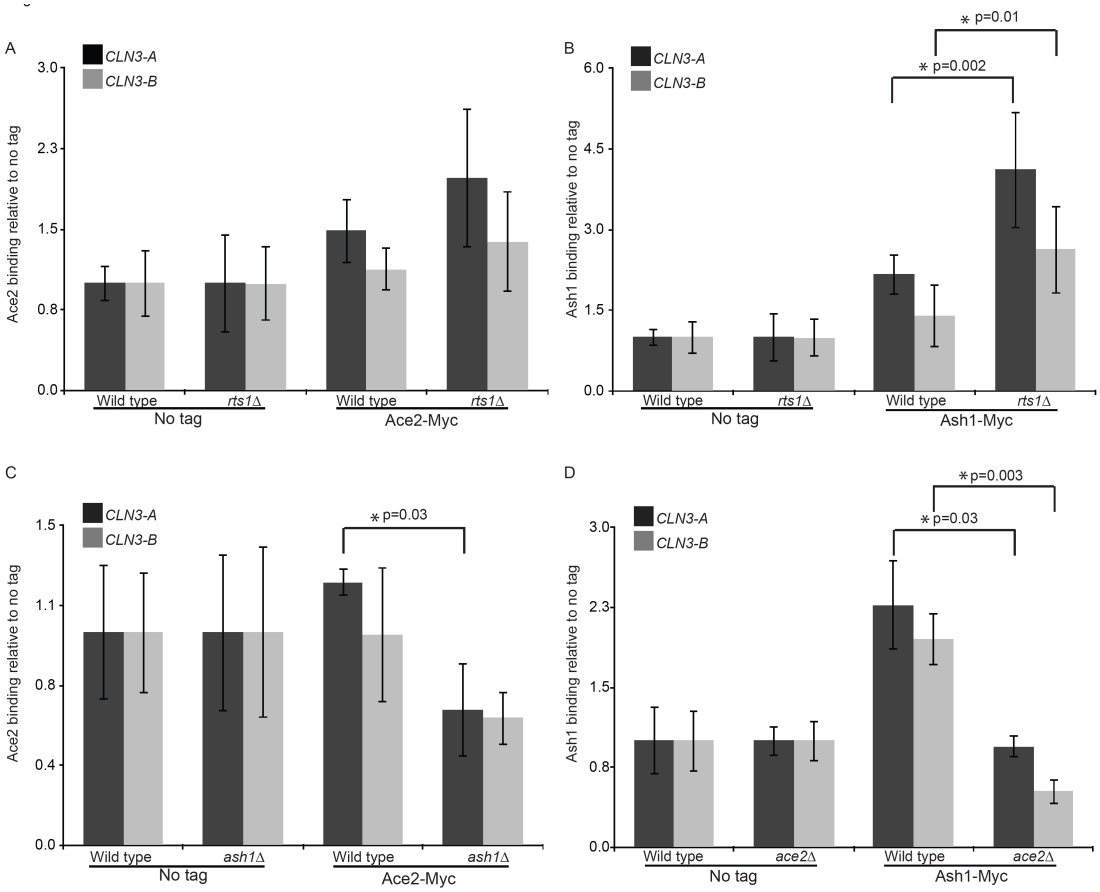
A
CLN3-A
CLN3-B
Ace2 binding relative to no tag
3.0
2.3
1.5
0.8
0.0
Wild type
rts1Δ
Wild type
rts1Δ
No tag
Ace2-Myc
B
CLN3-A
CLN3-B
∗ p=0.01
∗ p=0.002
Ash1 binding relative to no tag
6.0
4.5
3.0
1.5
0.0
Wild type
rts1Δ
Wild type
rts1Δ
No tag
Ash1-Myc
C
CLN3-A
CLN3-B
∗ p=0.03
Ace2 binding relative to no tag
1.5
1.1
0.8
0.4
0.0
Wild type
ash1Δ
Wild type
ash1Δ
No tag
Ace2-Myc
D
CLN3-A
CLN3-B
∗ p=0.003
∗ p=0.03
Ash1 binding relative to no tag
3.0
2.3
1.5
0.8
0.0
Wild type
ace2Δ
Wild type
ace2Δ
No tag
Ash1-Myc

Figure 10: Ace2 is hyperphosphorylated in small unbudded daughter cells.

Small unbudded cells in G1 were isolated by centrifugal elutriation and released into YPD medium at 25˚C. (A) Cell size was analyzed using a Coulter counter and plotted as a function of time. (B) The percentage of budded cells was plotted as a function of time. (C) Ace2 phosphorylation and Cln3-6XHA levels were assayed by Western blot. All samples in A-C were taken from the same time course. (D) Samples from an independent time course were probed for *CLN3* mRNA. The same membrane was probed for *ACT1* mRNA as a loading control. E) A model for $PP2A^{Rts1}$- dependent mechanisms that control *CLN3* transcription via Ace2. For simplicity, mitotic regulation of Ace2 by Cdk1 is not shown in the model.

Figure 10

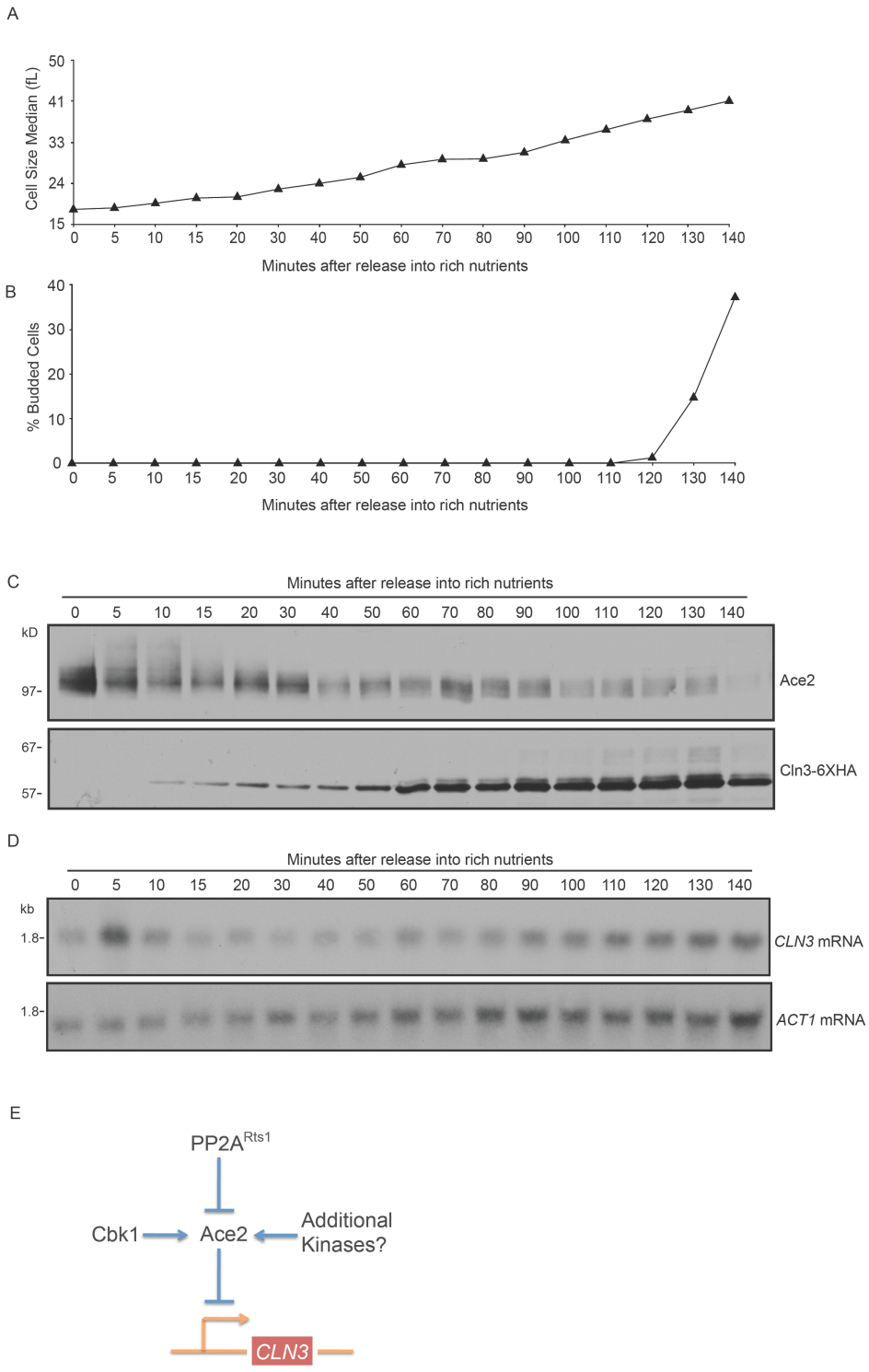
A
Cell Size Median (fL)
50
41
33
24
15
0 5 10 15 20 30 40 50 60 70 80 90 100 110 120 130 140
Minutes after release into rich nutrients
B
% Budded Cells
40
30
20
10
0
0 5 10 15 20 30 40 50 60 70 80 90 100 110 120 130 140
Minutes after release into rich nutrients
C
Minutes after release into rich nutrients
0 5 10 15 20 30 40 50 60 70 80 90 100 110 120 130 140
kD
97-
Ace2
67-
57-
Cln3-6XHA
D
Minutes after release into rich nutrients
0 5 10 15 20 30 40 50 60 70 80 90 100 110 120 130 140
kb
1.8-
CLN3 mRNA
1.8-
ACT1 mRNA
E
PP2A^Rts1
Cbk1
Ace2
Additional Kinases?
CLN3

Figure S1: **Phosphopeptide quantification.**
(A) A narrow region of a single MS1 scan corresponding to a doubly phosphorylated Ace2p peptide is shown. Both heavy (541.9324) and light (537.9073) forms of the peptide, derived from *rts1*Δ and wild type samples respectively, were observed. (B) Multiple scans like that shown in (A), taken as the peptides eluted off the reverse-phase column and entered the mass spectrometer over time were used to generate extracted ion chromatograms for the heavy and light peptide species. The ratio of the calculated areas under the curve provide a relative abundance measurement.

Figure S1

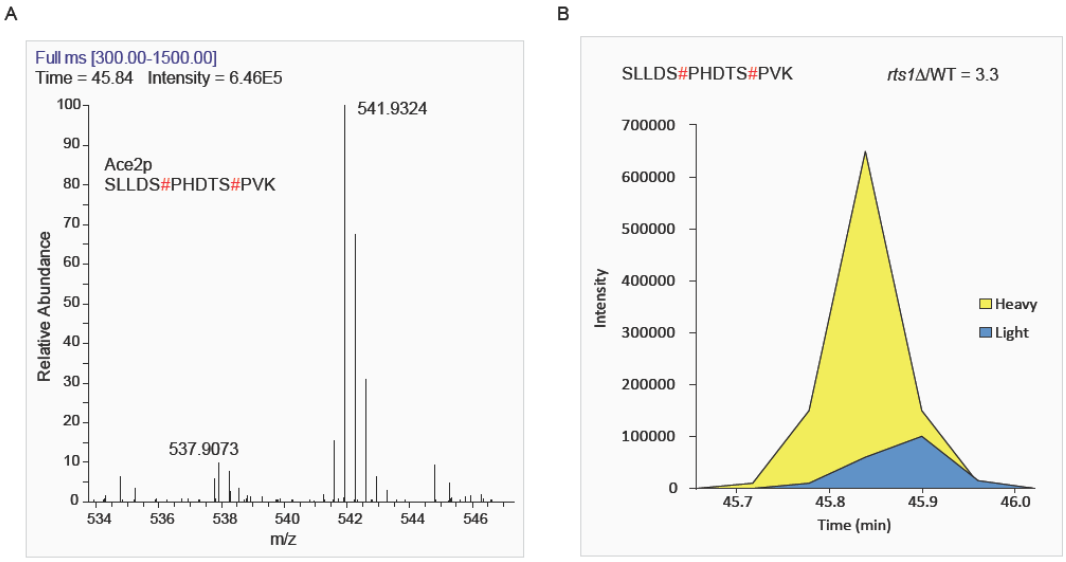
A
Full ms [300.00-1500.00]
Time = 45.84 Intensity = 6.46E5
541.9324
Ace2p
SLLDS#PHDTS#PVK
537.9073
Relative Abundance
m/z
B
SLLDS#PHDTS#PVK
rts1Δ/WT = 3.3
Intensity
Time (min)
Heavy
Light

Figure S2: Loading Controls

(A) Loading controls for the *CLN3* northern blots shown in Figure 6A were carried out by probing the same membrane for *ACT1* mRNA. (B) Loading controls for the Cln3-6XHA western blots in Figures 6C and 6D were generated by probing for Nap1.

Figure S2

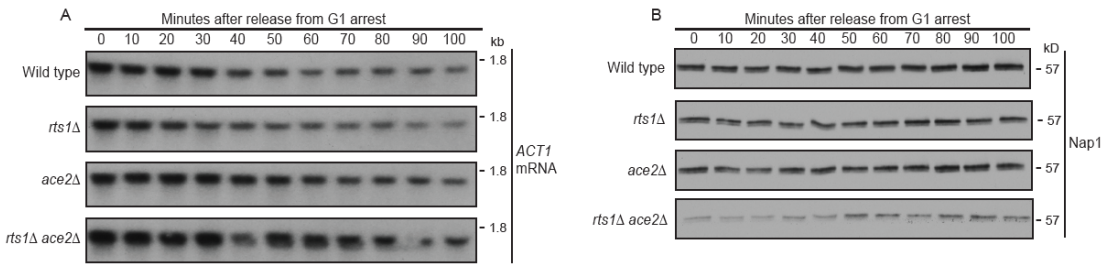
A
Minutes after release from G1 arrest
0 10 20 30 40 50 60 70 80 90 100
kb
Wild type
rts1Δ
ace2Δ
rts1Δ ace2Δ
1.8
1.8
1.8
1.8
ACT1 mRNA
B
Minutes after release from G1 arrest
0 10 20 30 40 50 60 70 80 90 100
kD
Wild type
rts1Δ
ace2Δ
rts1Δ ace2Δ
57
57
57
57
Nap1

CHAPTER III

$PP2A^{Rts1}$ IS REGULATED BY THE CONSERVED PDK1 PATHWAY

ABSTRACT

Nutrient modulation of cell size is thought to play an important role in cell size control, yet the pathways that link nutrient sensing and cell size with entry into the cell cycle are poorly understood. A specific form of protein phosphatase 2A (PP2A) associated with the Rts1 regulatory subunit ($PP2A^{Rts1}$) is required for nutrient modulation of cell size in budding yeast, yet little is known about the signals that control $PP2A^{Rts1}$. We set out to characterize regulation of Rts1 and found that Rts1 phosphorylation is dependent on the budding yeast homologs of vertebrate phosphoinositide-dependent kinase 1 (PDK1) and protein kinase C (PKC). We also found that hyperphosphorylation of Rts1 in response to poor nutrients is dependent on PDK1, PKC and casein kinase 1. Together these results suggest a complex signaling network comprised of conserved kinases and phosphatases that act together to sense nutrient availability and possibly to achieve proper nutrient-modulation of cell size.

INTRODUCTION

The ability of cells to maintain a specific size is essential for their survival and function, yet the molecular mechanisms involved are poorly understood (Jorgensen and Tyers, 2004). Cell size checkpoints control cell size by ensuring that key cell cycle transitions are initiated only when sufficient growth has occurred. In budding yeast, cell size is controlled by two major cell size checkpoints that act in G1 and entry into mitosis.

The G1 cell size checkpoint is thought to work through regulation of G1 cyclin transcription (Cross, 1990; Richardson et al., 1989). Transcription of late G1 cyclins Cln1 and Cln2 is dependent on transcription factor SBF, which is composed of Swi4 and Swi6. Before cells reach a critical size, SBF is kept inactive by a repressor called Whi5. When sufficient growth has occurred, Cdk1/Cln3 triggers transcription of late G1 cyclins by phosphorylating and inhibiting Whi5 (Costanzo et al., 2004; de Bruin et al., 2004). Loss of Whi5 causes premature transcription of late G1 cyclins, leading to premature entry into the cell cycle and reduced cell size, suggesting that the mechanisms that control timing of late G1 cyclin transcription are likely to play a critical role in regulating cell size. In the absence of Cln3, late G1 cyclin transcription is delayed but is eventually triggered by a poorly understood mechanism that works through the Bck2 protein (Di Como et al., 1995; Epstein and Cross, 1994).

A second cell size checkpoint monitors bud growth at entry into mitosis and is likely regulated by the Wee1 kinase and Cdc25 phosphatase (Nurse, 1975; Nurse et al., 1976). Wee1 phosphorylates and inhibits Cdk1, delaying entry into mitosis, whereas Cdc25 promotes mitotic entry by removing this inhibitory phosphorylation (Dunphy and Kumagai, 1991; Gautier et al., 1991; Gould and Nurse, 1989; Kumagai

and Dunphy, 1991; Russell and Nurse, 1986). Loss of Wee1 causes premature entry into mitosis resulting in small cell size (Nurse, 1975). Conversely, mutations in Cdc25 result in delayed entry into mitosis and a large cell size phenotype (Nurse, 1975; Russell and Nurse, 1986).

Although some components involved in cell size checkpoints are known, the molecular mechanisms involved in sensing and relaying cell size information are unknown. In an effort to find components acting upstream of cell size checkpoints we focused on the highly conserved serine-threonine phosphatase PP2A. PP2A plays a central role in regulating a variety of cell functions (Artiles et al., 2009; Chan and Amon, 2009; Healy et al., 1991; Lin and Arndt, 1995; Ronne et al., 1991). It is a trimeric complex comprised of a catalytic subunit, a scaffolding subunit, and a regulatory subunit (Janssens and Goris, 2001). PP2A specificity and localization are determined by the regulatory subunit. In budding yeast, there are two regulatory subunits, Rts1 and Cdc55. They bind to PP2A in a mutually exclusive manner and form two distinct complexes: $PP2A^{Rts1}$ and $PP2A^{Cdc55}$ (Shu et al., 1997; Zhao et al., 1997). $PP2A^{Rts1}$ promotes timely expression of late G1 cyclins and bud emergence (Artiles et al., 2009). In addition, Rts1 is required for nutrient modulation of cell size, in which cells reduce their cell size in response to poor nutrients (Artiles et al., 2009). These findings are interesting because they suggest that $PP2A^{Rts1}$ links G1 transcription to cell size. Therefore, understanding the regulation and function of Rts1 will help us better understand the function of PP2A and its link to entry into the cell cycle and cell size.

In addition to cell size, cells also monitor nutrient availability in order to make the decision to enter the cell cycle. In budding yeast there are two conserved

pathways that play a role in nutrient sensing, cell growth and cell cycle entry (Zaman et al., 2008). The Ras/PKA pathway responds to carbon sources and is required for control of cell size (Zaman et al., 2008). A second pathway involves the TOR kinases, which respond to nitrogen availability and trigger activation of pathways involved in control of cell growth and nutrient utilization (Zaman et al., 2008). One of the key targets of the TOR pathway is the Sch9 kinase, a conserved member of the AGC family of kinases and a homolog of vertebrate Akt (Zaman et al., 2008). Sch9 is also regulated by Pkh1/2, a pair of redundant kinases that correspond to mammalian phosphoinositide-dependent kinase 1 (PDK1) (Casamayor et al., 1999; Roelants et al., 2004). The PDK1/Akt pathway is a survival pathway that has been shown to be deregulated in various diseases, including cancer (Carnero et al., 2008; Fresno Vara et al., 2004). In addition to Sch9, Pkh1/2 are also regulators of Pkc1, the budding yeast homolog of protein kinase C (PKC) involved in control of cell growth and cell wall integrity events (Davenport et al., 1995; Levin et al., 1990; Nanduri and Tartakoff, 2001; Roelants et al., 2004). The signals that regulate Pkh1/2 are poorly understood.

In this study we show that in rich media Rts1 phosphorylation is dependent on Pkh1/2 and Pkc1. We also found that hyperphosphorylation of Rts1 that occurs when cells are shifted to a poor carbon source is dependent on Pkh1/2, Pkc1 and casein kinase 1. Furthermore, loss of Pkh1/2 leads to a large decrease in cell size and delay of early G1 cyclins. Loss of Pkc1 also results in a delay in late G1 cyclin transcription, similar to the delay in *rts1*Δ cells. Interestingly, Rts1 hyperphosphorylation in response to poor nutrients is independent of the TOR and PKA pathways.

Together, these observations suggest a complex signaling network consisting of conserved kinases and phosphatases that act together to achieve proper cell cycle control in response to nutrient availability. Additionally, our results support a model in which Pkh1/2 controls cell size and entry into the cell cycle through regulation of Pkc1 and Rts1.

RESULTS

Rts1 does not undergo changes in phosphorylation during the cell cycle that can be detected by electrophoretic mobility shifts

Previous studies have shown that Rts1 phosphorylation can be detected as an electrophoretic shift by western blotting (Shu et al., 1997). To test if Rts1 phosphorylation is regulated in a cell cycle-dependent manner, we assayed Rts1 phosphorylation in wild type cells after release from a pheromone-induced G1 arrest (Figure 1A). In addition to Rts1, the G1 cyclin Cln2 and the mitotic cyclin Clb2 levels were assayed to monitor timing of the cell cycle (Figure 1A. Rts1 migrated as two phosphoforms with similar intensities throughout the cell cycle, suggesting that Rts1 does not undergo changes in phosphorylation during the cell cycle that can be detected by electrophoretic mobility shifts.

We also assayed Rts1 phosphorylation in wild type cells after arresting in metaphase. To synchronize cells in metaphase, *CDC20* was placed under the control of the *GAL1* promoter. *GAL1-CDC20* cells grown in dextrose will arrest in metaphase because Cdc20 is required for mitotic cyclin destruction. Consistent with the G1 arrest, no detectable differences in Rts1 phosphorylation were observed (Figure 1B.

These observations suggest that Rts1 phosphorylation events that cause electrophoretic mobility shifts are not regulated in a cell cycle-dependent manner and are compatible with Karen Artiles' previous observations. However, they do not rule out the possibility that Rts1 undergoes cell cycle-dependent changes in phosphorylation that cannot be detected by shifts in electrophoretic mobility.

A screen to identify essential kinases that phosphorylate Rts1

The kinases that phosphorylate Rts1 are unknown. In order to identify the kinase responsible for phosphorylating Rts1, Karen Artiles and Matt Nordstrom screened through a collection of strains containing single deletions of every non-essential kinase in the budding yeast genome. They reasoned that deletion of the kinase responsible for Rts1 phosphorylation would result in an electrophoretic shift detectable by western blotting. The screen failed to identify a non-essential kinase that is required for Rts1 phosphorylation. This suggested that Rts1 phosphorylation is due to the activity of an essential kinase, or that multiple non-essential kinases act redundantly to phosphorylate Rts1.

To screen for essential kinases that phosphorylate Rts1 we first used a tiled array of 2-micron high copy number yeast vectors, each containing several kinase genes. We hypothesized that overexpressing the kinase required for Rts1 phosphorylation might result in a detectable hyperphosphorylated form by western blotting. We selected vectors containing essential kinases and candidate non-essential kinases found by Karen Artiles and Matt Nordstrom. A list of kinases tested is shown in Table 1. No differences in Rts1 phosphorylation in any of the mutant strains tested were observed. Overexpression of the kinases was verified for several vectors by western blotting; the results for *GIN4* and *CLB2* are shown in Figure 2A.

Pkh1/2 and Pkc1 regulate Rts1 phosphorylation in rich media

An alternative approach to screen for essential kinases is to test conditional loss-of-function mutations in the essential kinases to determine whether they are required for Rts1 phosphorylation. We used a combination of temperature-sensitive,

analog-sensitive and degrons to test the effects of inactivating essential kinases on Rts1 phosphorylation. We found that loss of Hrr25, Kin28, Tor1/2, Tpk1/2/3 and Cdk1 function did not affect Rts1 phosphorylation (Figure 2B-F). However, loss of Pkc1, Pkh1/2, and to a lesser extent Ypk1/2 and Yck1/2 resulted in dephosphorylation of Rts1 (Figure 2G-J). Interestingly, all of these kinases are highly conserved and are involved in metabolism, growth and proliferation in vertebrate cells (Casamayor et al., 1999).

Pkh1/2 are the budding yeast homologs of vertebrate phosphoinositide-dependent kinase 1 (PDK1). In *pkh1-ts pkh2*Δ cells, Rts1 was rapidly dephosphorylated within 10 minutes of shifting to the restrictive temperature, reaching its maximum dephosphorylation by 60 minutes (Figure 2H).

Pkc1 is the budding yeast homolog of vertebrate protein kinase C (PKC). Previous studies have shown that Pkc1 is a direct target of Pkh1/2, suggesting that Pkh1/2 could affect Rts1 phosphorylation through Pkc1 (Inagaki et al., 1999). To test the effects of Pkc1 on Rts1 phosphorylation we used cells containing a temperature-sensitive allele of Pkc1. Loss of Pkc1 resulted in gradual loss of Rts1 phosphorylation within 60 minutes after shifting to the restrictive temperature, reaching maximum dephosphorylation by 90 minutes (Figure 2G). Together these results show that Pkh1/2 and Pkc1 regulate Rts1 phosphorylation.

Loss of function of Ypk1/Yrk2 and Yck1/2, the budding yeast homologs of serum/glucocorticoid-induced regulated kinase (SGK) and casein kinase 1, lead to partial dephosphorylation of Rts1 (Figure 2I-J). Interestingly, neither mutant led to complete dephosphorylation of Rts1.

Pkh1/2 regulates Gin4 phosphorylation

It was previously shown that *rts1*Δ rescues the elongated cell phenotype caused by loss of septin kinases Gin4, Hsl1 and Kcc4 (Artiles et al., 2009). Interestingly, Rts1, Gin4, Hsl1 and Kcc4 are all synthetically lethal with late G1 cyclins Cln1/2 (Benton et al., 1993; Cvrckova and Nasmyth, 1993). These observations suggested the possibility that Rts1 and the septin kinases could be acting in the same pathway. To test this hypothesis we assayed Rts1 phosphorylation in *gin4*Δ *hsl1*Δ *kcc4*Δ cells in log phase by western blotting and found that Rts1 is slightly dephosphorylated in this context (Figure 3A). We were unable to detect any Rts1 in *hsl1*Δ cells. It is unclear if this result is real or a loading error.

Since Pkh1/2 regulate Rts1 phosphorylation, we wanted to test if they also had an effect on Gin4 phosphorylation. Wild type and *pkh1-ts pkh2*Δ cells were shifted to the restrictive temperature and Gin4 phosphorylation was assayed by western blotting. Loss of Pkh1/2 function resulted in dephosphorylation of Gin4 by 40 minutes after shifting to the restrictive temperature (Figure 3B). These results suggest that Pkh1/2, Gin4, and Rts1 could be acting in the same pathway.

Overexpression of Pkc1 leads to Rts1 hyperphosphorylation

To further test the effect of Pkc1 on Rts1 phosphorylation we tested whether overexpression of a hyperactive allele of *PKC1* (*PKC1**) increases Rts1 phosphorylation. Induction of *GAL1-PKC1** was achieved by addition of galactose and changes in Rts1 phosphorylation were monitored by electrophoretic mobility shift on a western blot. Rts1 hyperphosphorylation began 30 minutes after addition of

galactose (Figure 4). These results suggest that Pkc1 hyperactivity leads to increased Rts1 phosphorylation. The rapid timing of the mobility shift suggests that Rts1 may be a direct target of Pkc1.

Pkh1/2 and Pkc1 are required for normal accumulation of G1 cyclin Cln2

Rts1 is known to be required for normal accumulation of G1 cyclin Cln2 and timely entry into the cell cycle (Artiles et al., 2009). To further test the hypothesis that Pkh1/2 and Pkc1 are regulators of Rts1, we assayed Cln2 accumulation and bud emergence in wild type, *pkh1*Δ *pkh2-ts* and *pkc1-ts* cells after release from a G1 arrest and shifting to the restrictive temperature.

In wild type cells, Cln2 levels peaked in late G1 at 50 minutes and disappeared as cells progressed through the cell cycle (Figure 5A). 50% of cells budded between 50-60 minutes after release from G1 (Figure 5B). In *pkh1*Δ *pkh2-ts*, accumulation of Cln2 was significantly reduced and delayed by 30 minutes (Figure 5A). Defects in bud emergence were even more dramatic, with less than 50% budded cells 90 minutes after release from G1 (Figure 5B).

Loss of Pkc1 resulted in a 20-minute delay in Cln2 accumulation (Figure 5C); however, Cln2 levels did not change significantly. Interestingly, once Cln2 reached maximum accumulation at around 50 minutes, it was gradually dephosphorylated and remained present throughout the rest of the time course (Figure 5C), presumably because of non-specific phosphatase activity due to cell death.

Together these results show that Pkh1/2 and Pkc1 are important for normal accumulation of Cln2 and timely entry into the cell cycle.

Partial loss of Pkh1/2 causes reduced cell size

The Pkh1/2 homolog in vertebrate cells, PDK1, is known to affect cell size in vertebrate cells (Lawlor et al., 2002). Pkh1/2 are also known regulators of Sch9, the yeast homolog of the Akt kinase, known to regulate cell size in budding yeast (Roelants et al., 2004). Furthermore, loss of Rts1 results in defective cell size (Artiles et al., 2009; Shu et al., 1997). To test if Pkh1/2 are involved in cell size control we measured size in cells with compromised Pkh1/2 function using a coulter counter. The *pkh1-ts pkh2*Δ strain used in this study shows partial loss of function at the permissive temperature. We found that *pkh1-ts pkh2*Δ grown at the permissive temperature show a significant decrease in cell size (Figure 6), suggesting an important role for Pkh1/2 in cell size control.

***rts1*Δ cells show additive effects on bud emergence and Cln2 accumulation in Pkh1/2 mutant cells**

In order to test if Rts1 and Pkh1/2 are components of the same pathway, we looked at Cln2 accumulation, bud emergence and cell size in wild type and *pkh1*Δ *pkh2-ts rts1*Δ cells released from a G1 arrest at 37˚C. In wild type cells, Cln2 accumulated by 75 minutes and peaked at 90-105 minutes (Figure 7A) after release from a G1 arrest. Moreover, 50% of all cells budded by 70 minutes (Figure 7B) after release from the arrest. In contrast, Cln2 failed to accumulate in *pkh1-ts pkh2*Δ *rts1*Δ cells (Figure 7A), and only 20% of all cells had budded by 90 minutes (Figure 7B). It is odd that at 37˚C, wild type cells took so long to accumulate Cln2 and undergo bud emergence. However, the delay in the triple mutant strain is more striking than the effects seen in each individual deletion.

As mentioned earlier, *rts1*Δ cells have a large cell phenotype, whereas *pkh1*Δ *pkh2-ts* cells are small (Figure 6). Interestingly, *pkh1*Δ *pkh2-ts rts1*Δ cells restore cell size to wild type (Figure 7C).

These observations suggest that Rts1 and Pkh1/2 possibly function in additional signaling pathways that control entry into the cell cycle. However, to make any conclusive remarks, the effects of the individual deletions need to be tested in the same experiment.

Rts1 is hyperphosphorylated in poor nutrients

When budding yeast cells are shifted from rich nutrients to poor nutrients, they readjust their cell size and become overall smaller (Fantes and Nurse, 1977; Johnston et al., 1979). Previous work in the lab showed that loss of Rts1 results in the inability of cells to readjust their size in response to nutrient shifts (Artiles et al., 2009). Furthermore, Karen Artiles found that Rts1 undergoes rapid hyperphosphorylation 20 minutes after shifting cells to poor nutrients, reaching maximum phosphorylation by 90 minutes after the nutrient shift (Figure 8A). We hypothesized that hyperphosphorylation of Rts1 in cells grown in poor media should disappear in cells shifted back to rich media.

To test this hypothesis we grew wild type cells in poor media during 90 minutes, allowing maximum Rts1 hyperphosphorylation to occur, and shifted them to rich media. Rts1 phosphorylation was assayed by western blotting. Rts1 started out hyperphosphorylated and was rapidly dephosphorylated 5 minutes after shifting to rich nutrients (Figure 8B). These results show that Rts1 is rapidly regulated in response to nutrient availability.

Rts1 hyperphosphorylation in poor nutrients is independent of the PKA pathway

The TOR and PKA pathways are the major nutrient sensing and utilization pathways in budding yeast (Zaman et al., 2008). The homologs of PKA in budding yeast are a triplet of redundant kinases called Tpk1, Tpk2 and Tpk3. We had previously observed that cells with compromised PKA and TOR pathways grown in rich media did not display any changes in Rts1 phosphorylation in comparison to wild type (Figure 2E-F).

To test if the PKA pathway is required for Rts1 hyperphosphorylation in response to poor nutrients, we used wild type and *tpk1-as tpk2-as tpk3-as* cells, shifted them to poor nutrients, and added the analog inhibitor 1NM-PP1 to abolish all Tpk activity. Changes in Rts1 hyperphosphorylation in 1NMPP1-treated cells shifted to poor nutrients were comparable to wild type (Figure 9A).

We were unable to rule out the involvement of the TOR pathway in Rts1 hyperphosphorylation in poor nutrients because the *tor2-ts* allele requires a temperature of 37˚C to be inactivated. At high temperatures Rts1 hyperphosphorylation in response to poor nutrients cannot be observed due to a heat shock response that abolishes all Rts1 phosphorylation. However, we tested the effect of a well-known target of the TOR pathway called Sch9 (Zaman et al., 2008). Sch9 is a member of the AGC kinase family, and corresponds to mammalian S6K (Urban et al., 2007). To test if Sch9 is required for Rts1 hyperphosphorylation in response to poor nutrients, we used wild type and *sch9-as* cells shifted to poor nutrients and added analog inhibitor 1NM-PP1. No changes in Rts1 hyperphosphorylation were observed (Figure 9B).

Pkh1/2, Pkc1 and Yck1/2 are required for Rts1 hyperphosphorylation in response to poor nutrients

Pkh1/2, Pkc1 and to a lesser extent Ypk1/2 and Yck1/2 had effects on Rts1 phosphorylation in rich nutrients (Figure 2G-J). We hypothesized that one or several of these kinases are responsible for Rts1 hyperphosphorylation in cells shifted to poor nutrients. To test this hypothesis we assayed Rts1 phosphorylation in wild type, *pkh1*Δ *pkh2-ts*, *pkc1-ts*, and *yck1-as yck2*Δ cells shifted from rich to poor nutrients at 30C. We were unable to test *ypk1*Δ *ypk2-ts* because the restrictive temperature for *ypk2-ts* is 37˚C, which inhibits Rts1 phosphorylation in wild type control cells. Rts1 became partially hyperphosphorylated in *pkh1*Δ *pkh2-ts* (Figure 10A). The inability to see complete loss of Rts1 hyperphosphorylation could be because *pkh2-ts* has a restrictive temperature of 34C and is still partially active at 30C. *pkc1-ts* and *yck1-as yck2*Δ cells failed to undergo Rts1 hyperphosphorylation in response to poor nutrients (Figure 10B-C). These results suggest that Pkc1, Yck1/2 and potentially Pkh1/2 are responsible for Rts1 hyperphosphorylation after shifting cells to poor nutrients.

DISCUSSION

Identification of kinases that regulate Rts1 phosphorylation

To identify kinases required for Rts1 phosphorylation, we screened through most kinases in the budding yeast genome using different approaches. Karen Artiles and Matt Nordstrom assayed Rts1 phosphorylation in strains containing single deletions for every non-essential kinase. None of the non-essential kinases were required for Rts1 phosphorylation; however, budding yeast have many redundant genes, making it difficult to observe a phenotype when only one gene is knocked out. It is also possible that more than one kinase contribute to Rts1 phosphorylation.

A second approach used high copy vectors that overexpress essential kinases. We reasoned that overexpression of the kinase might induce Rts1 hyperphosphorylation. We did not observe any effects on Rts1 phosphorylation. One explanation could be that the kinase requires a regulator to be active. Thus, when the kinase is overexpressed, the regulator becomes a limiting factor. Another possibility is that the kinase is already present at saturation and overexpressing it will not cause any further effects due to lack of available substrate.

The final approach was to test conditional alleles for essential kinases. This approach identified Pkh1/2, Pkc1, and to a lesser extent Yck1/2 and Ypk1/2. Interestingly, most of these kinases act on interrelated pathways involved in cell growth, nutrient sensing, cell wall integrity, and stress response.

Rts1 is regulated in response to nutrient availability

Previous work by Karen Artiles showed that Rts1 becomes rapidly hyperphosphorylated in response to poor nutrients (Figure 8A). This hyperphosphorylation is rapidly reversed when cells are shifted back to rich media (Figure 8B) suggesting that regulation of Rts1 is important in nutrient sensing. Interestingly, Karen Artiles showed that cells lacking Rts1 are unable to regulate their size in response to poor nutrients and remain large, which further supports a role for Rts1 in nutrient response and size regulation (Artiles et al., 2009). It is possible that Rts1 is required to sense nutrient availability; therefore, *rts1*Δ cells would be unable to readjust their critical size threshold in poor nutrients.

Hyperphosphorylation of Rts1 in poor nutrients seems to be regulated by the same kinases that regulate Rts1 in rich nutrients, Pkh1/2, Pkc1 and Yck1/2. These results further support a model in which Rts1 is regulated by the Pkh1/2 pathway in response to nutrient availability.

Pkh1/2 are required for cell size control

It is known that the Pkh1/2 homolog in animal cells, PDK1, affects cell size (Bayascas et al., 2008; Cho et al., 2001; Haga et al., 2009; Radimerski et al., 2002). In addition, mice expressing a hypomorphic allele of PDK1 are 40-50% smaller than their wild type counterparts, and their organ size is proportionately smaller (Lawlor et al., 2002). These studies show that deficiency in PDK1 causes decreased cell size.

Interestingly, Pkh1/2 are known regulators of Sch9 (Roelants et al., 2004). Cells lacking Sch9 are small and unable to regulate their size in response to poor nutrients (Jorgensen et al., 2004). Consistent with these results, we find that cells

deficient in Pkh1/2 function also have a small size phenotype (Fig 6). This is exciting because it hints at a conserved mechanism for regulation of cell size between budding yeast and vertebrates. We also tested whether Pkh1/2 are required for nutrient modulation of cell size (data not shown) and found that poor nutrients did not further decrease the size of *pkh1-ts pkh2*Δ cells. However, it is possible that these cells are already too small to reduce their size further.

Rts1 is also required for cell size control. Our findings that Pkh1/2 are required for phosphorylation of Rts1 suggest that these two proteins act in a pathway required for cell size regulation.

Pkh1/2 and Pkc1 regulate Rts1 phosphorylation

Our results show that Pkh1/2 and Pkc1 affect Rts1 phosphorylation in both rich and poor nutrients. Furthermore, Pkh1/2 and Pkc1 mutants show delayed G1 cyclin accumulation and entry into the cell cycle, similar to that observed in *rts1*Δ cells (Artiles et al., 2009). Previous work has shown that Pkc1 is a direct target of Pkh1/2 (Inagaki et al., 1999). Our results show that overexpression of Pkc1 causes rapid hyperphosphorylation of Rts1. Therefore, it is plausible that Rts1 is a direct target of Pkc1. I propose a model in which Pkh1/2 respond to nutrient availability by signaling to Pkc1 which in turn regulates Rts1 to control cell size and entry into the cell cycle (Figure 11).

In this model, the Pkh1/2-Pkc1 pathway is hyperactive in poor nutrients, leading to inhibitory hyperphosphorylation of Rts1. This would cause a prolonged delay in G1 cyclin transcription and reduce the critical cell size threshold, yielding an overall population of small cells. In rich media, Rts1 would set a threshold, allowing

cells to enter the cell cycle in a timely fashion once sufficient growth has occurred. In the absence of Rts1, cells would delay entry into the cell cycle but keep growing because they would not be able to sense their size, consistent with the large cell phenotype observed in these cells. In this model Rts1 is a sensor that relays nutrient information and growth signals to the cell cycle.

Although this model fits with most of our data, we still don't know if Rts1 phosphorylation/hyperphosphorylation is inhibitory. It is also uncertain how Pkh1/2 is regulated in response to growth. Additionally, *pkh1*Δ *pkh2-ts rts1*Δ cells have additive effects on G1 cyclin accumulation and entry into the cell cycle. This suggests that different pathways coordinate and integrate signals regarding nutrients and cell size and that it can't all be explained with one linear pathway.

Further analysis of the mechanisms that regulate Rts1 will help us understand how information regarding size and nutrient availability is relayed to the cell cycle.

MATERIALS AND METHODS

Yeast strains, culture conditions and plasmids

Most strains are in the W303 background (*leu2-3,112 ura3-1 can1-100 ade2-1 his3-11,15 trp1-1 GAL+ ssd1-d2*). The genotypes of the strains used for this study are listed in Table II. Full length constitutively active *PKC1* was expressed from the GAL1 promoter using the plasmid *pGAL1-PKC1* CEN URA*. One-step PCR-based gene replacement was used for construction of deletions and epitope tags at the endogenous locus. Strains that contain *GAL1-CDC20* strains were made by genetic crosses (Bhoite et al., 2001) or by using a PCR-based approach to integrate the *GAL1* promoter in front of the endogenous *CDC20* gene in the appropriate background.

Cells were grown in YEPD media (1% yeast extract, 2% peptone, 2% dextrose) supplemented with 40mg/L adenine or in YEP media (1% yeast extract, 2% peptone) supplemented with an added carbon source, as noted.

Cell cycle time courses and log phase cells

To synchronize cells in G1 with mating pheromone, cells were grown to log phase in YEPD overnight at room temperature prior to synchronization. Cells at an OD_{600} of 0.6 were arrested in G1 by addition of 0.5 mg/ml of α factor for 3.5 hours. *BAR1* strains were arrested by addition of 15mg/ml α factor. Cells were released into a synchronous cell cycle by washing 3X with fresh YEPD pre-warmed to 30ºC, 34˚C or 37˚C, as noted. To prevent cells from re-entering the cell cycle, a factor was added back at 65 minutes post-release.

To synchronize cells at metaphase, cells containing *GAL1-CDC20* were grown overnight in YEP media containing 2% raffinose and 2% galactose. Cells were arrested by washing into media containing 2% raffinose and incubated at room temperature for 4 hours. Cells were released from the metaphase arrest by adding 2% galactose and were then shifted to 30ºC for western blotting experiments.

For induced expression experiments, cells were grown overnight in YEP medium containing 2% glycerol and 2% ethanol. Expression of genes from the *GAL1* promoter was induced by addition of 2% galactose and the cells were shifted to 30ºC.

For time courses using analog-sensitive alleles, cells were grown overnight in YEPD without adenine. The adenine-analog inhibitors 1NMPP1 and CZ31 were added to log phase cells at a final concentration of 0.15-25μM and 10μM respectively; the cells were then shifted to 30ºC.

To analyze log phase cells, cultures were grown in YEPD, YEPD+2% galactose or YEPD+2% glycerol/ethanol overnight at room temperature. 1.6ml of cells at an OD_{600} of 0.6 were collected and centrifuged at 13000rpm for 30s, the supernatant was removed and 250ul of glass beads were added before freezing in liquid nitrogen.

Western blotting

To collect samples for western blotting, 1.6 ml samples were collected at each time point and centrifuged at 13000 rpm for 30s. The supernatant was removed and 250ml of glass beads were added before freezing in liquid nitrogen. Cells were lysed using 140ml of 1X sample buffer (65mM Tris-HCl pH 6.8, 3% SDS,

10% glycerol, 50mM NaF, 100mM b-glycerophosphate, 5% 2-mercaptoethanol, bromophenol blue). Phenyl methyl sulfonyl fluoride (PMSF) was added to the sample buffer to 2mM immediately before use. Cells were lysed in a Biospec Multibeater-8 at top speed for 2 minutes. The samples were removed and centrifuged for 15s at 13000 rpm in a microfuge and placed in boiling water for 5 min. After boiling, the samples were centrifuged for 5min at 13000 rpm and loaded on a SDS polyacrylamide gel.

SDS-PAGE was carried out as previously described (Harvey et al., 2005). Gels were run at a constant current of 20 mA. For Cln2, Clb2 and Nap1, electrophoresis was carried out on 10% polyacrylamide gels until a 29kD prestained marker ran to the bottom of the gel. For Rts1, 10% polyacrylamide gels were run until a 66.5kD prestained marker ran to the bottom of the gel. Gin4 was ran on 9% polyacrylamide gels until the 29kD marker ran to the bottom of the gel. Protein was transferred to nitrocellulose membranes for 1h 30min at 800 mA at 4ºC in a Hoeffer transfer tank in buffer containing 20 mM Tris base, 150 mM glycine, and 20% methanol. Blots were probed overnight at 4ºC with affinity-purified rabbit polyclonal antibodies raised against, Clb2, Gin4, Nap1, Rts1 or HA peptide. All blots were probed with an HRP-conjugated donkey anti-rabbit secondary antibody (GE Healthcare) for 45-90 minutes at room temperature.

Analysis of cell size and bud emergence

Triplicate cell cultures were grown overnight to log phase at room temperature in YEPD. A 0.9 ml sample of each culture was fixed with 100 ml of 37% formaldehyde for 1 hour, and then washed twice with 1X PBS+0.04% sodium azide

+0.02% Tween-20. Cell size was measured using a Channelizer Z2 Coulter counter as previously described (Jorgensen et al., 2002). Briefly, 150ml of fixed culture was diluted in 20ml of Isoton II® diluent (Beckman Coulter) and sonicated for 20 seconds prior to cell sizing. Each plot is the average of three independent experiments in which three independent samples were analyzed per strain. The percentage of budded cells was measured by counting the number of small-unbudded cells over a total of at least 200 cells.

ACKNOWLEDGEMENTS

I thank members of the laboratory for advice and support, especially Karen Artiles who started this project and mentored me. I would also like to thank Rafael Lucena who contributed Figure 5C, and Duy Nguyen who contributed Figure 4.

REFERENCES

Artiles, K., S. Anastasia, D. McCusker, and D.R. Kellogg. 2009. The Rts1 regulatory subunit of protein phosphatase 2A is required for control of G1 cyclin transcription and nutrient modulation of cell size. *PLoS genetics*. 5:e1000727.

Bayascas, J.R., S. Wullschleger, K. Sakamoto, J.M. Garcia-Martinez, C. Clacher, D. Komander, D.M. van Aalten, K.M. Boini, F. Lang, C. Lipina, L. Logie, C. Sutherland, J.A. Chudek, J.A. van Diepen, P.J. Voshol, J.M. Lucocq, and D.R. Alessi. 2008. Mutation of the PDK1 PH domain inhibits protein kinase B/Akt, leading to small size and insulin resistance. *Mol Cell Biol*. 28:3258-3272.

Benton, B.K., A.H. Tinkelenberg, D. Jean, S.D. Plump, and F.R. Cross. 1993. Genetic analysis of Cln/Cdc28 regulation of cell morphogenesis in budding yeast. *EMBO J*. 12:5267-5275.

Bhoite, L.T., Y. Yu, and D.J. Stillman. 2001. The Swi5 activator recruits the Mediator complex to the HO promoter without RNA polymerase II. *Genes Dev*. 15:2457-2469.

Carnero, A., C. Blanco-Aparicio, O. Renner, W. Link, and J.F. Leal. 2008. The PTEN/PI3K/AKT signalling pathway in cancer, therapeutic implications. *Current cancer drug targets*. 8:187-198.

Casamayor, A., P.D. Torrance, T. Kobayashi, J. Thorner, and D.R. Alessi. 1999. Functional counterparts of mammalian protein kinases PDK1 and SGK in budding yeast. *Curr Biol*. 9:186-197.

Chan, L.Y., and A. Amon. 2009. The protein phosphatase 2A functions in the spindle position checkpoint by regulating the checkpoint kinase Kin4. *Genes Dev*. 23:1639-1649.

Cho, K.S., J.H. Lee, S. Kim, D. Kim, H. Koh, J. Lee, C. Kim, J. Kim, and J. Chung. 2001. Drosophila phosphoinositide-dependent kinase-1 regulates apoptosis and growth via the phosphoinositide 3-kinase-dependent signaling pathway. *Proc Natl Acad Sci U S A*. 98:6144-6149.

Costanzo, M., J.L. Nishikawa, X. Tang, J.S. Millman, O. Schub, K. Breitkreuz, D. Dewar, I. Rupes, B. Andrews, and M. Tyers. 2004. CDK activity antagonizes Whi5, an inhibitor of G1/S transcription in yeast. *Cell*. 117:899-913.

Cross, F. 1990. Cell cycle arrest caused by CLN gene deficiency in Saccharomyces cerevisiae resembles START-I arrest and is independent of the mating-pheromone signalling pathway. *Mol. Cell. Biol.* 10:6482-6490.

Cvrckova, F., and K. Nasmyth. 1993. Yeast G1 cyclins CLN1 and CLN2 and a GAP-like protein have a role in bud formation. *EMBO J*. 12:5277-5286.

Davenport, K.R., M. Sohaskey, Y. Kamada, D.E. Levin, and M.C. Gustin. 1995. A second osmosensing signal transduction pathway in yeast. Hypotonic shock activates the PKC1 protein kinase-regulated cell integrity pathway. *The Journal of biological chemistry*. 270:30157-30161.

de Bruin, R.A., W.H. McDonald, T.I. Kalashnikova, J. Yates, 3rd, and C. Wittenberg. 2004. Cln3 activates G1-specific transcription via phosphorylation of the SBF bound repressor Whi5. *Cell*. 117:887-898.

Di Como, C.J., H. Chang, and K.T. Arndt. 1995. Activation of CLN1 and CLN2 G1 cyclin gene expression by BCK2. *Molec. Cell. Biol.* 15:1835-1846.

Dunphy, W.G., and A. Kumagai. 1991. The cdc25 protein contains an intrinsic phosphatase activity. *Cell*. 67:189-196.

Epstein, C.B., and F. Cross. 1994. Genes that can bypass the CLN requirement for Saccharomyces cerevisiae. *Mol Cell Biol*. 14:2041-2047.

Fantes, P., and P. Nurse. 1977. Control of cell size in fission yeast by a growth modulated size control over nuclear division. *Exp. Cell Res.* 107:377-386.

Fresno Vara, J.A., E. Casado, J. de Castro, P. Cejas, C. Belda-Iniesta, and M. Gonzalez-Baron. 2004. PI3K/Akt signalling pathway and cancer. *Cancer treatment reviews*. 30:193-204.

Gautier, J., M.J. Solomon, R.N. Booher, J.F. Bazan, and M.W. Kirschner. 1991. cdc25 is a specific tyrosine phosphatase that directly activates p34cdc2. *Cell*. 67:197-211.

Gould, K.L., and P. Nurse. 1989. Tyrosine phosphorylation of the fission yeast $cdc2^{+}$ protein kinase regulates entry into mitosis. *Nature*. 342:39-45.

Haga, S., M. Ozaki, H. Inoue, Y. Okamoto, W. Ogawa, K. Takeda, S. Akira, and S. Todo. 2009. The survival pathways phosphatidylinositol-3 kinase (PI3-K)/phosphoinositide-dependent protein kinase 1 (PDK1)/Akt modulate liver regeneration through hepatocyte size rather than proliferation. *Hepatology*. 49:204-214.

Harvey, S.L., A. Charlet, W. Haas, S.P. Gygi, and D.R. Kellogg. 2005. Cdk1-dependent regulation of the mitotic inhibitor Wee1. *Cell*. 122:407-420.

Healy, A.M., S. Zolnierowicz, A.E. Stapleton, M. Goebl, A.A. DePaoli-Roach, and J.R. Pringle. 1991. Cdc55, a *Saccharomyces cerevisiae* gene involved in cellular morphogenesis: identification, characterization, and homology to the B subunit of mammalian type 2A protein phosphatase. *Mol. Cell. Biol.* 11:5767-5780.

Inagaki, M., T. Schmelzle, K. Yamaguchi, K. Irie, M.N. Hall, and K. Matsumoto. 1999. PDK1 homologs activate the Pkc1-mitogen-activated protein kinase pathway in yeast. *Mol Cell Biol*. 19:8344-8352.

Janssens, V., and J. Goris. 2001. Protein phosphatase 2A: a highly regulated family of serine/threonine phosphatases implicated in cell growth and signalling. *Biochem J*. 353:417-439.

Johnston, G.C., C.W. Ehrhardt, A. Lorincz, and B.L. Carter. 1979. Regulation of cell size in the yeast Saccharomyces cerevisiae. *Journal of bacteriology*. 137:1-5.

Jorgensen, P., J.L. Nishikawa, B.J. Breitkreutz, and M. Tyers. 2002. Systematic identification of pathways that couple cell growth and division in yeast. *Science*. 297:395-400.

Jorgensen, P., I. Rupes, J.R. Sharom, L. Schneper, J.R. Broach, and M. Tyers. 2004. A dynamic transcriptional network communicates growth potential to ribosome synthesis and critical cell size. *Genes Dev*. 18:2491-2505.

Jorgensen, P., and M. Tyers. 2004. How cells coordinate growth and division. *Curr Biol*. 14:R1014-1027.

Kumagai, A., and W.G. Dunphy. 1991. The cdc25 protein controls tyrosine dephosphorylation of the cdc2 protein in a cell-free system. *Cell*. 64:903-914.

Lawlor, M.A., A. Mora, P.R. Ashby, M.R. Williams, V. Murray-Tait, L. Malone, A.R. Prescott, J.M. Lucocq, and D.R. Alessi. 2002. Essential role of PDK1 in regulating cell size and development in mice. *EMBO J*. 21:3728-3738.

Levin, D.E., F.O. Fields, R. Kunisawa, J.M. Bishop, and J. Thorner. 1990. A candidate protein kinase C gene, *PKC1*, is required for the S. cerevisiae cell cycle. *Cell*. 62:213-224.

Lin, F.C., and K.T. Arndt. 1995. The role of *Saccharomyces cerevisiae* type 2A phosphatase in the actin cytoskeleton and in entry into mitosis. *EMBO J.* 14:2745-2759.

Nanduri, J., and A.M. Tartakoff. 2001. The arrest of secretion response in yeast: signaling from the secretory path to the nucleus via Wsc proteins and Pkc1p. *Mol Cell*. 8:281-289.

Nurse, P. 1975. Genetic control of cell size at cell division in yeast. *Nature*. 256:547-551.

Nurse, P., P. Thuriaux, and K. Nasmyth. 1976. Genetic control of the cell division cycle in the fission yeast *Schizosaccharomyces pombe*. *Molec. Gen. Genet.* 146:167-178.

Radimerski, T., J. Montagne, F. Rintelen, H. Stocker, J. van der Kaay, C.P. Downes, E. Hafen, and G. Thomas. 2002. dS6K-regulated cell growth is dPKB/dPI(3)K-independent, but requires dPDK1. *Nat Cell Biol*. 4:251-255.

Richardson, H.E., C.W. Wittenberg, F. Cross, and S.I. Reed. 1989. An essential G1 function for cyclin-like proteins in yeast. *Cell*. 59:1127-1133.

Roelants, F.M., P.D. Torrance, and J. Thorner. 2004. Differential roles of PDK1- and PDK2-phosphorylation sites in the yeast AGC kinases Ypk1, Pkc1 and Sch9. *Microbiology*. 150:3289-3304.

Ronne, J., M. Carlberg, G.-z. Hu, and J.O. Nehlin. 1991. Protein Phosphatase 2A in *Saccharomyces cerevisiae*: Effects on Cell Growth and Bud Morphogenesis. *Mol. Cell. Biol.* 11:4876-4884.

Russell, P., and P. Nurse. 1986. cdc25+ functions as an inducer in the mitotic control of fission yeast. *Cell*. 45:145-153.

Shu, Y., H. Yang, E. Hallberg, and R. Hallberg. 1997. Molecular genetic analysis of Rts1p, a B' regulatory subunit of Saccharomyces cerevisiae protein phosphatase 2A. *Mol. Cell Biol.* 17:3242-3253.

Urban, J., A. Soulard, A. Huber, S. Lippman, D. Mukhopadhyay, O. Deloche, V. Wanke, D. Anrather, G. Ammerer, H. Riezman, J.R. Broach, C. De Virgilio, M.N. Hall, and R. Loewith. 2007. Sch9 is a major target of TORC1 in Saccharomyces cerevisiae. *Mol Cell*. 26:663-674.

Zaman, S., S.I. Lippman, X. Zhao, and J.R. Broach. 2008. How Saccharomyces responds to nutrients. *Annu Rev Genet*. 42:27-81.

Zhao, Y., G. Boguslawski, R.S. Zitomer, and A.A. DePaoli-Roach. 1997. Saccharomyces cerevisiae homologs of mammalian B and B' subunits of protein phosphatase 2A direct the enzyme to distinct cellular functions. *The Journal of biological chemistry*. 272:8256-8262.

Table I: List of kinases tested using the Yeast Tiling Array 2-micron yeast vectors.

Strain name	Overexpressed gene of interest
DK1174	Control (*pYEplac181*)
DK1175	*KIN28*
DK1176	*CLN3*
DK1177	*CDC15*
DK1178	*PKC1*
DK1179	*CDC7*
DK1180	*MPS1*
DK1181	*CDC28*
DK1184	*CKB1*
DK1185	*TAF1*
DK1187	*CAK1*
DK1188	*GUK1*
DK1191	*MSS4*
DK1202	*BCY1*
DK1203	*YCK1*
DK1204	*PRK1*
DK1205	*CKA1*
DK1206	*TOR2*
DK1207	*TPK1*
DK1208	*SLN1*
DK1209	*CDC5*
DK1210	*TPK3*
DK1211	*RIO2*
DK1212	*CKB2*
DK1213	*YCK2*
DK1214	*CBK1*
DK1215	*STT4*
DK1234	*STE20*
DK1235	*SGV1*
DK1236	*CLB5*
DK1237	*SLT2*
DK1238	*RAD53*
DK1239	*PHO85*
DK1240	*PIK1 [ ]*[1]
DK1241	*ELM1*
DK1242	*CLA4*
DK1243	*RIO1*
DK1244	*CKA2*
DK1245	*IPL1*
DK1246	*CLN2*
DK1247	*CLB2*
DK1248	*TRA1 [ ]*[2] means*
DK1249	*MEC1 [ ]*
DK1250	*HRR25, TPK2*
DK1251	*SCH9*
DK1252	*YOR287C*
DK1253	*BUD32*
DK1254	*BCK1 [ ]*
DK1255	*GIN4*
DK1256	*KCC4*
DK1257	*VHS1 [ ]*
DK1258	*HSL1*
DK1259	*TRA1 [ ] * &*[3]
DK1261	*FUS3*
DK1264	*ARK1*
DK1265	*PAK1*

[1] [ ] denotes an intact ORF that might be missing upstream or downstream regulatory sequences.
[2] [ ]* denotes that the 3' end of the gene is missing.
[3] [ ]& denotes that the 5' end of the gene is missing.

Table II: Strains used in this study

Strain	*MAT*	Genotype	Reference or Source
DK186	a	*bar1*	Altman *et al*., 1997
DK351	a	*bar1 cdk1::cdk1-as1*	Bishop *et al*., 2000
DK458	a	*tor2Δ::ADE2 pJK4 [TOR2::LEU]*	Helliwell *et al.,* 1998
DK459	a	*tor1Δ::HIS3 tor2Δ::ADE2 pJK4 [TOR2::LEU]*	Helliwell *et al.,* 1998
DK460	a	*tor1Δ::HIS3 tor2Δ::ADE2 YCplac111 [tor2-21::CEN/LEU2]*	Helliwell *et al.,* 1998
DK794	?	*hrr25Δ::KanMX pKK204 [GAL1-3XHA-HRR25 degron]*	Kadafor *et al.,* 2003
DK888	a	*bar1 gin4Δ::LEU2*	Mortensen *et al.,* 2002
DK1174	a	*bar1 pYEplac181 [2μ/LEU2]*	This study
DK1247	a	*bar1 pYGPM3e23 {(YPR118W, tk(UUU)P, CLB2, [YPR117W]&, [CLB5]&)::LEU}*	This study
DK1255	a	*bar1 pYGPM25o09 {(GIN4, GNP1, YDR509W, SMT3, YDR510C-A, ACN9, EMI1, TTR1, [tL(CAA)D], [YDR514C]&)::LEU}*	This study
DK1292	a	*bar1 yck1Δ::KanMX6 yck2-as*	This study
DK1312	?	*kin28Δ::TRP pGP457 [KIN28::URA]*	Hartzog Laboratory[4]
DK1313	?	*kin28Δ::TRP pGH215 [KIN28-16::LEU]*	Hartzog Laboratory
DK1332	a	*yck1Δ::KanMX6*	This study
DK1356	?		Sikorski *et al.,* 1989
DK1357	a	*ypk1-ts::HIS3 ykr2Δ::TRP1*	Casamayor *et al.,* 1999
DK1358	a		Richardson *et al.,* 1989
DK1359	?	*pkh1-D398G pkh2Δ::LEU2*	Inagaki *et al.,* 1999
DK1524	a	*CLN2-3XHA::ADE2*	This study
DK1529	a	*CLN2-3XHA::ADE2 pkh1-D398G pkh2Δ::LEU2*	This study
DK1561	a	*bar1 CLN2-3XHA::LEU2 GAL1-CDC20::HIS5*	Artiles *et al.,* 2009
DK1615	α		Broach Laboratory[5]
DK1616	α	*tpk1-M164G tpk2-M147G tpk3-M165G*	Zaman *et al.,* 2009
DK1631	a	*bar1 PKC1::HIS3*	Anastasia *et al*., 2012
DK1641	a	*bar1 pGAL1-PKC1**	Delley *et al.,* 1999
DK1693	a	*bar1 pkc1-17::HIS*	This study
DK1697	a	*bar1 pkc1-21::HIS*	This study
DK1721	a	*bar1 CLN2-3XHA::ADE2 pkh1-D398G pkh2Δ::LEU2 rts1Δ::HIS*	This study
DK1831	a	*bar1 CLN2-3XHA::ADE2 pkc1-21::HIS*	This study
EM22	a	*gin4Δ::LEU hsl1::HIS kcc4Δ::URA*	This study
HT159	a	*bar1 hsl1Δ::HIS5*	This study
ZZ1	a	*kcc4Δ::URA*	This study
ZZ41	a	*bar1 CLN2-3XHA::LEU2*	Artiles *et al*., 2009

[4] University of California, Santa Cruz
[5] Princeton University

Figure 1: Rts1 phosphorylation throughout the cell cycle.

A) Cells were released from a G1 arrest and the behavior of Rts1, Cln2-3XHA and Clb2 was assayed by western blotting. B) Cells were released from a metaphase arrest and Rts1 phosphorylation was assayed by western blotting.

Figure 1

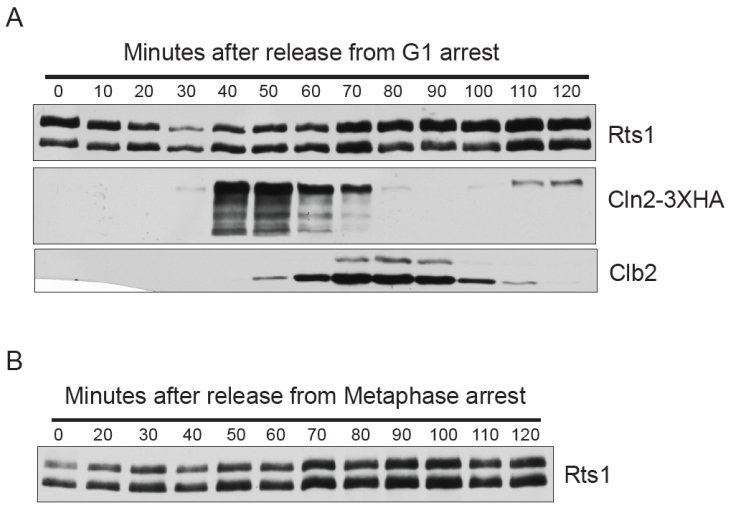
A
Minutes after release from G1 arrest
0 10 20 30 40 50 60 70 80 90 100 110 120
Rts1
Cln2-3XHA
Clb2
B
Minutes after release from Metaphase arrest
0 20 30 40 50 60 70 80 90 100 110 120
Rts1

Figure 2: A screen to identify kinases that regulate Rts1 phosphorylation.

For panels B-J, Rts1 was assayed by western blot. A) Gin4 and Clb2 levels were assayed by western blot in log phase cells carrying 2 micron vectors that express *GIN4* or *CLB2* from their endogenous promoters. Nap1 was used as a loading control. B) Wild type and *HRR25-degron* cells were grown to log phase in 2% galactose media and switched to 2% dextrose media to induce degradation of Hrr25. C) Wild type and *kin28-ts* cells were grown to log phase in YPD and then shifted to the restrictive temperature (37˚C). Samples were taken at the indicated times and loaded in an intercalated manner. D) *cdk1-as* log phase cells were taken at the indicated times after addition of DMSO or 1NMPP1. E) Wild type and *tpk1/2/3-as* log phase cells were taken at the indicated times after addition of 5μM 1NMPP1. F) Control, *tor1*Δ and *tor1*Δ *tor2-ts* cells were grown to log phase in YPD and then shifted to the restrictive temperature (37˚C). G) Wild type and *pkc1-ts* cells were grown to log phase in YPD and then shifted to the restrictive temperature (34˚C). Samples were taken at the indicated times. H) Wild type and *pkh1-ts pkh2*Δ cells were grown to log phase in YPD and then shifted to the restrictive temperature (37˚C). Samples were taken at the indicated times. I) Wild type and *ypk1-ts yrk2*Δ cells were grown to log phase in YPD and then shifted to the restrictive temperature (37˚C). Samples were taken at the indicated times. J) *yck1*Δ *yck2-as* log phase cells were taken at the indicated times after addition of 10μM CZ31.

Figure 2

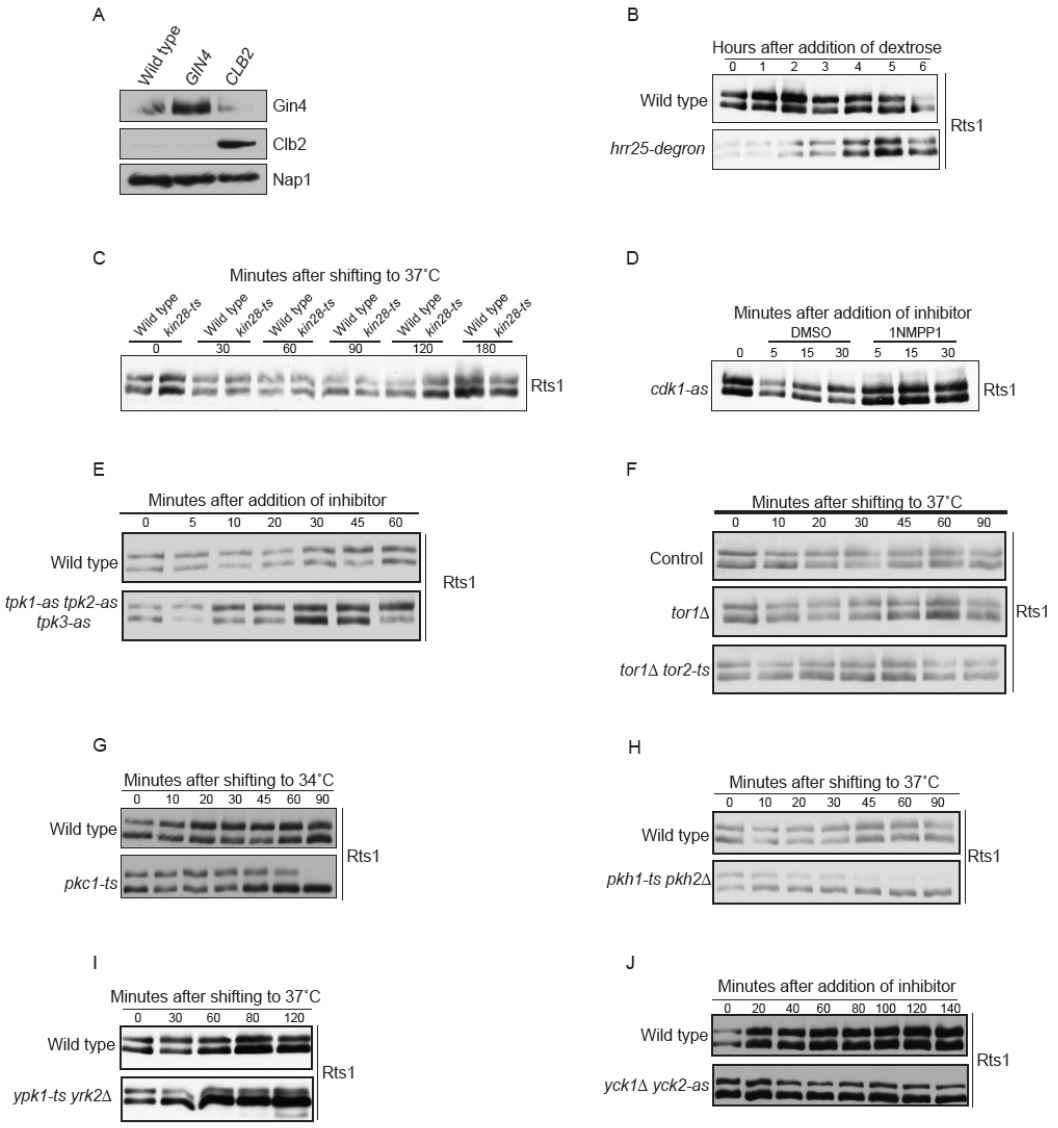
A
Wild type
GIN4
CLB2
Gin4
Clb2
Nap1
B
Hours after addition of dextrose
0 1 2 3 4 5 6
Wild type
hrr25-degron
Rts1
C
Minutes after shifting to 37˚C
Wild type
kin28-ts
0 30 60 90 120 180
Rts1
D
Minutes after addition of inhibitor
DMSO
1NMPP1
0 5 15 30 5 15 30
cdk1-as
Rts1
E
Minutes after addition of inhibitor
0 5 10 20 30 45 60
Wild type
tpk1-as tpk2-as tpk3-as
Rts1
F
Minutes after shifting to 37˚C
0 10 20 30 45 60 90
Control
tor1Δ
tor1Δ tor2-ts
Rts1
G
Minutes after shifting to 34˚C
0 10 20 30 45 60 90
Wild type
pkc1-ts
Rts1
H
Minutes after shifting to 37˚C
0 10 20 30 45 60 90
Wild type
pkh1-ts pkh2Δ
Rts1
I
Minutes after shifting to 37˚C
0 30 60 80 120
Wild type
ypk1-ts yrk2Δ
Rts1
J
Minutes after addition of inhibitor
0 20 40 60 80 100 120 140
Wild type
yck1Δ yck2-as
Rts1

Figure 3: Pkh1/2 regulate Gin4 phosphorylation.

A) Cells of the indicated genotypes were grown to log phase in YPD and Rts1 phosphorylation was assayed by western blot. B) Wild type and *pkh1-ts pkh2*Δ cells were grown to log phase in YPD and then shifted to the restrictive temperature (37˚C). Samples were taken at the indicated times and Gin4 phosphorylation was assayed by western blot.

Figure 3

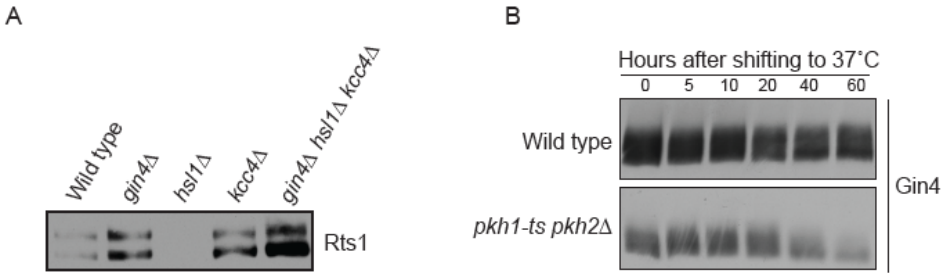
A
Wild type
gin4Δ
hsl1Δ
kcc4Δ
gin4Δ hsl1Δ kcc4Δ
Rts1
B
Hours after shifting to 37°C
0
5
10
20
40
60
Wild type
pkh1-ts pkh2Δ
Gin4

Figure 4. Overexpression of Pkc1 results in Rts1 hyperphosphorylation.

Wild type and *GAL1-PKC1** cells were grown to log phase in YPD. Overexpression of *PKC1** was achieved by switching to media containing 2% galactose and samples were taken at the indicated time points. Rts1 phosphorylation was assayed by western blot.

Figure 4

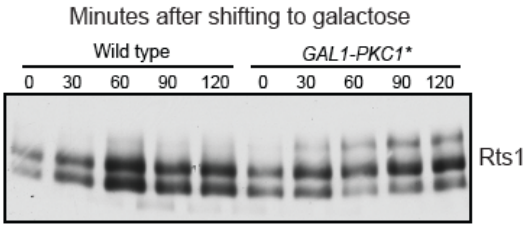
Minutes after shifting to galactose
Wild type
GAL1-PKC1*
0 30 60 90 120 0 30 60 90 120
Rts1

Figure 5: Loss of Pkh1/2 and Pkc1 delays G1 cyclin accumulation; Pkh1/2 also delay bud emergence.

A) Wild type and *pkh1-ts pkh2*Δ cells were arrested in G1 and shifted to the restrictive temperature (34˚C). Samples were taken at the indicated times and the behavior of Cln2-3XHA was assayed by western blot. B) The percentage of budded cells was plotted as a function of time in the same sample used in A. C) Wild type and *pkc1-ts* cells were arrested in G1 and shifted to the restrictive temperature (34˚C). Samples were taken at the indicated times and the behavior of Cln2-3XHA was assayed by western blot.

Figure 5

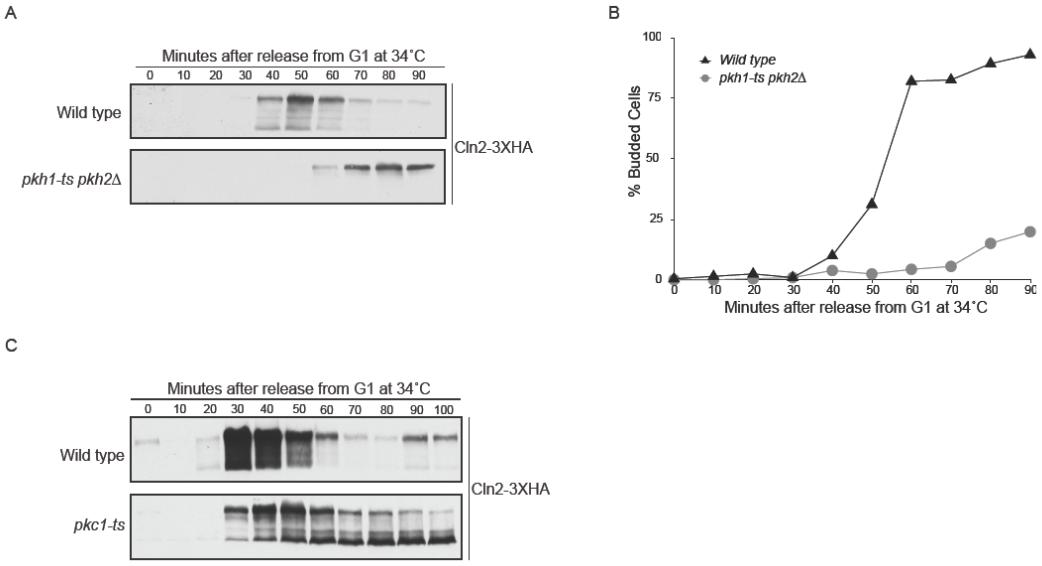
A
Minutes after release from G1 at 34˚C
0 10 20 30 40 50 60 70 80 90
Wild type
pkh1-ts pkh2Δ
Cln2-3XHA
B
Wild type
pkh1-ts pkh2Δ
% Budded Cells
0 25 50 75 100
0 10 20 30 40 50 60 70 80 90
Minutes after release from G1 at 34˚C
C
Minutes after release from G1 at 34˚C
0 10 20 30 40 50 60 70 80 90 100
Wild type
pkc1-ts
Cln2-3XHA

Figure 6. Partial loss of Pkh1/2 results in reduced cell size.

Cells were grown to log phase in YPD and cell size distributions were measured using a Coulter Counter. The Y-axis corresponds to percentage of cells.

Figure 6

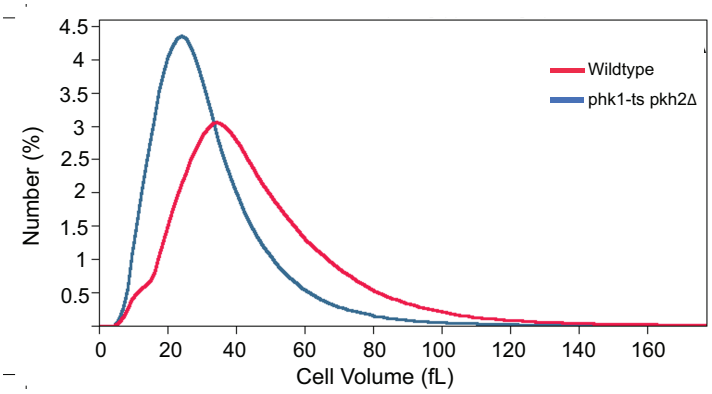
4.5
4
3.5
3
2.5
2
1.5
1
0.5
Number (%)
0
20
40
60
80
100
120
140
160
Cell Volume (fL)
Wildtype
phk1-ts pkh2Δ

Figure 7: *pkh1-ts pkh2*Δ *rts1*Δ further delay G1 cyclin accumulation and bud emergence.

A) Wild type and *pkh1-ts pkh2*Δ *rts1*Δ cells were arrested in G1 and shifted to the restrictive temperature (37˚C). Samples were taken at the indicated times and the behavior of Cln2-3XHA was assayed by western blot. B) The percentage of budded cells was plotted as a function of time in the same sample used in A. C) Cells were grown to log phase in YPD and cell size distributions were measured using a Coulter Counter. The Y-axis corresponds to percentage of cells.

Figure 7

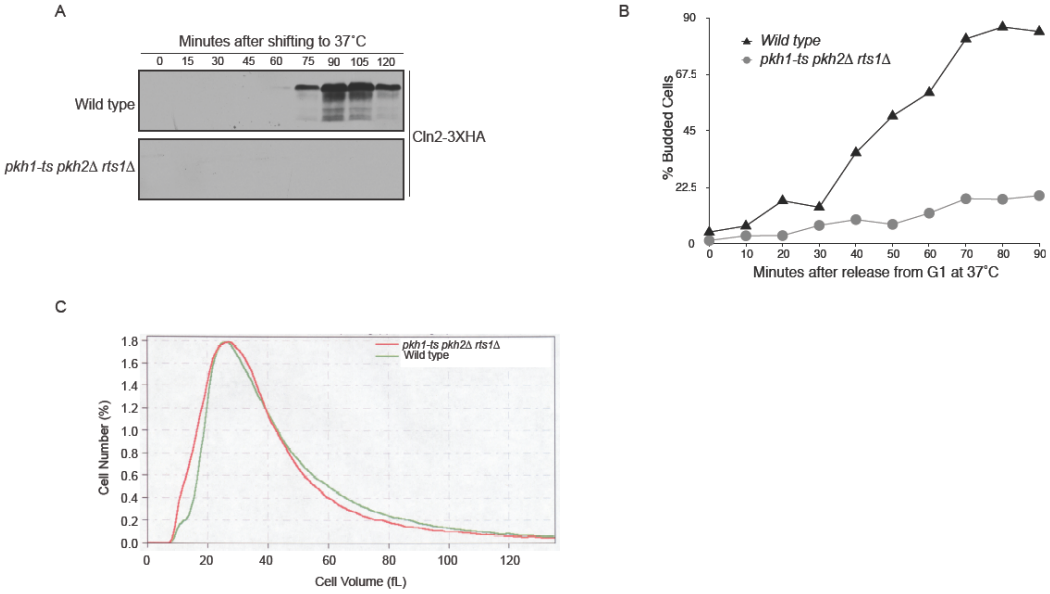
A
Minutes after shifting to 37°C
0 15 30 45 60 75 90 105 120
Wild type
pkh1-ts pkh2Δ rts1Δ
Cln2-3XHA
B
Wild type
pkh1-ts pkh2Δ rts1Δ
% Budded Cells
0
22.5
45
67.5
90
0 10 20 30 40 50 60 70 80 90
Minutes after release from G1 at 37°C
C
pkh1-ts pkh2Δ rts1Δ
Wild type
Cell Number (%)
0.0 0.2 0.4 0.6 0.8 1.0 1.2 1.4 1.6 1.8
0 20 40 60 80 100 120
Cell Volume (fL)

Figure 8. Rts1 phosphorylation is regulated in response to nutrient conditions. A) Wild type cells were grown to log phase in YPD and then shifted to media containing 2% glycerol/ethanol. Samples were taken at the indicated times and Rts1 phosphorylation was assayed by western blot. B) Wild type cells were grown to log phase in YPD and shifted to media containing 2% glycerol/ethanol. After 90 minutes in 2% galactose, cells were shifted back to YPD and samples were taken at the indicated times. Rts1 phosphorylation was assayed by western blot.

Figure 8

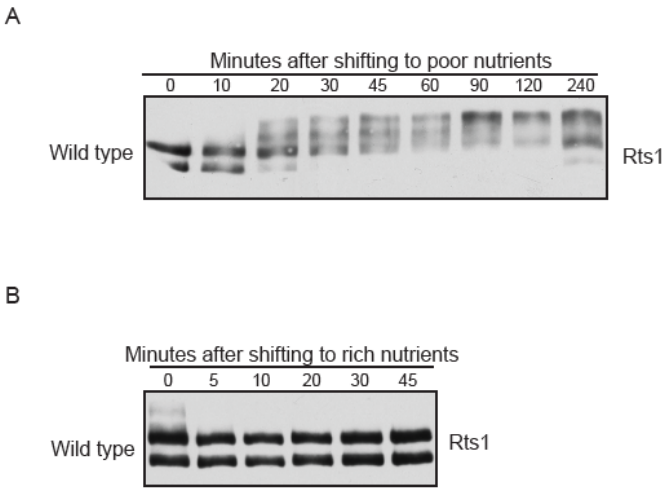
A
Minutes after shifting to poor nutrients
0 10 20 30 45 60 90 120 240
Wild type
Rts1
B
Minutes after shifting to rich nutrients
0 5 10 20 30 45
Wild type
Rts1

Figure 9. The Tpk pathway have no effect on Rts1 phosphorylation

A) Wild type and *tpk1/2/3-as* log phase cells were grown to log phase in YPD -Ade and washed twice with media containing 2% glycerol/ethanol –Ade. 5 μM 1NMPP1 was added 7.5 minutes after the nutrient shift. Samples were taken at the indicated times and Rts1 phosphorylation was assayed by western blot. B) Wild type and *sch9-as* cells were grown to log phase in YPD –Ade and washed twice with media containing 2% glycerol/ethanol –Ade. DMSO or 0.15μM 1NMPP1 were added 8.5 minutes after the nutrient shift.

Figure 9

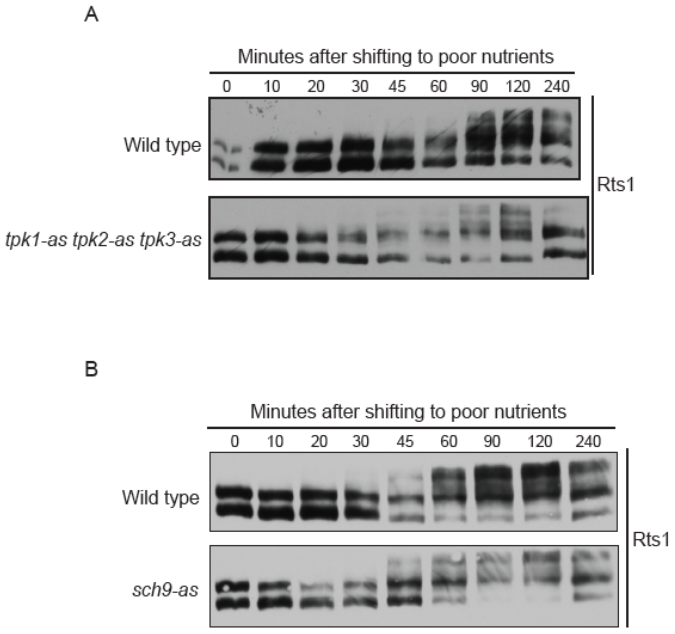
A
Minutes after shifting to poor nutrients
0 10 20 30 45 60 90 120 240
Wild type
tpk1-as tpk2-as tpk3-as
Rts1
B
Minutes after shifting to poor nutrients
0 10 20 30 45 60 90 120 240
Wild type
sch9-as
Rts1

Figure 10. Pkh1/2, Pkc1, and Yck1/2 are required for Rts1 hyperphosphorylation in poor nutrients.

A) Wild type and *pkh1-ts pkh2*Δ log phase cells were grown in YPD. Cells were then shifted to media containing 2% glycerol/ethanol and a semi-restrictive temperature of 30˚C. Samples were taken at the indicated times and Rts1 phosphorylation was assayed by western blot. B) Wild type and *pkc1-ts* log phase cells were grown in YPD. Cells were then shifted to media containing 2% glycerol/ethanol and a restrictive temperature of 30˚C. Samples were taken at the indicated times and Rts1 phosphorylation was assayed by western blot. C) Wild type and *yck1*Δ *yck2-ts* log phase cells were grown in YPD-Ade. Cells were then shifted to media containing 2% glycerol/ethanol -Ade and 10μM CZ31. Samples were taken at the indicated times and Rts1 phosphorylation was assayed by western blot.

Figure 10

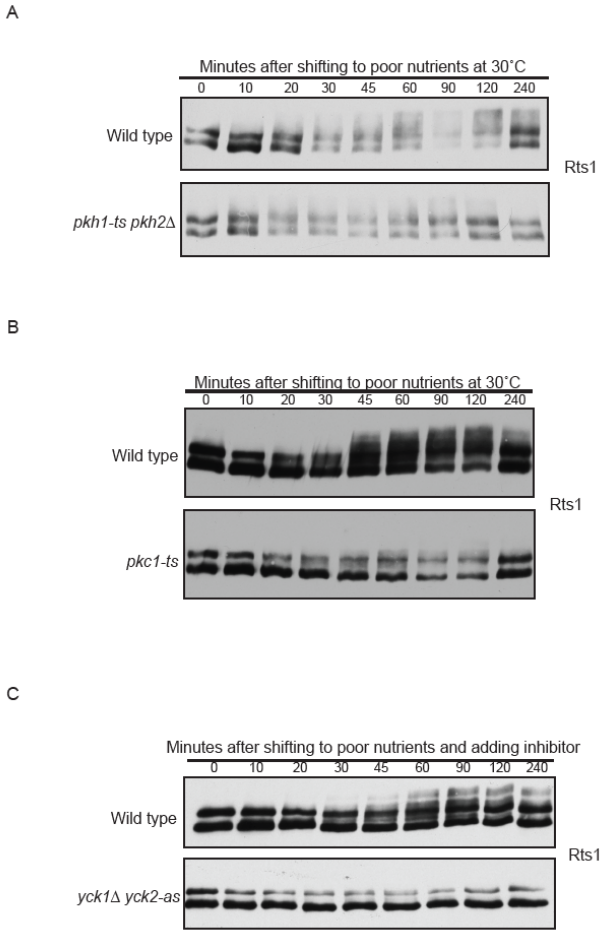
A
Minutes after shifting to poor nutrients at 30°C
0 10 20 30 45 60 90 120 240
Wild type
pkh1-ts pkh2Δ
Rts1
B
Minutes after shifting to poor nutrients at 30°C
0 10 20 30 45 60 90 120 240
Wild type
pkc1-ts
Rts1
C
Minutes after shifting to poor nutrients and adding inhibitor
0 10 20 30 45 60 90 120 240
Wild type
yck1Δ yck2-as
Rts1

Figure 11. Pkh1/2 and PP2A^{Rts1} are part of a pathway that senses nutrient availability.

In poor nutrients, Rts1 becomes inhibited by hyperphosphorylation, lowering the amount of growth that needs to occur to trigger late G1 cyclin transcription; therefore, these cells enter the cell cycle at a smaller size. In rich nutrients, there needs to be more growth to overcome the higher threshold set by PP2A^{Rts1}.

Figure 11

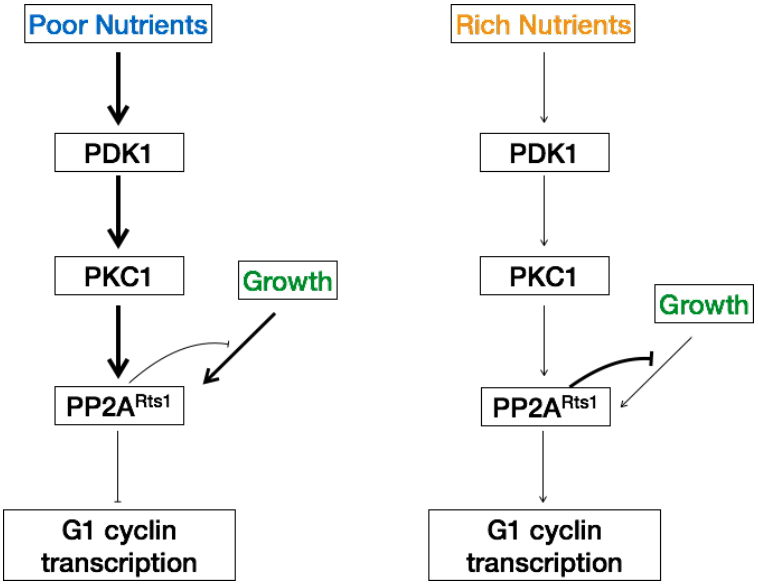
Poor Nutrients
PDK1
PKC1
Growth
PP2A Rts1
G1 cyclin transcription
Rich Nutrients
PDK1
PKC1
Growth
PP2A Rts1
G1 cyclin transcription

CHAPTER IV

REGULATION OF ENTRY INTO THE CELL CYCLE IN POOR NUTRIENTS

ABSTRACT

Cell size at entry into the cell cycle is regulated by nutrient availability, but the underlying mechanisms are unknown. Rts1, a specific regulatory subunit of protein phosphatase 2A ($PP2A^{Rts1}$), is required for nutrient modulation of cell size in budding yeast, and it undergoes rapid hyperphosphorylation in cells shifted to poor nutrients. Furthermore, Rts1 is required for timely entry into the cell cycle through control of G1 cyclin transcription. These observations suggest that $PP2A^{Rts1}$ controls cell cycle entry in response to nutrient availability. We found that Rts1 is required for normal accumulation of G1 cyclins Cln2 and Cln3 in poor nutrients. We also found that the kinases required for hyperphosphorylation of Rts1 in response to poor nutrients undergo changes in phosphorylation upon shifting to poor nutrients. These results support a model in which Rts1 links nutrient availability and cell size to entry into the cell cycle.

INTRODUCTION

Cells adapt to changing environments by monitoring and responding to external cues. Nutrient availability, cell size and entry into the cell cycle are all integrated (Jorgensen and Tyers, 2004); however, the molecular mechanisms involved remain unclear. The link between nutrient availability, cell size and cell cycle entry is clearly observed in budding yeast, where poor nutrient conditions cause a prolonged delay in G1 and a lower critical size threshold (Johnston et al., 1979; Tyson et al., 1979). Thus, yeast cells growing in poor media have a longer cell cycle and are smaller than cells growing in rich media. Readjustment of cell size in response to nutrient conditions is commonly known as “nutrient modulation of cell size” and it represents one of the most informative models to study cell size control.

In budding yeast, there are four proteins known to be required for nutrient modulation of cell size: AGC-type kinase Sch9, Sfp1, protein kinase A (PKA), and the protein phosphatase 2A (PP2A) regulatory subunit, Rts1 (Artiles et al., 2009; Jorgensen et al., 2002). The first three proteins are involved in ribosome biogenesis and their link to nutrient-modulation of cell size led to the “ribosome biogenesis model” which states that cells growing in rich media have a higher rate of ribosome biogenesis, inhibiting G1 cyclin transcription and allowing the cell to grow larger (Jorgensen et al., 2004). On the other hand, Rts1 is required for normal G1 cyclin transcription and timely entry into the cycle (Artiles et al., 2009). Until now, no link has been shown between ribosome biogenesis and Rts1.

Karen Artiles showed that Rts1 is extensively hyperphosphorylated in response to poor nutrients, suggesting a role in nutrient sensing. Hyperphosphorylation of Rts1 in poor nutrients is dependent on protein kinase C

(Pkc1), casein kinase 2 (Yck1/2) and Pkh1/2, which correspond to mammalian phosphoinositide-dependent kinase 1 (PDK1). All of these proteins are highly conserved and are involved in cell growth and cell cycle control (Anastasia et al., 2012; Liu et al., 2005a; Liu et al., 2005b; Robinson et al., 1999; Robinson et al., 1993).

We hypothesize that Rts1 links nutrient availability and cell size to entry into the cell cycle. In this study we try to shed light on how Rts1 may be linking nutrient sensing and cell division.

RESULTS

Rts1 becomes hyperphosphorylated in poor carbon sources

Rts1 becomes rapidly hyperphosphorylated when cells are shifted from dextrose to glycerol/ethanol (see Figure 8A, Chapter III). To compare Rts1 phosphorylation in different carbon sources, we grew wild type cells to log phase in media containing dextrose, galactose, raffinose or glycerol/ethanol.

In wild type cells grown in dextrose, Rts1 migrates as two phosphoforms that can be detected by western blot (Figure 1A, lane 1). Cells grown in glycerol/ethanol show Rts1 hyperphosphorylation (Figure 1A, lane 4), as previously shown in Figure 8A, Chapter III. Cells grown in galactose and raffinose do not show extensive hyperphosphorylation of Rts1, although there is a faint smear above the upper band that may correspond to a hyperphosphorylated form of Rts1 (Figure 1A, lanes 2-3). These results suggest that the extent of Rts1 phosphorylation is carbon-source dependent, with the most dramatic effects occurring in cells grown in glycerol/ethanol.

To test if Rts1 hyperphosphorylation in poor nutrients is regulated in a cell cycle-dependent manner, wild type cells were arrested in G1 in rich media and released into media containing glycerol/ethanol. Rts1 underwent hyperphosphorylation within 15 minutes and reached maximum hyperphosphorylation by 30 minutes (Figure 1B). No further changes in Rts1 phosphorylation were observed for the remainder of the time course. Throughout the time course Rts1 is observed as three distinct phosphoforms. The lower

phosphoform does not disappear entirely, in contrast with the results obtained in log phase cells where the lower form disappears completely (see Figure 8A, Chapter III).

These results verify that Rts1 phosphorylation is regulated in response to nutrients. It is unclear whether this phosphorylation is cell cycle dependent because the cells were arrested in rich media. It is possible the changes observed at the beginning of the cell cycle are a consequence of the nutrient change and not the stage of the cell cycle.

Rts1 is required for normal accumulation of G1 cyclin Cln2 in poor nutrients

Entry into the cell cycle is controlled by G1 cyclin transcription (Futcher, 2002). Cells grown in poor media delay the cell cycle to allow more time to grow and reach a critical size. To test if Rts1 has an effect on G1 cyclin levels in poor media, we examined the behavior of Cln2 in wild type and *rts1*∆ log phase cells shifted from rich nutrients to poor nutrients.

In wild type cells, Cln2 gradually disappears and is undetectable by 45 minutes after the nutrient shift (Figure 2A). Cln2 reappears 90 minutes after the nutrient shift, presumably when cells have readjusted to the new nutrient conditions and are ready to resume the cell cycle (Figure 2A). In *rts1*∆ cells, Cln2 disappears by 20 minutes and reappears 150 minutes after wild type (Figure 2A), suggesting these cells need more time to adjust to the new environment before they can enter the cell cycle. Cln2 levels are significantly lower in *rts1*∆ (Figure 2A).

Rts1 is required for normal accumulation of Cln2 in rich media (Artiles et al., 2009). To test if Rts1 affects Cln2 levels in poor nutrients in a cell cycle-dependent

manner, we assayed Cln2 accumulation in wild type and *rts1*Δ cells arrested in G1 in rich media and released into poor media.

In wild type cells, Cln2 began accumulating 50 minutes after release and peaked at 70 minutes (Figure 2B). In contrast, *rts1*Δ cells showed a delay of 30 minutes in Cln2 accumulation (Figure 2B). These results show that Rts1 is also required for normal Cln2 accumulation in poor nutrients.

Rts1 is required for normal regulation of G1 cyclin Cln3 and transcription factor Ace2 in poor nutrients

Budding yeast cells shifted from rich to poor nutrients immediately undergo budding because most are above the critical size. We hypothesized that in poor nutrients Ace2 becomes dephosphorylated, allowing transcription of Cln3 and entry into the cell cycle in an Rts1-dependent manner. To test this hypothesis, we used wild type and *rts1*Δ log phase cells shifted from rich nutrients to poor nutrients and probed for Cln3 and Ace2 by western blot.

In wild type cells shifted from rich to poor media, Ace2 is transiently dephosphorylated 5 minutes after the nutrient shift, correlating with a peak in Cln3 levels (Figure 3A). In *rts1*Δ cells, Ace2 phosphorylation does not change significantly and Cln3 levels remain low (Figure 3A). This suggests that dephosphorylation of Ace2 and the consequent burst of Cln3 upon changing to poor nutrients is Rts1-dependent.

Conversely, in wild type cells shifted from poor to rich media, we would expect Ace2 to be actively inhibiting *CLN3* to allow cells more time to grow. However, no detectable changes were observed on Ace2 phosphorylation nor Cln3

levels (Figure 3B). In *rts1*Δ cells, levels of both Ace2 and Cln3 are much lower (Figure 3B).

One explanation for Cln3 levels not correlating with Ace2 phosphorylation in wild type cells is that transcription of *CLN3* in response to dextrose is independent of Ace2. Studies have shown that transcription factor Azf1 positively regulates *CLN3* transcription in response to glucose (Newcomb et al., 2002). Additionally, it is possible that in *rts1*Δ cells, Azf1 becomes inactive and cannot trigger *CLN3* transcription, and that this is independent from Ace2 activity.

Pkh1/2 is not required for nutrient modulation of cell size

Previous studies found that *rts1*Δ cells are unable to undergo nutrient modulation of cell size (Artiles et al., 2009). Additionally, we had shown that Pkh1/2 are required for Rts1 phosphorylation (see Figure 2F and 10A, Chapter III). Based on these observations we hypothesized that Pkh1/2 control cell size through regulation of Rts1. To test this hypothesis we measured cell size in wild type and *pkh1-ts pkh2*Δ cells grown in rich or poor media. Strikingly, even though *pkh1-ts pkh2*-Δ are much smaller than wild type cells, they still undergo normal nutrient modulation of cell size (Figure 4). It is important to note that this experiment was done at room temperature, and it is possible that residual Pkh1/2 activity is enough to modulate cell size in response to poor nutrients.

Pkc1 gets dephosphorylated in response to poor nutrients, whereas Yck2 gets phosphorylated

We had previously seen that Pkc1 and Yck1/2 are required for Rts1 hyperphosphorylation in response to poor nutrients (see Figure 10B-C, Chapter III). We hypothesized that Pkc1 and/or Yck2 are themselves regulated in poor nutrients. To test this hypothesis, we shifted wild type cells from rich to poor media and probed for Pkc1 and Yck2 by western blot.

After shifting to poor nutrients, Pkc1 gets rapidly dephosphorylated (Figure 5). If Pkc1 is inactive in the dephosphorylated form, then this result argues against Pkc1 being responsible for phosphorylating Rts1 in poor nutrients. One possibility is that the hyperphosphorylated form of Rts1 is active and is constantly dephosphorylating Pkc1.

Yck2 seems to get phosphorylated by 60 minutes but the effect is very subtle (Figure 5). However, Rts1 hyperphosphorylation is observed within 20 minutes after shifting to poor nutrients (Figure 8A, Chapter III). It is hard to reach any significant conclusions from this experiment due the difficulty resolving the different phosphoforms of Yck2.

Rts1 hyperphosphorylation in poor nutrients is dependent on the strain background

We wanted to test if Rts1 hyperphosphorylation in poor nutrients was dependent on the strain background. To test this, we compared W303 and S288C cells, two widely used budding yeast strain backgrounds, shifted from rich to poor media. W303 defers from S288C in that it lacks the *SSD1* gene. *SSD1* interacts with

the TOR pathway and is thought to be important in nutrient sensing (Reinke et al., 2004).

W303 cells shifted to poor nutrients show significant Rts1 hyperphosphorylation by 20 minutes, reaching maximum hyperphosphorylation by 90-120 minutes after the nutrient shift (Figure 6). Conversely, in S288C cells shifted to poor nutrients, Rts1 does not get hyperphosphorylated until 90 minutes after the nutrient shift and nowhere to the extent observed in W303 cells.

To test if this difference was *SSD1*-dependent, we used a W303 strain expressing *SSD1*. These cells still undergo dramatic hyperphosphorylation of Rts1 in response to poor nutrients, arguing that *SSD1* is not responsible for the difference observed between W303 and S288C (Figure 6). If anything, these cells show further hyperphosphorylation of Rts1 as seen in time points 90-240 minutes after the nutrient shift (Figure 6).

Tracy MacDonough looked at other backgrounds and found that Rts1 also gets hyperphosphorylated in response to poor nutrients (data not shown), contrasting with the view in the field that S288C is more similar to wild type yeast than W303.

MATERIALS AND METHODS

Yeast strains, culture conditions and plasmids

Most strains are in the W303 background (*leu2-3,112 ura3-1 can1-100 ade2-1 his3-11,15 trp1-1 GAL+ ssd1-d2*). The genotypes of the strains used for this study are listed in Table I. One-step PCR-based gene replacement was used for construction of deletions and epitope tags at the endogenous locus (oligonucleotide sequences available upon request).

Cells were grown in YEPD media (1% yeast extract, 2% peptone, 2% dextrose) supplemented with 40mg/L adenine or in YEP media (1% yeast extract, 2% peptone) supplemented with an added carbon source, as noted.

Cell cycle time courses and log phase cells

To synchronize cells in G1 with mating pheromone, cells were grown to log phase in YEPD overnight at room temperature prior to synchronization. Cells at an OD_{600} of 0.6 were arrested in G1 by addition of 0.5 mg/ml of α factor for 3.5 hours. Cells were released into a synchronous cell cycle by washing 3X with fresh YEP media supplemented with an added carbon source, as noted. To prevent cells from re-entering the cell cycle, a factor was added back when half of the cells had undergone budding.

To analyze log phase cells, cultures were grown in YEPD, YEPD+2% galactose, YEPD+2% raffinose or YEPD+2% glycerol/ethanol overnight at room temperature. 1.6ml of cells at an OD_{600} of 0.6 were collected and centrifuged at

13000rpm for 30s, the supernatant was removed and 250ul of glass beads were added before freezing in liquid nitrogen.

Western blotting

To collect samples for western blotting, 1.6 ml samples were collected at each time point and centrifuged at 13000 rpm for 30s. The supernatant was removed and 250ml of glass beads were added before freezing in liquid nitrogen. Cells were lysed using 140ml of 1X sample buffer (65mM Tris-HCl pH 6.8, 3% SDS, 10% glycerol, 50mM NaF, 100mM b-glycerophosphate, 5% 2-mercaptoethanol, bromophenol blue). Phenyl methyl sulfonyl fluoride (PMSF) was added to the sample buffer to 2mM immediately before use. Cells were lysed in a Biospec Multibeater-8 at top speed for 2 minutes. The samples were removed and centrifuged for 15s at 13000 rpm in a microfuge and placed in boiling water for 5 min. After boiling, the samples were centrifuged for 5min at 13000 rpm and loaded on a SDS polyacrylamide gel.

SDS-PAGE was carried out as previously described (Harvey et al., 2005). Gels were run at a constant current of 20 mA. For Ace2, Cln2, Cln3 and Nap1, electrophoresis was carried out on 10% polyacrylamide gels until a 29kD prestained marker ran to the bottom of the gel. For Rts1, 10% polyacrylamide gels were run until a 66.5kD prestained marker ran to the bottom of the gel. Protein was transferred to nitrocellulose membranes for 1h 30min at 800 mA at 4ºC in a Hoeffer transfer tank in buffer containing 20 mM Tris base, 150 mM glycine, and 20% methanol. Blots were probed overnight at 4ºC with affinity-purified rabbit polyclonal antibodies raised against, Ace2, Gin4, Nap1, Rts1, Swe1 or HA peptide. All blots were probed with an

HRP-conjugated donkey anti-rabbit secondary antibody (GE Healthcare) for 45-90 minutes at room temperature.

Analysis of cell size

Triplicate cell cultures were grown overnight to log phase at room temperature in YEPD. A 0.9 ml sample of each culture was fixed with 100 ml of 37% formaldehyde for 1 hour, and then washed twice with 1X PBS+0.04% sodium azide +0.02% Tween-20. Cell size was measured using a Channelizer Z2 Coulter counter as previously described (Jorgensen et al., 2002). Briefly, 150ml of fixed culture was diluted in 20ml of Isoton II® diluent (Beckman Coulter) and sonicated for 20 seconds prior to cell sizing. Each plot is the average of three independent experiments in which three independent samples were analyzed per strain.

ACKNOWLEDGEMENTS

I thank members of the laboratory for advice and support, especially Tracy McDonough who invested a lot of time and effort throughout this project.

REFERENCES

Anastasia, S.D., D.L. Nguyen, V. Thai, M. Meloy, T. MacDonough, and D.R. Kellogg. 2012. A link between mitotic entry and membrane growth suggests a novel model for cell size control. *J Cell Biol*. 197:89-104.

Artiles, K., S. Anastasia, D. McCusker, and D.R. Kellogg. 2009. The Rts1 regulatory subunit of protein phosphatase 2A is required for control of G1 cyclin transcription and nutrient modulation of cell size. *PLoS genetics*. 5:e1000727.

Futcher, B. 2002. Transcriptional regulatory networks and the yeast cell cycle. *Curr Opin Cell Biol*. 14:676-683.

Harvey, S.L., A. Charlet, W. Haas, S.P. Gygi, and D.R. Kellogg. 2005. Cdk1-dependent regulation of the mitotic inhibitor Wee1. *Cell*. 122:407-420.

Johnston, G.C., C.W. Ehrhardt, A. Lorincz, and B.L. Carter. 1979. Regulation of cell size in the yeast Saccharomyces cerevisiae. *Journal of bacteriology*. 137:1-5.

Jorgensen, P., J.L. Nishikawa, B.J. Breitkreutz, and M. Tyers. 2002. Systematic identification of pathways that couple cell growth and division in yeast. *Science*. 297:395-400.

Jorgensen, P., I. Rupes, J.R. Sharom, L. Schneper, J.R. Broach, and M. Tyers. 2004. A dynamic transcriptional network communicates growth potential to ribosome synthesis and critical cell size. *Genes Dev*. 18:2491-2505.

Jorgensen, P., and M. Tyers. 2004. How cells coordinate growth and division. *Curr Biol*. 14:R1014-1027.

Liu, K., X. Zhang, R.L. Lester, and R.C. Dickson. 2005a. The sphingoid long chain base phytosphingosine activates AGC-type protein kinases in Saccharomyces cerevisiae including Ypk1, Ypk2, and Sch9. *The Journal of biological chemistry*. 280:22679-22687.

Liu, K., X. Zhang, C. Sumanasekera, R.L. Lester, and R.C. Dickson. 2005b. Signalling functions for sphingolipid long-chain bases in Saccharomyces cerevisiae. *Biochem Soc Trans*. 33:1170-1173.

Newcomb, L.L., D.D. Hall, and W. Heideman. 2002. AZF1 is a glucose-dependent positive regulator of CLN3 transcription in Saccharomyces cerevisiae. *Mol Cell Biol*. 22:1607-1614.

Reinke, A., S. Anderson, J.M. McCaffery, J. Yates, 3rd, S. Aronova, S. Chu, S. Fairclough, C. Iverson, K.P. Wedaman, and T. Powers. 2004. TOR complex 1 includes a novel component, Tco89p (YPL180w), and cooperates with Ssd1p to maintain cellular integrity in Saccharomyces cerevisiae. *The Journal of biological chemistry*. 279:14752-14762.

Robinson, L.C., C. Bradley, J.D. Bryan, A. Jerome, Y. Kweon, and H.R. Panek. 1999. The Yck2 yeast casein kinase 1 isoform shows cell cycle-specific localization to sites of polarized growth and is required for proper septin organization. *Mol Biol Cell*. 10:1077-1092.

Robinson, L.C., M.M. Menold, S. Garrett, and M.R. Culbertson. 1993. Casein kinase I-like protein kinases encoded by YCK1 and YCK2 are required for yeast morphogenesis. *Mol Cell Biol*. 13:2870-2881.

Tyson, C.B., P.G. Lord, and A.E. Wheals. 1979. Dependency of size of Saccharomyces cerevisiae cells on growth rate. *Journal of bacteriology*. 138:92-98.

Table I: Strains used in this study

Strain	*MAT*	Genotype	Reference or Source
DK186	a	*bar1*	Altman *et al*., 1997
DK751	a	*bar1 CLN2-3XHA::LEU2 rts1Δ::kanMX6*	Artiles *et al*., 2009
DK1524	a	*CLN2-3XHA::ADE2*	This study
DK1529	a	*CLN2-3XHA::ADE2 pkh1-D398G pkh2Δ::LEU2*	This study
DK1771	a	*SSD1-V (W303)*	Li *et al.,* 2009
DK1914	a	*bar1 ACE2-3XHA::kanMX6*	This study
DK1916	a	*bar1 ACE2-3XHA::kanMX6 rts1Δ::HIS*	This study
DK2017	a	*bar1 CLN3-6XHA::HIS*	Zapata *et al.,* 2014
DK2019	a	*bar1 CLN3-6XHA::HIS rts1Δ::kanMX4*	Zapata *et al.,* 2014
SH507	a	*SSD1-V*	This study
ZZ41	a	*bar1 CLN2-3XHA::LEU2*	Artiles *et al*., 2009

Figure1: Rts1 is hyperphosphorylated in poor nutrients.

(A) Cells were grown to log phase in media containing 2% dextrose, 2% galactose, 2% raffinose or 2% glycerol ethanol. Samples were probed for Rts1 by western blot. (B) Wild type cells were G1-arrested in rich media and released into 2% glycerol/ethanol. Samples were taken at the indicated time points and probed for Rts1 by western blot.

Figure 1

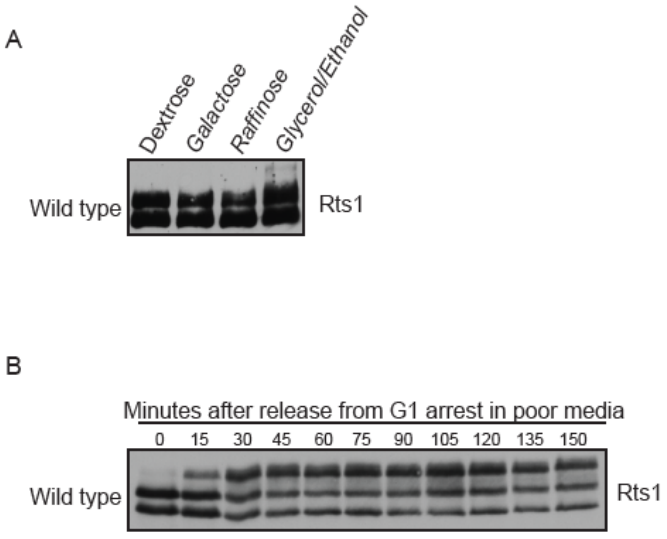
A
Dextrose
Galactose
Raffinose
Glycerol/Ethanol
Wild type
Rts1
B
Minutes after release from G1 arrest in poor media
0 15 30 45 60 75 90 105 120 135 150
Wild type
Rts1

Figure 2: Rts1 is required for regulation of Cln2 in poor nutrients.

(A) Wild type and *rts1*Δ cells were grown to log phase in rich media and then washed into 2% glycerol/ethanol. Samples were taken at the indicated time points and probed for Cln2-3XHA by western blot. The loading control corresponds to a background band from the same blot. (B) Wild type and *rts1*Δ cells were G1-arrested in rich media and released into 2% glycerol/ethanol. Samples were taken at the indicated time points and probed for Cln2-3XHA by western blot. The loading control corresponds to a background band from the same blot.

Figure 2

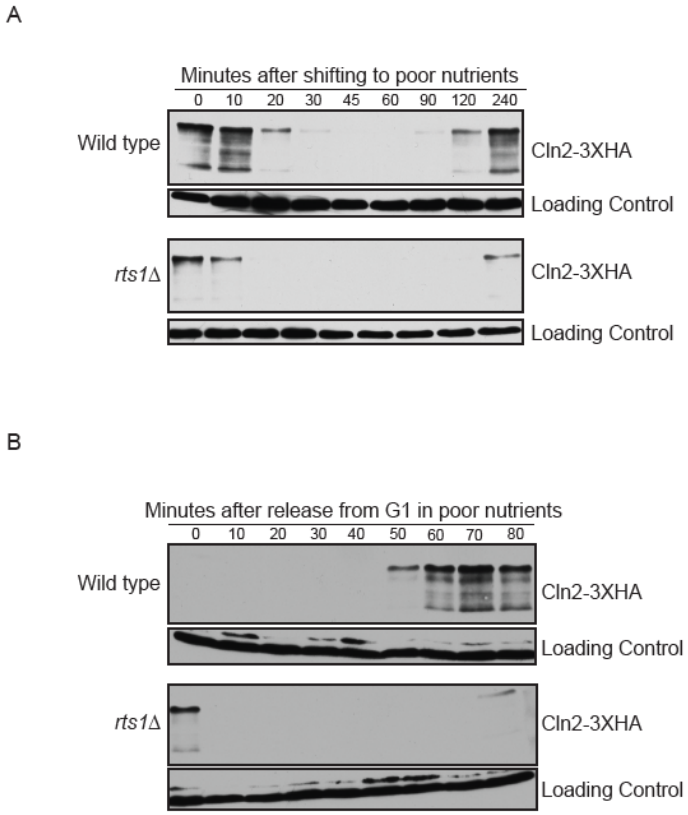
A
Minutes after shifting to poor nutrients
0 10 20 30 45 60 90 120 240
Wild type
Cln2-3XHA
Loading Control
rts1Δ
Cln2-3XHA
Loading Control
B
Minutes after release from G1 in poor nutrients
0 10 20 30 40 50 60 70 80
Wild type
Cln2-3XHA
Loading Control
rts1Δ
Cln2-3XHA
Loading Control

Figure 3: Regulation of Ace2 and Cln3 in poor nutrients is Rts1-dependent.

(A) Wild type and *rts1*Δ cells were grown to log phase in rich media and shifted to 2% glycerol/ethanol. Samples were taken at the indicated time points and probed for Ace2 or Cln3-6XHA by western blot. (B) Wild type and *rts1*Δ cells were grown to log phase in 2% glycerol/ethanol and then shifted to rich media. Samples were taken at the indicated time points and probed for Ace2 or Cln3-6XHA by western blot.

Figure 3

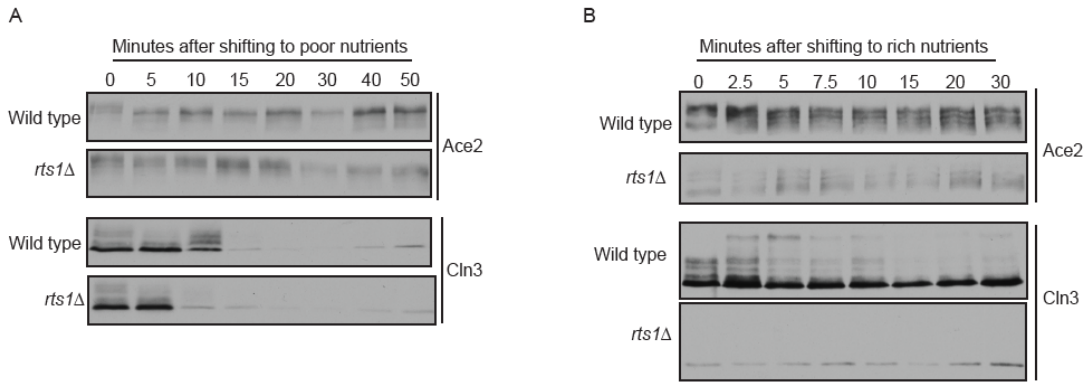
A
Minutes after shifting to poor nutrients
0 5 10 15 20 30 40 50
Wild type
rts1Δ
Ace2
Wild type
rts1Δ
Cln3
B
Minutes after shifting to rich nutrients
0 2.5 5 7.5 10 15 20 30
Wild type
rts1Δ
Ace2
Wild type
rts1Δ
Cln3

Figure 4: Pkh1/2 mutants undergo nutrient modulation of cell size.

Cells were grown lo log phase in media containing either 2% dextrose or 2% glycerol/ethanol. Cell size distributions were determined using a Coulter counter. Each plot represents three independent biological replicates in which three independent samples were analyzed for each strain

Figure 4

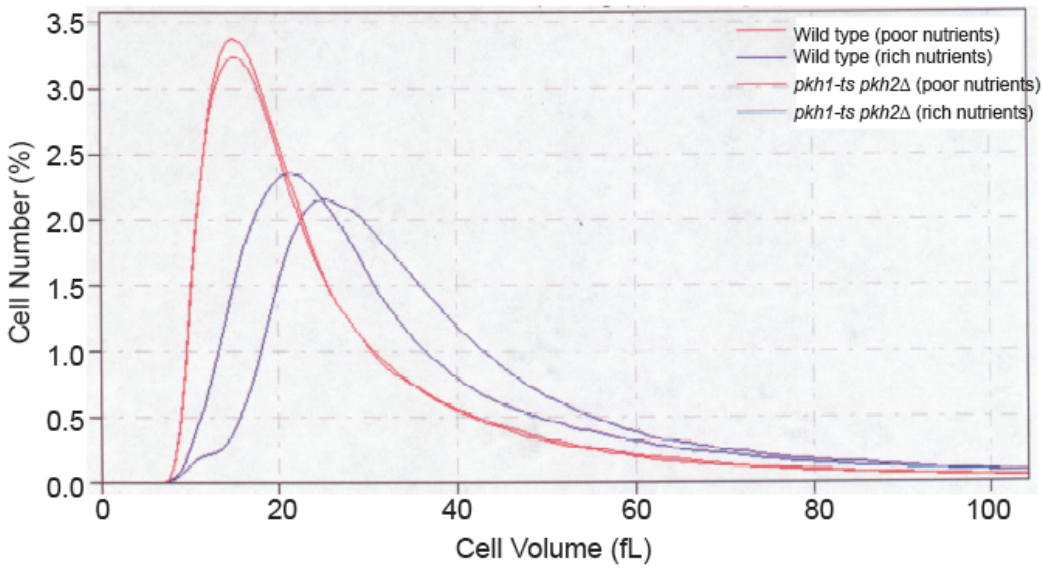
Wild type (poor nutrients)
Wild type (rich nutrients)
pkh1-ts pkh2Δ (poor nutrients)
pkh1-ts pkh2Δ (rich nutrients)
Cell Number (%)
3.5
3.0
2.5
2.0
1.5
1.0
0.5
0.0
0
20
40
60
80
100
Cell Volume (fL)

Figure 5: Phosphorylation of Pkc1 and Yck2 is regulated in poor nutrients.

Wild type cells were grown to log phase in rich media and then shifted to 2% glycerol ethanol. The behavior of Pkc1 and Yck2 was assayed by western blot.

Figure 5

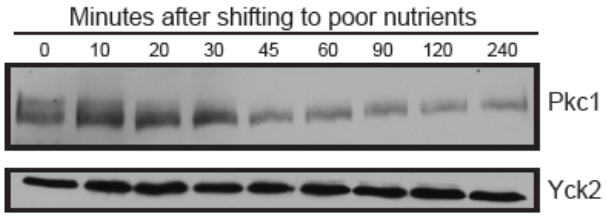
Minutes after shifting to poor nutrients
0
10
20
30
45
60
90
120
240
Pkc1
Yck2

Figure 6:Hyperphosphorylation of Rts1 in poor nutrients is background-dependent and independent of *SSD1.*

Wild type cells from the W303 and S288C backgrounds, as well as W303 cells with a copy of *SSD1*, were grown to log phase in rich media and shifted to 2% glycerol/ethanol. Rts1 phosphorylation was assayed by western blot.

Figure 6

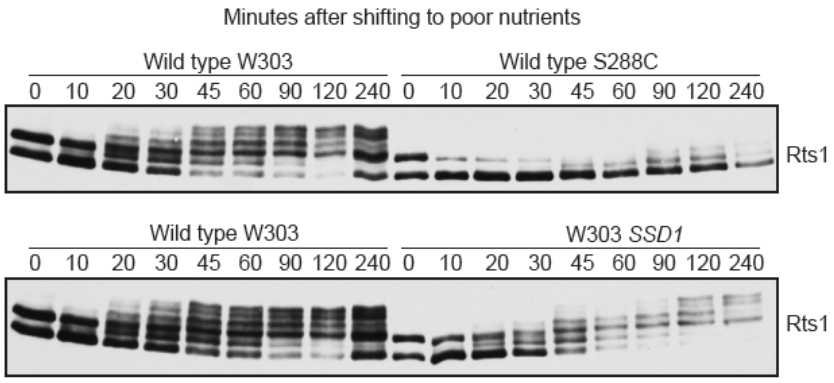
Minutes after shifting to poor nutrients
Wild type W303
Wild type S288C
0 10 20 30 45 60 90 120 240 0 10 20 30 45 60 90 120 240
Rts1
Wild type W303
W303 SSD1
0 10 20 30 45 60 90 120 240 0 10 20 30 45 60 90 120 240
Rts1

CHAPTER V

MISCELLANEOUS EXPERIMENTS

RESULTS

The effect of additional phosphatases on Ace2

The function and localization of transcription factor Ace2 is regulated by phosphorylation and dephosphorylation (Mazanka and Weiss, 2010). During mitosis, Cdk1 phosphorylates Ace2 to block its nuclear import and prevent repression of *CLN3* transcription (Mazanka and Weiss, 2010; O'Conallain et al., 1999; Sbia et al., 2008). We previously showed that $PP2A^{Rts1}$ does not oppose Ace2 phosphorylation by Cdk1 (see Figure 3A, Chapter II). This result provided evidence that a second phosphatase was acting on Ace2. The literature suggests that phosphatase Cdc14 acts on Ace2; however, we were unable to find conclusive evidence (Mazanka and Weiss, 2010; Sbia et al., 2008). To find additional phosphatases that act on Ace2 we used a combination of deletions and conditional alleles of some of the major phosphatases in budding yeast.

To test if the catalytic subunits of PP2A, called Pph21 and Pph22, affect Ace2 phosphorylation, we used two different temperature sensitive alleles of Pph22 in a *pph21 pph3*Δ background and assayed Ace2 phosphorylation by western blot. Temperature sensitive alleles are often times compromised at the permissive temperature. Because Ace2 is very sensitive to high temperatures, the experiment was done at the permissive and restrictive temperature. At 30˚C, there were no differences on Ace2 phosphorylation in wild type and *pph22-ts* mutants (Figure 1A).

At 37˚C, Ace2 gets rapidly dephosphorylated in response to the temperature change and then gradually becomes phosphorylated (Figure 1B). If Pph21/Pph22 were acting on Ace2, we would expect Ace2 to become hyperphosphorylated after inhibiting the phosphatase; however, in both *pph22-ts* mutants, Ace2 stays dephosphorylated after shifting to 37˚C (Figure 1B).

The same approach as above was used to test the effect of two temperature-sensitive alleles of Tap42 and one temperature-sensitive allele of Sit4 on Ace2 phosphorylation. Sit4 is a type 2A-related phosphatase required for the G1/S transition (Sutton et al., 1991). Tap42 physically interacts with phosphatase Sit4 and the catalytic subunits of PP2A, presumably activating them in response to nutrient signals (Di Como and Arndt, 1996). At 30˚C, there are no differences on Ace2 phosphorylation between wild type, *tap42-ts* and *sit4-ts* mutants (Figure 1C and E). At the restrictive temperature, the same effect seen for *pph22-ts* mutants is observed (Figure 1D and F), arguing that neither Sit4 nor Tap42 have an effect on Ace2 phosphorylation.

We next tested if the catalytic subunit of protein phosphatase 1 (PP1), Glc7, affected Ace2 phosphorylation. We tested two temperature-sensitive alleles of Glc7 and found no effect on Ace2 phosphorylation (Figure 1G).

Finally, we tested if a second regulatory subunit of PP2A called Cdc55 had an effect on Ace2 phosphorylation. We used wild type, *rts1*Δ*, cdc55*Δ*,* and *rts1*Δ *cdc55*Δ log phase cells and probed for Ace2. In *rts1*Δ cells, Ace2 was hyperphosphorylated as previously reported (see Figure 2, Chapter II) (Figure 1H). Interestingly, deleting Cdc55 also causes hyperphosphorylation of Ace2, and deletion of both regulatory subunits causes further hyperphosphorylation of Ace2

(Figure 1H). These results suggest that the Cdc55-bound form of PP2A leads to Ace2 dephosphorylation, similarly to $PP2A^{Rts1}$.

Screening for kinases that phosphorylate Ace2 in *rts1*Δ cells

In our previous work, we found that Cbk1 phosphorylates Ace2 in *rts1*Δ cells (see Figure 3B-D, Chapter II). However, *cbk1*Δ *rts1*Δ cells still show Ace2 phosphorylation, arguing that there are additional kinases that act on Ace2 in *rts1*Δ cells. We set out to find additional kinases required for Ace2 phosphorylation in *rts1*Δ cells.

There are two cyclin-dependent kinases in budding yeast, Cdk1 and Pho85. We had already ruled out Cdk1 (see Figure 3A, Chapter II), which is a known regulator of Ace2. We hypothesized that if Rts1 opposes Pho85 phosphorylation of Ace2, then the double deletion should abolish all or some of the hyperphosphorylation observed in *rts1*Δ cells. To test this hypothesis we assayed Ace2 phosphorylation in wild type, *rts1*Δ*, pho85*Δ, and *pho85*Δ *rts1*Δ cells by western blot. Ace2 was hyperphosphorylated in *rts1*Δ cells as expected; however, *pho85*Δ had no effect on Ace2 phosphorylation (Figure 2A). These results argue that Pho85 does not act on Ace2.

Next, we tested Kin4, a serine/threonine kinase that inhibits mitotic exit in response to spindle alignment defects (D'Aquino et al., 2005; Pereira and Schiebel, 2005). To test if Kin4 opposes Rts1, we assayed Ace2 phosphorylation in wild type, *rts1*Δ*, kin4*Δ, and *kin4*Δ *rts1*Δ cells by western blot. Ace2 remained hyperphosphorylated in *kin4*Δ *rts1*Δ cells, suggesting Kin4 does not phosphorylate Ace2 in *rts1*Δ cells (Figure 2B).

We then tested Yak1, a serine/threonine kinases that responds to glucose availability by inhibiting growth (Moriya et al., 2001). *yak1*Δ cells had no effect on Ace2 phosphorylation (Figure 2C); therefore, testing the double mutant seemed unnecessary .

The Glycogen Synthase Kinase 3 (GSK3) homologs in budding yeast activate transcription of stress-response genes (Andoh et al., 2000; Hirata et al., 2003). We used a strain that has all 4 homologs deleted to test Ace2 phosphorylation in *rts1*Δ cells. No effect on Ace2 phosphorylation in *rts1*Δ cells was observed (Figure 2D).

To test if Pkh1/2, Sch9 or Yck1/2 were responsible for phosphorylating Ace2 in *rts1*Δ cells, we used a variety of conditional alleles. None showed any effect on Ace2 phosphorylation in *rts1*Δ cells (Figure 2E-G).

Despite and extensive effort to find additional kinases opposing Rts1 on Ace2, we were unable to find them. There are still several kinases left to test, such as the septin kinases Gin4, Hsl1, Kcc4; the homologs of mammalian serum/glucocorticoid-induced kinases (SGK), Ypk1/Yrk2; and DNA damage checkpoint proteins, Mec1/Tel1.

Neither PP2A^{Rts1} nor PP2A^{Cdc55} dephosphorylate Ace2 in vitro

We had previously shown that loss of Rts1 leads to Ace2 hyperphosphorylation; however, we did not know if this effect was direct (see Figure 2, Chapter II). To test if PP2A directly dephosphorylates Ace2, we used purified hyperphosphorylated Ace2 from *rts1*Δ cells and added purified PP2A bound to either Rts1 or Cdc55. Neither PP2A complex dephosphorylated Ace2 (Figure 3). One explanation is that neither complex acts directly on Ace2; instead, they could be

acting on upstream regulators of Ace2. Another possibility is that the purified PP2A complexes were inactive.

Both Cdk1-Cln3 and Cdk1-Cln1/2 affect Ace2 phosphorylation

Mitotic Cdk1 is known to phosphorylate Ace2 during mitosis to keep it in the cytoplasm (Mazanka and Weiss, 2010). However, it was unknown if Cdk1 bound to the G1 cyclins also acted on Ace2. To test this, we assayed Ace2 phosphorylation in *cln3*Δ and *cln1*Δ *cln2*Δ cells. Ace2 was partially dephosphorylated in *cln3*Δ cells in comparison to wild type; this effect was more dramatic in *cln1*Δ *cln2*Δ cells (Figure 4). These results suggest that Cdk1 also regulates Ace2 during G1.

CLN2-3XHA* acts like a hyperactive form of *CLN2

When we initially looked at Ace2 phosphorylation in *rts1*Δ cells, we used a Cln2-3XHA background. We found that 0-15 minutes after release from G1, Ace2 was significantly hyperphosphorylated in *rts1*Δ *CLN2-3XHA* cells in comparison to wild type (Figure 5B). However, in untagged *CLN2* strains, Ace2 hyperphosphorylation in *rts1*Δ was much more subtle (Figure 5A). We hypothesized that the tag on *CLN2* was making it hyperactive. To test this hypothesis, we looked at Ace2 phosphorylation in cells overexpressing *CLN2* from the *GAL1* promoter. We found that in *GAL1-CLN2 rts1*Δ cells, Ace2 was significantly hyperphosphorylated, comparable to the effects seen in *CLN2-3XHA rts1*Δ cells (Figure 5C). These results suggest that the *3XHA* tag is making Cln2 hyperactive and the results obtained using these strains must be interpreted with caution.

Growth inhibition causes Ace2 dephosphorylation

To test if Ace2 phosphorylation was sensitive to growth signals, we used a Sec6 temperature sensitive mutant that blocks vesicle fusion (*sec6-4*) and assayed Ace2 phosphorylation by western blot. In *sec6-4* cells shifted to the restrictive temperature, Ace2 was dephosphorylated by 20 minutes (Figure 6). This result suggests that Ace2 phosphorylation might respond to growth signals. However, this result must be interpreted with caution because Ace2 phosphorylation is very sensitive to increasing temperatures.

Loss of Pkh1/2 affects phosphorylation of Ace2 and Mih1

$PP2A^{Rts1}$ is an inhibitor of Ace2 (see Figures 4 and 5, Chapter II). Additionally, Rts1 phosphorylation is dependent on Pkh1/2 (see Figure 2H, Chapter III). These results suggested that regulation of Rts1 by the Pkh1/2 pathway may affect Ace2 phosphorylation. To test this hypothesis, we used wild type and *pkh1-ts pkh2*Δ cells and assayed Ace2 phosphorylation by western blot.

Initially cells were shifted to a semi-permissive temperature of 30˚C to avoid heat shock-induced dephosphorylation of Ace2. No differences in Ace2 phosphorylation were observed between wild type and *pkh1/*2 mutants (Figure 7A).

In wild type and *pkh1-ts pkh2*Δ cells shifted to the restrictive temperature (37˚C), dephosphorylation of Ace2 occurred immediately after the shift and then gradually became phosphorylated; however, in the mutant, Ace2 is less phosphorylated in comparison to wild type (Figure 7B). These results suggest that the Pkh1/2 pathway may be involved in regulating Ace2 phosphorylation.

To test if Pkh1/2 had an effect on proteins involved in the G2/M checkpoint, we used wild type and *pkh1-ts pkh2*Δ cells shifted to the restrictive temperature and assayed Mih1 and Swe1 phosphorylation. Loss of Pkh1/2 function had no effect on Swe1 phosphorylation, but resulted in hyperphosphorylation of Mih1 (Figure 7C-D). This result is counterintuitive because inactivating the kinase should result in dephosphorylation of the target protein. It is possible that Pkh1/2 is required to activate a phosphatase that acts on Mih1.

Loss of Cdc55 causes hyperphosphorylation of Cbk1

Cbk1 is a member of the Ndr/LATS family known to phosphorylate Ace2, keeping it in the nucleus and activating its transcription factor functions (Mazanka and Weiss, 2010). Since Cbk1 is also regulated by phosphorylation, we hypothesized that PP2A could possibly affect Cbk1 phosphorylation (Jansen et al., 2006). To test this hypothesis, we used wild type, *rts1*Δ, *cdc55*Δ, *rts1*Δ *cdc55*Δ log phase cells and assayed Cbk1 phosphorylation. Loss of Rts1 had no effect on Cbk1 phosphorylation, whereas loss of Cdc55 resulted in dramatic hyperphosphorylation of Cbk1 (Figure 8). These results suggest that $PP2A^{Cdc55}$ maybe required for control of Cbk1 phosphorylation.

***ace2*Δ recues the Cln2 accumulation delay observed in *rts1*Δ cells**

Rts1 is required for normal control of Cln3 (see Figure 6 and 7, Chapter II) and Cln2 accumulation (Artiles et al., 2009). We previously showed that many of the defects observed in *rts1*Δ cells are rescued by *ace2*Δ (see Figures 6 and 7, Chapter II). To test if this was also true for Cln2 accumulation, we released wild type, *rts1*Δ,

*ace2*Δ and *rts1*Δ *ace2*Δ from a G1 arrest and assayed the behavior of Cln2 by western blot.

In wild type cells, Cln2 gradually accumulates and peaks in G1, 50 minutes after release (Figure 9). Loss of Rts1 delayed Cln2 accumulation by 10 minutes, and this delay was rescued by *ace2*Δ (Figure 9).

These observations are consistent with the results previously obtained for Cln3 (see Figures 6 and 7, Chapter II) and argue that Rts1 also controls Cln2 accumulation via Ace2.

MATERIALS AND METHODS

Yeast strains, culture conditions and plasmids

Most strains are in the W303 background (*leu2-3,112 ura3-1 can1-100 ade2-1 his3-11,15 trp1-1 GAL+ ssd1-d2*). The genotypes of the strains used for this study are listed in Table I. Full length *CLN2* was expressed from the GAL1 promoter using the integrating plasmid pSL201-5 [*GAL1-CLN2-3XHA URA3*]. One-step PCR-based gene replacement was used for construction of deletions and epitope tags at the endogenous locus.

Cells were grown in YEPD media (1% yeast extract, 2% peptone, 2% dextrose) supplemented with 40mg/L adenine or in YEP media (1% yeast extract, 2% peptone) supplemented with an added carbon source, as noted.

Cell cycle time courses and log phase cells

To synchronize cells in G1 with mating pheromone, cells were grown to log phase in YEPD overnight at room temperature prior to synchronization. Cells at an OD_{600} of 0.6 were arrested in G1 by addition of 0.5 mg/ml of α factor for 3.5 hours. Cells were released into a synchronous cell cycle by washing 3X with fresh YEPD pre-warmed to 30ºC, 34˚C, 37˚C or 38˚C, as noted. To prevent cells from re-entering the cell cycle, a factor was added back when 50% of cells were budded.

For induced expression experiments, cells were grown overnight in YEP medium containing 2% glycerol and 2% ethanol. Expression of genes from the *GAL1* promoter was induced by addition of 2% galactose and the cells were shifted to 30ºC.

For time courses using analog-sensitive alleles, cells were grown overnight in YEPD without adenine. The adenine-analog inhibitors 1NMPP1 and CZ31 were added to log phase cells at a final concentration of 25μM and 10μM respectively; the cells were then shifted to 30ºC.

To analyze log phase cells, cultures were grown in YEPD, YEPD+2% galactose or YEPD+2% glycerol/ethanol overnight at room temperature. 1.6ml of cells at an OD_{600} of 0.6 were collected and centrifuged at 13000rpm for 30s, the supernatant was removed and 250ul of glass beads were added before freezing in liquid nitrogen.

Western blotting

To collect samples for western blotting, 1.6 ml samples were collected at each time point and centrifuged at 13000 rpm for 30s. The supernatant was removed and 250ml of glass beads were added before freezing in liquid nitrogen. Cells were lysed using 140ml of 1X sample buffer (65mM Tris-HCl pH 6.8, 3% SDS, 10% glycerol, 50mM NaF, 100mM b-glycerophosphate, 5% 2-mercaptoethanol, bromophenol blue). Phenyl methyl sulfonyl fluoride (PMSF) was added to the sample buffer to 2mM immediately before use. Cells were lysed in a Biospec Multibeater-8 at top speed for 2 minutes. The samples were removed and centrifuged for 15s at 13000 rpm in a microfuge and placed in boiling water for 5 min. After boiling, the samples were centrifuged for 5min at 13000 rpm and loaded on a SDS polyacrylamide gel.

SDS-PAGE was carried out as previously described (Harvey et al., 2005). Gels were run at a constant current of 20 mA. For Ace2, Cln2, Clb2, Cbk1 and Mih1,

electrophoresis was carried out on 10% polyacrylamide gels until a 29kD prestained marker ran to the bottom of the gel. Swe1 was ran on 10% polyacrylamide gels until a 66.5kD prestained marker ran to the bottom of the gel. Protein was transferred to nitrocellulose membranes for 1h 30min at 800 mA at 4ºC in a Hoeffer transfer tank in buffer containing 20 mM Tris base, 150 mM glycine, and 20% methanol. Blots were probed overnight at 4ºC with affinity-purified rabbit polyclonal antibodies raised against, Ace2, Clb2, Cbk1, Gin4, Swe1, Mih1 or HA peptide. All blots were probed with an HRP-conjugated donkey anti-rabbit secondary antibody (GE Healthcare) for 45-90 minutes at room temperature.

Immunoaffinity Purifications and in vitro Assays

Immunoaffinity purification of Ace2-3XHA, Rts1-3XHA was carried out in the presence of 1M KCl as previously described with the following changes (Mortensen et al., 2002). Affinity beads were prepared by binding 0.6mg of anti-HA antibody to 0.5 ml of protein A beads overnight at 4˚C. 14 grams of frozen cell powder was resuspended in 30 ml of lysis buffer (50 mM HEPES-KOH pH7.6, 1 M KCL, 1 mM EGTA, 1 mM $MgCl_2$, 0.25% Tween-20, 5% glycerol) containing 1mM PMSF by stirring at 4˚C for 15 min. The cell extract was centrifuged at 40,000 rpm for 1 h. The elution buffer contained 50 mM HEPES-KOH pH 7.6, 250 mM KCl, 1 mM EGTA, 1 mM $MgCl_2$, 5% glycerol, 0.5mg/ml HA dipeptide. The Ace2-3XHA was treated with lambda phosphatase before elution.

To test if Rts1 directly dephosphorylates Ace2, purified Ace2 and Rts1 were mixed in the presence of phosphatase assay buffer (50mM HEPES-KOH pH 7.6, 2 mM $MgCl_2$, 1 mM DTT, 10% glycerol, 0.05% Tween-20, 1mM DTT). The reactions

were incubated for 30 min at 30°C and then quenched with 4X SDS-PAGE sample buffer (260mM Tris-HCl pH 6.8, 12% SDS, 40% Glycerol, 0.04% bromophenol blue). The samples were loaded onto a 10% SDS-PAGE gel, which was transferred to nitrocellulose and probed with anti-Ace2. Similar approaches were used to test the effects of purified Cdc55 (Harvey et al., 2011).

REFERENCES

Andoh, T., Y. Hirata, and A. Kikuchi. 2000. Yeast glycogen synthase kinase 3 is involved in protein degradation in cooperation with Bul1, Bul2, and Rsp5. *Mol Cell Biol*. 20:6712-6720.

Artiles, K., S. Anastasia, D. McCusker, and D.R. Kellogg. 2009. The Rts1 regulatory subunit of protein phosphatase 2A is required for control of G1 cyclin transcription and nutrient modulation of cell size. *PLoS genetics*. 5:e1000727.

D'Aquino, K.E., F. Monje-Casas, J. Paulson, V. Reiser, G.M. Charles, L. Lai, K.M. Shokat, and A. Amon. 2005. The protein kinase Kin4 inhibits exit from mitosis in response to spindle position defects. *Mol Cell*. 19:223-234.

Di Como, C.J., and K.T. Arndt. 1996. Nutrients, via the Tor proteins, stimulate the association of Tap42 with type 2A phosphatases. *Genes Dev*. 10:1904-1916.

Harvey, S.L., A. Charlet, W. Haas, S.P. Gygi, and D.R. Kellogg. 2005. Cdk1-dependent regulation of the mitotic inhibitor Wee1. *Cell*. 122:407-420.

Harvey, S.L., G. Enciso, N.E. Dephoure, S.P. Gygi, J. Gunawardena, and D.R. Kellogg. 2011. A phosphatase threshold sets the level of Cdk1 activity in early mitosis. *Mol Biol. Cell*. 22:3595-3608.

Hirata, Y., T. Andoh, T. Asahara, and A. Kikuchi. 2003. Yeast glycogen synthase kinase-3 activates Msn2p-dependent transcription of stress responsive genes. *Mol Biol Cell*. 14:302-312.

Jansen, J.M., M.F. Barry, C.K. Yoo, and E.L. Weiss. 2006. Phosphoregulation of Cbk1 is critical for RAM network control of transcription and morphogenesis. *J Cell Biol*. 175:755-766.

Mazanka, E., and E.L. Weiss. 2010. Sequential counteracting kinases restrict an asymmetric gene expression program to early G1. *Mol Biol Cell*. 21:2809-2820.

Moriya, H., Y. Shimizu-Yoshida, A. Omori, S. Iwashita, M. Katoh, and A. Sakai. 2001. Yak1p, a DYRK family kinase, translocates to the nucleus and

phosphorylates yeast Pop2p in response to a glucose signal. *Genes Dev*. 15:1217-1228.

Mortensen, E., H. McDonald, J. Yates, and D.R. Kellogg. 2002. Cell cycle-dependent assembly of a Gin4-septin complex. *Molec. Biol. Cell*. 13:2091-2105.

O'Conallain, C., M.T. Doolin, C. Taggart, F. Thornton, and G. Butler. 1999. Regulated nuclear localisation of the yeast transcription factor Ace2p controls expression of chitinase (CTS1) in Saccharomyces cerevisiae. *Molecular & general genetics : MGG*. 262:275-282.

Pereira, G., and E. Schiebel. 2005. Kin4 kinase delays mitotic exit in response to spindle alignment defects. *Mol Cell*. 19:209-221.

Sbia, M., E.J. Parnell, Y. Yu, A.E. Olsen, K.L. Kretschmann, W.P. Voth, and D.J. Stillman. 2008. Regulation of the yeast Ace2 transcription factor during the cell cycle. *The Journal of biological chemistry*. 283:11135-11145.

Sutton, A., D. Immanuel, and K.T. Arndt. 1991. The SIT4 protein phosphatase functions in late G1 for progression into S phase. *Mol Cell Biol*. 11:2133-2148.

Table I: Strains used in this study

Strain	*MAT*	Genotype	Reference or Source
DK186	a	*bar1*	Altman *et al*., 1997
DK346	a	*pph21Δ1::HIS3 pph22-12::URA3 pph3Δ1::LYS2*	Evans and Stark, 1997
DK360	a	*CDC28::TRP1*	Sorger and Murray, 1992
DK494	a	*glc7Δ::LEU2 glc7-10::TRP1*	Andrews and Stark, 2000
DK495	a	*glc7Δ::LEU2 glc7-12::TRP1*	Andrews and Stark, 2000
DK496	a	*GLC7::TRP1*	Andrews and Stark, 2000
DK647	a	*bar1 rts1Δ::kanMX6*	Artiles *et al*., 2009
DK853	a	*bar1 pho85Δ::kanMX6 rts1Δ::HIS*	Artiles *et al*., 2009
DK1233	a	*bar1 rts1Δ::HIS3MX6 pSL201-5[GAL1-CLN2-3XHA::URA3]*	Artiles *et al*., 2009
DK1275	a	*bar1 yck1Δ::KanMX6 yck2-as*	This study
DK1314	?	*bar1 sit4Δ::HIS3 YCp50[sit4-102::URA3]*	Arndt Laboratory[1]
DK1408	a	*bar1 rts1Δ::kanMX6 yplac33[URA3]*	Artiles *et al*., 2009
DK1475	a	*bar1 sec6-4::kanMX*	Anastasia *et al.,* 2012
DK1524	a	*CLN2-3XHA::ADE2*	This study
DK1529	a	*CLN2-3XHA::ADE2 pkh1-D398G pkh2Δ::LEU2*	This study
DK1619	a	*sch9 (T492G)*	Zaman *et al.,* 2009
DK1721	a	*bar1 CLN2-3XHA::ADE2 pkh1-D398G pkh2Δ::LEU2 rts1Δ::HIS*	This study
DK1868	a	*mck1Δ::TRP1 mds1Δ::HIS3 mrk1Δ::URA3 yol128C::LEU2*	Kikuchi Laboratory[2]
DK1906	a	*bar1 CLN2-3XHA::LEU2 rts1Δ::HIS ace2Δ::kanMX4*	This study
DK1908	a	*bar1 CLN2-3XHA::LEU2 ace2Δ::kanMX4*	Zapata *et al.,* 2014
DK2017	a	*bar1 CLN3-6XHA::HIS*	Zapata *et al.,* 2014
DK2019	a	*bar1 CLN3-6XHA::HIS rts1Δ::kanMX4*	Zapata *et al.,* 2014
DK2049	a	*bar1 CLN3-6XHA::HIS rts1Δ::kanMX4 ace2Δ::hphNT1*	Zapata *et al.,* 2014
DK2055	a	*bar1 CLN3-6XHA::HIS ace2Δ::natMX4*	Zapata *et al.,* 2014
DK2093	a	*bar1 cbk1Δ::HIS*	Zapata *et al.,* 2014
DK2238	a	*bar1 kin4Δ::hphNT1 CLN3-6XHA::HIS*	This study
DK2242	a	*bar1 kin4Δ::hphNT1 rts1Δ::kanMX6 CLN3-6XHA::HIS*	This study
DK2288	a	*mck1Δ::TRP1 mds1Δ::HIS3 mrk1Δ::URA3 yol128C::LEU2 rts1Δ::kanMX*	This study
DK2290	a	*bar1 yck1Δ::KanMX6 yck2-as rts1Δ::HIS*	This study
DK2291	a	*sch9 (T492G) rts1Δ::kanMX4*	This study
DK2298	a	*bar1 yak1Δ::kanMX4*	This study
KA61	a	*bar1 cln1Δ::TRP1 cln2Δ::LEU2*	Egelhofer *et al.,* 2008
SH183	a	*bar1 pho85Δ::kanMX4*	Egelhofer *et al.,* 2008
SH184	a	*bar1 cln3Δ::HIS3MX6*	Egelhofer *et al.,* 2008
SH403	a	*pph21Δ1::HIS3 pph22-172::URA3 pph3Δ1::LYS2*	This study
SH454	a	*CDC28::TRP1 cdc55Δ::LEU2*	This study
SH491	a	*CDC28::TRP1 cdc55Δ::LEU2 rts1Δ::kanMX4*	This study
SH497	a	*CDC28::TRP1 rts1Δ::kanMX4*	This study
SH533	a	*tap42Δ::HIS3 pRS414[TAP42::TRP1]*	Broach Laboratory[3]
SH534	a	*tap42Δ::HIS3 pRS414[tap42-106::TRP1]*	Broach Laboratory
SH535	a	*tap42Δ::HIS3 pRS414[tap42-109::TRP1]*	Broach Laboratory
ZZ41	a	*bar1 CLN2-3XHA::LEU2*	Artiles *et al*., 2009

[1] Pfizer, New York
[2] University of Tokyo, Japan
[3] Princeton University

Figure 1: Identification of additional phosphatases that regulate Ace2 phosphorylation.

For all panels, Ace2 was assayed by western blot. A-B) Wild type, *pph21*Δ *pph22-ts* *pph3*Δ were grown to log phase in YPD and then shifted to a semi-permissive (30˚C) or restrictive temperature (37˚C). Samples were taken at the indicated time points. C-D) Wild type and *tap42-ts* log phase cells were taken at the indicated times after shifting to a semi-permissive (30˚C) or restrictive temperature (37˚C). E-F) Wild type and *sit4-102* cells were grown to log phase in YPD and then shifted to a semi-permissive (30˚C) or restrictive temperature (38˚C). Samples were taken at the indicated time points. G) An isogenic control and *glc7-ts* cells were grown to log phase in YPD and then shifted to the restrictive temperature (34˚C). Samples were taken at the indicated time points. H) Control, *rts1*Δ, *cdc55*Δ, and *rts1*Δ *cdc55*Δ cells were grown to log phase and processed for western blot.

Figure 1

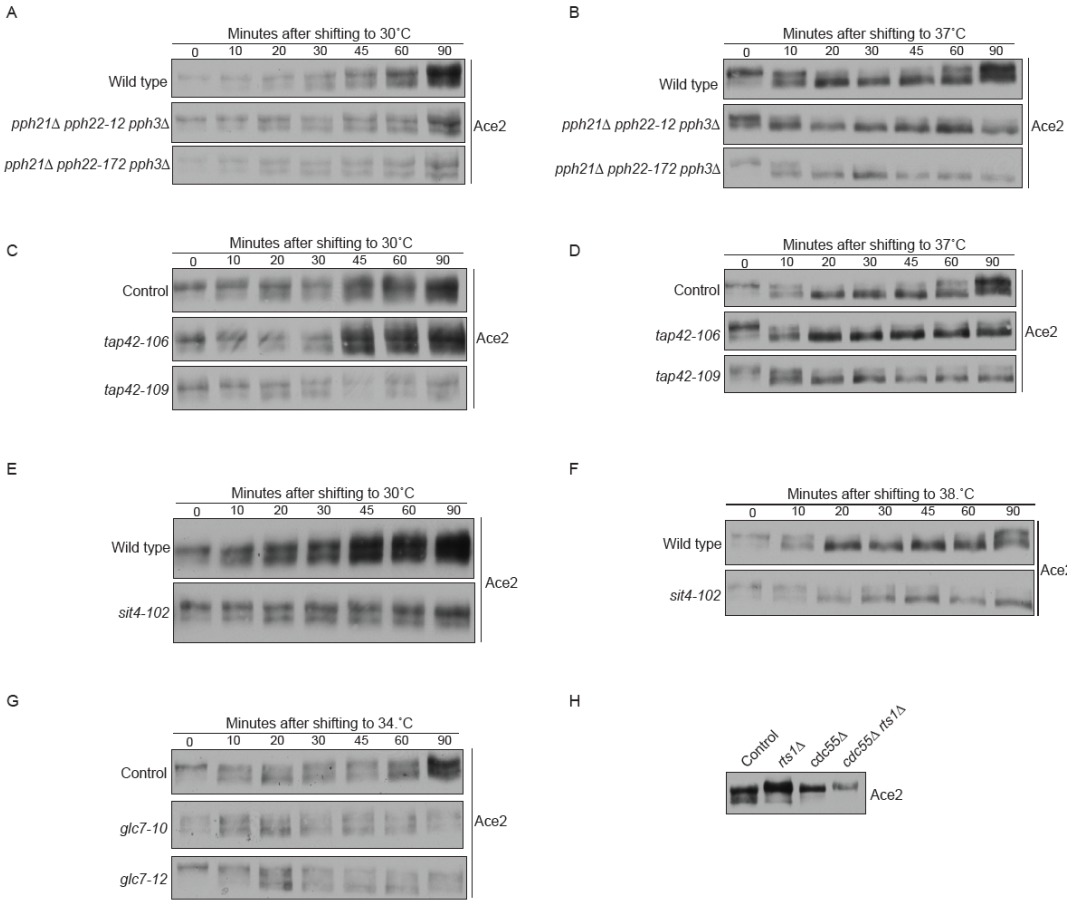
A
Minutes after shifting to 30°C
0 10 20 30 45 60 90
Wild type
pph21Δ pph22-12 pph3Δ
pph21Δ pph22-172 pph3Δ
Ace2
B
Minutes after shifting to 37°C
0 10 20 30 45 60 90
Wild type
pph21Δ pph22-12 pph3Δ
pph21Δ pph22-172 pph3Δ
Ace2
C
Minutes after shifting to 30°C
0 10 20 30 45 60 90
Control
tap42-106
tap42-109
Ace2
D
Minutes after shifting to 37°C
0 10 20 30 45 60 90
Control
tap42-106
tap42-109
Ace2
E
Minutes after shifting to 30°C
0 10 20 30 45 60 90
Wild type
sit4-102
Ace2
F
Minutes after shifting to 38.°C
0 10 20 30 45 60 90
Wild type
sit4-102
Ace2
G
Minutes after shifting to 34.°C
0 10 20 30 45 60 90
Control
glc7-10
glc7-12
Ace2
H
Control
rts1Δ
cdc55Δ
cdc55Δ rts1Δ
Ace2

Figure 2: A screen to identify kinases that regulate Ace2 phosphorylation in *rts1*Δ cells.

For all panels, Ace2 was assayed by western blot. A-D) Cells from the indicated genotypes were grown to log phase in YPD and processed for western blotting. E) Wild type, *rts1*Δ, *pkh1-ts pkh2*Δ, and *pkh1-ts pkh2*Δ *rts1*Δ cells were grown to log phase in YPD and then shifted to a semi-permissive temperature of 30˚C. Samples were taken at the indicated times and loaded in an intercalated manner to compare differences in phosphorylation. F) Wild type, *rts1*Δ, *sch9-as*, and *sch9-as rts1*Δ log phase cells were taken at the indicated times after addition of 1μM 1NMPP1. Samples were loaded in an intercalated manner. G) Wild type, *rts1*Δ*, yck1*Δ *yck2-as,* and *yck1*Δ *yck2-as rts1*Δ log phase cells were taken at the indicated times after addition of 10μM CZ31. Samples were loaded in an intercalated manner.

Figure 2

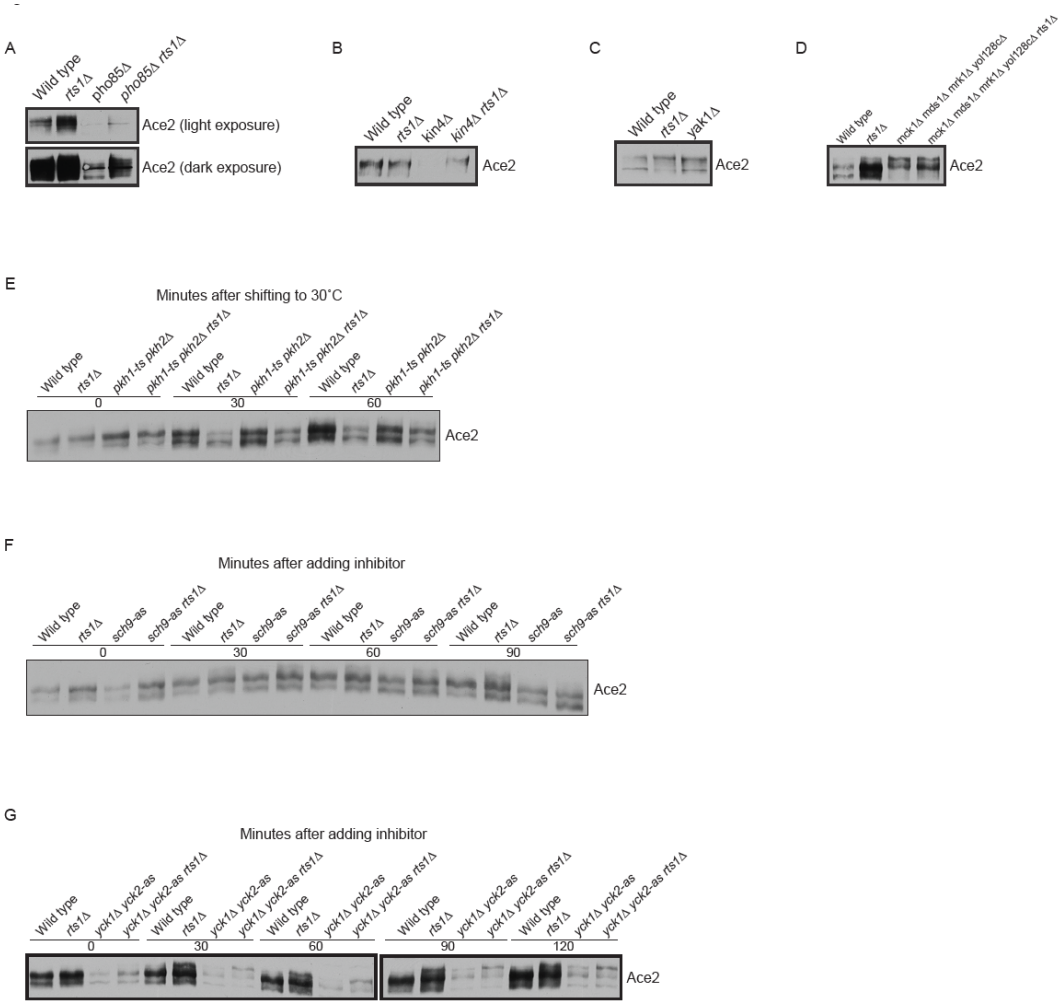
A
Wild type
rts1Δ
pho85Δ
pho85Δ rts1Δ
Ace2 (light exposure)
Ace2 (dark exposure)
B
Wild type
rts1Δ
kin4Δ
kin4Δ rts1Δ
Ace2
C
Wild type
rts1Δ
yak1Δ
Ace2
D
Wild type
rts1Δ
mck1Δ mds1Δ mrk1Δ yor128cΔ
mck1Δ mds1Δ mrk1Δ yor128cΔ rts1Δ
Ace2
E
Minutes after shifting to 30˚C
Wild type
rts1Δ
pkh1-ts pkh2Δ
pkh1-ts pkh2Δ rts1Δ
0
30
60
Ace2
F
Minutes after adding inhibitor
Wild type
rts1Δ
sch9-as
sch9-as rts1Δ
0
30
60
90
Ace2
G
Minutes after adding inhibitor
Wild type
rts1Δ
yck1Δ yck2-as
yck1Δ yck2-as rts1Δ
0
30
60
90
120
Ace2

Figure 3: Ace2 dephosphorylation by PP2A in vitro.

Phosphatase reactions containing affinity-purified Ace2-3XHA, Rts1-3XHA, and Cdc55-3XHA were incubated in phosphatase assay buffer for 30 minutes. Ace2 phosphorylation was assayed by western blot with anti-Ace2. Ace2 was purified in a hyperphosphorylated form from *rts1*Δ cells. As a control, Ace2 was dephosphorylated using λ phosphatase (1st lane).

Figure 3

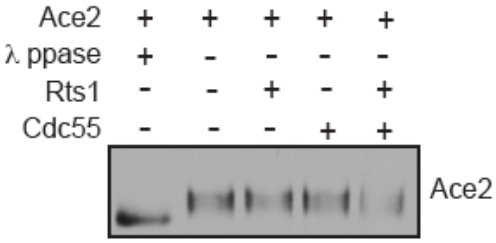

Figure 4: Ace2 phosphorylation in cells lacking G1 cyclins.

Cells of the indicated genotypes were grown to log phase in YPD and samples were probed for Ace2 phosphorylation by western blot.

Figure 4

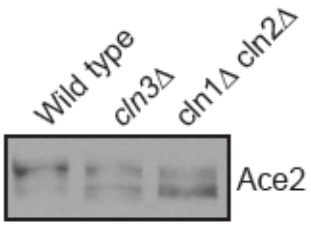

Figure 5: Ace2 phosphorylation in *rts1*∆ cells containing *CLN2-3XHA or GAL1-CLN2.*

A-B) Cells of the indicated genotypes were released from a G1 arrest and Ace2 phosphorylation was assayed at the indicated time points by western blot. Samples were loaded in an intercalated manner to compare differences in phosphorylation. C) Control and *GAL1-CLN2* cells were released from a G1 arrest into media containing 2% Galactose to induce expression of *CLN2.* Samples were probed for Ace2 phosphorylation by western blotting and loaded in an intercalated manner.

Figure 5

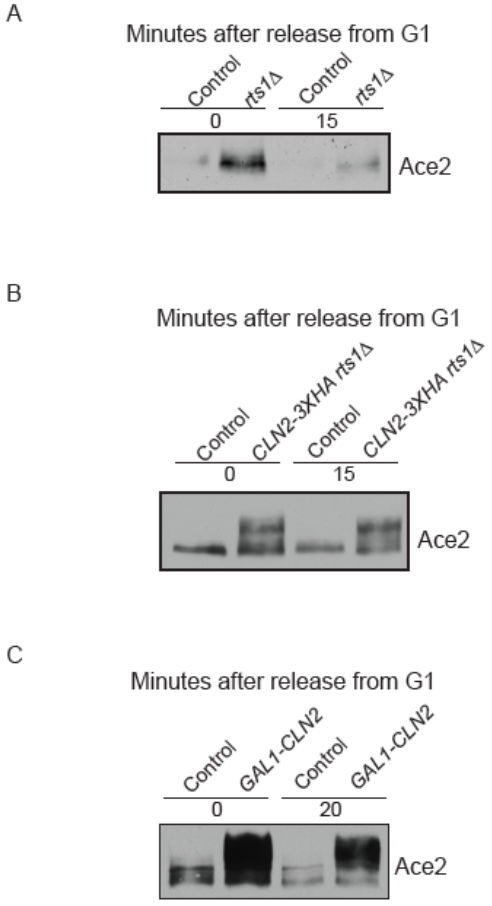
A
Minutes after release from G1
Control
rts1Δ
Control
rts1Δ
0
15
Ace2
B
Minutes after release from G1
Control
CLN2-3XHA rts1Δ
Control
CLN2-3XHA rts1Δ
0
15
Ace2
C
Minutes after release from G1
Control
GAL1-CLN2
Control
GAL1-CLN2
0
20
Ace2

Figure 6: Ace2 phosphorylation in *sec6-4* mutants.

Wild type and *sec6-4* cells were grown to log phase in YPD and shifted to the restrictive temperature (34˚C). Samples were taken at the indicated time points after the temperature shift, and probed for Ace2 phosphorylation by western blotting.

Figure 6

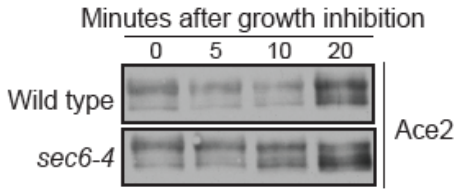
Minutes after growth inhibition
0
5
10
20
Wild type
sec6-4
Ace2

Figure 7: Effect of Pkh1/2 on Ace2, Swe1 and Mih1 phosphorylation.

A-D) Wild type and *pkh1-ts pkh2*Δ cells were grown to log phase in YPD and then shifted to a semi-permissive temperature of 30˚C (A), or a restrictive temperature of either 34˚C (B) or 37˚C (C-D). Samples were taken at the indicated and Ace2, Swe1, and Mih1 phosphorylation was assayed by western blotting.

Figure 7

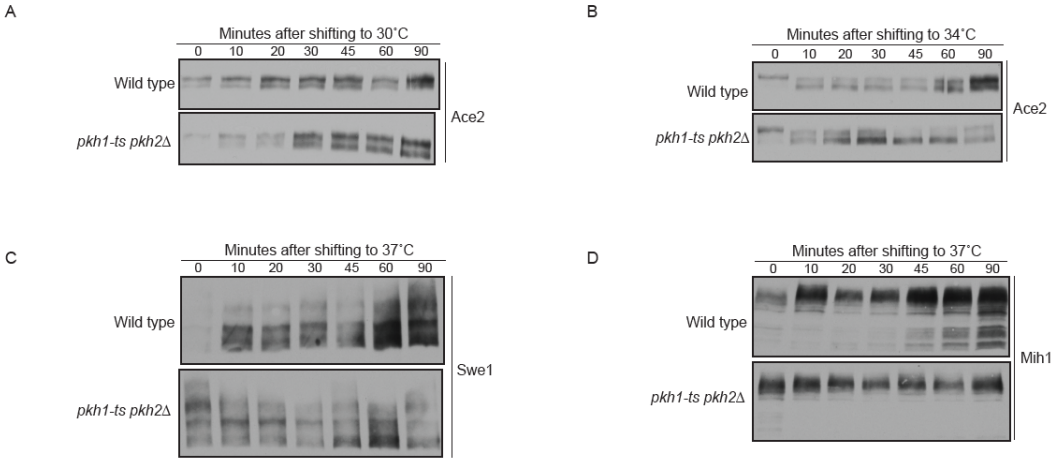
A
Minutes after shifting to 30˚C
0 10 20 30 45 60 90
Wild type
pkh1-ts pkh2Δ
Ace2
B
Minutes after shifting to 34˚C
0 10 20 30 45 60 90
Wild type
pkh1-ts pkh2Δ
Ace2
C
Minutes after shifting to 37˚C
0 10 20 30 45 60 90
Wild type
pkh1-ts pkh2Δ
Swe1
D
Minutes after shifting to 37˚C
0 10 20 30 45 60 90
Wild type
pkh1-ts pkh2Δ
Mih1

Figure 8: Loss of *cdc55*Δ causes hyperphosphorylation of Cbk1.

Cells of the indicated genotypes were grown to log phase in YPD and Cbk1 phosphorylation was assayed by western blotting. 1st lane is a negative control to the specificity of the Cbk1 antibody. The 2nd and 3rd lanes are both positive controls containing a wild type copy of Cbk1.

Figure 8

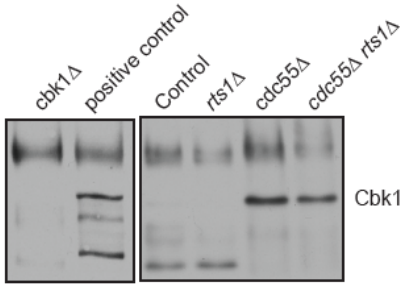
cbk1Δ
positive control
Control
rts1Δ
cdc55Δ
cdc55Δ rts1Δ
Cbk1

Figure 9: Rts1 is required for normal accumulation of Cln2 via Ace2.

Wild type, *rts1*Δ, *ace2*Δ, and *rts1*Δ *ace2*Δ cells were released from a G1 arrest and the behavior of Cln2 was assayed by western blotting.

Figure 9

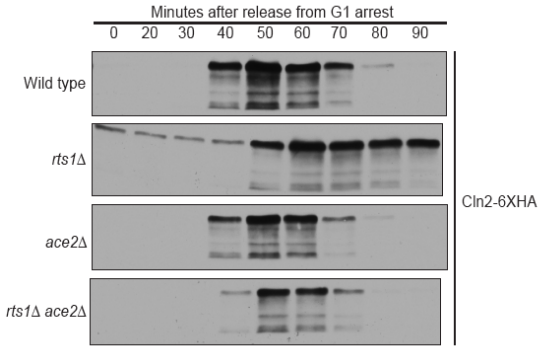
Minutes after release from G1 arrest
0 20 30 40 50 60 70 80 90
Wild type
rts1Δ
ace2Δ
rts1Δ ace2Δ
Cln2-6XHA